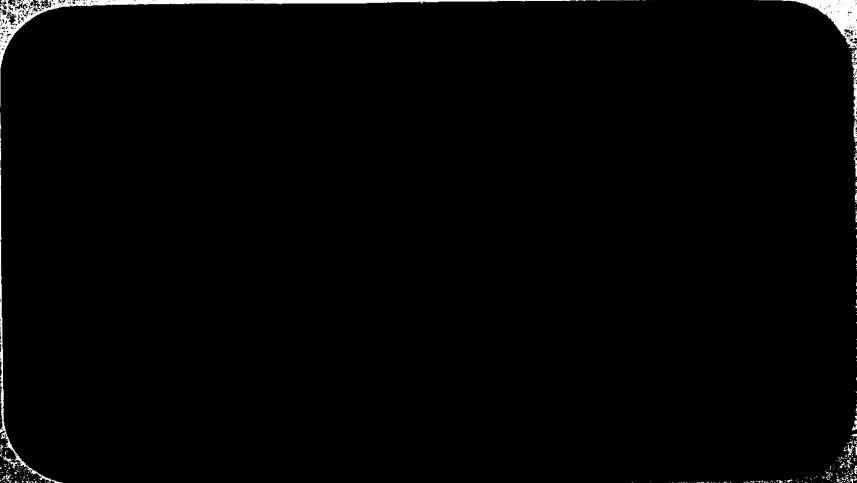


ITRI

N 66-13572

146 /
CR 68709 18



GPO PRICE \$ _____

CFSTI PRICE(S) \$ _____

Hard copy (HC) 4.00

Microfiche (MF) 1.00

IIT RESEARCH INSTITUTE
10 West 35th Street
Chicago, Illinois 60616

Contract No. NAS8-11333
IITRI Project No. G6002

DEVELOPMENT OF LIGHTWEIGHT
THERMAL INSULATION MATERIALS
FOR RIGID HEAT SHIELDS

IITRI-G6002-12
Summary Report No. 1
for the period
June 25, 1964 to June 25, 1965

Prepared by
A. J. Mountvala
H. H. Nakamura
H. L. Rechter

Prepared for
National Aeronautics and Space Administration
George C. Marshall Space Flight Center
Huntsville, Alabama 35812

June 25, 1965

IIT RESEARCH INSTITUTE

IITRI Project No. G-6002

DEVELOPMENT OF LIGHTWEIGHT

THERMAL INSULATION MATERIALS

FOR RIGID HEAT SHIELDS

National Aeronautics and Space Administration
George C. Marshall Space Flight Center
Huntsville, Alabama 35812

DEVELOPMENT OF LIGHTWEIGHT
THERMAL INSULATION MATERIALS
FOR RIGID HEAT SHIELDS

13572

ABSTRACT

Exposed structural members at the base of large, high-thrust rocket engines are subject to excessive heating, largely radiative, from the engine exhaust. A program of engineering and scientific research has been carried out to develop lightweight ceramic foams which will provide adequate insulation and survive the mechanical environment associated with launch operations.

Castable ceramic foams of zircon, mullite, and calcium aluminate have been prepared and evaluated for use as rigid heat shields in launch vehicles. The effects of various additives, including fibers and other opacifying materials to zircon foams, have been investigated.

Chemically bonded, castable-type zircon foams have been optimized to meet certain specific requirements. These foams of $\frac{1}{2}$ in. thickness show good insulative and mechanical characteristics when subjected to a heat flux of 40 Btu/ft²-sec with simultaneous vibration of 60 cps, $\frac{1}{2}$ in. double amplitude displacement and 90 g's acceleration. Property measurements on an optimized zircon foam disclosed very high optical reflectance in the near-infrared wavelength region and an extremely low thermal conductivity to 2300°F.

A comprehensive literature survey on foamed ceramics has been carried out. This survey includes a tabulation of commercially available materials and their properties, as obtained from certain manufacturers. A computer program to theoretically evaluate the thermal analysis on foamed insulation is also presented.

Butler

IIT RESEARCH INSTITUTE

TABLE OF CONTENTS

	<u>Page</u>
I. INTRODUCTION	1
II. THERMAL ANALYSIS OF FOAMED CERAMIC INSULATORS	2
A. Introduction	2
B. Thermal Analysis	3
C. Results of the Analysis	4
III. PREPARATION OF CERAMIC FOAMS	8
A. General Procedure	8
B. Zircon Foams	11
C. Mullite Foams	26
D. Calcium Aluminate Foams	26
IV. EFFECTS OF HEAT FLUX WITH SIMULTANEOUS VIBRATION AND ACCELERATION ON CERAMIC FOAMS	28
A. Screening Program	28
B. Final Test Program	44
V. CHARACTERISTICS OF OPTIMIZED ZIRCON FOAMS	59
A. Introduction	59
B. Flat-Wise Tensile Strength	60
C. Water Effect	60
D. Thermal Conductivity	62
E. Specific Heat	65
F. Reflectance	67
VI. SUMMARY	69
VII. LOGBOOK RECORDS	70
VIII. PERSONNEL	70
ACKNOWLEDGEMENTS	71
APPENDIX A - Numerical Analysis of the Thermal Properties of Foams	A-1
APPENDIX B - Literature and Technical Survey	B-1

LIST OF TABLES

	<u>PAGE</u>
Table I. Characteristics of Zircon Foams (1 in. Thick) Prepared by Mechanical Whipping	13
Table II. Characteristics of Chemically Bonded Castable Zircon Foams ($\frac{1}{2}$ in. Thick) on Steel Panels	16
Table III. Characteristics of Layered Composite Foams Based on Zircon Z-61 Composition ($\frac{1}{2}$ in. Thick)	20
Table IV. Characteristics of Chemically Bonded Castable Zircon Foams ($\frac{1}{2}$ in. Thick) on Honeycomb Substrates	23
Table V. Characteristics of Mullite Foams ($\frac{1}{2}$ in. Thick) Prepared by Mechanical Whipping.	27
Table VI. Characteristics of Calcium Aluminate Cement Foams ($\frac{1}{2}$ in. Thick) by Mechanical Whipping	29
Table VII. Screening Test Results on Zircon-Based Foams, 1 in. Thick	32
Table VIII. Screening Test Results on Zircon-Based Foams, $\frac{1}{2}$ in. Thick	34
Table IX. Screening Test Results on Foams on Steel Panels	37
Table X. Test Results on Foams ($\frac{1}{2}$ in. Thick) on Steel Panel Substrates at Heat Flux of 40 Btu/ft ² -sec	45
Table XI. Final Test Results on Zircon Foams ($\frac{1}{2}$ in. Thick) on 1 in. Thick Honeycomb Substrates	48
Table XII. Back Face Temperatures of Some Nearly Optimized Zircon Foams ($\frac{1}{2}$ in. Thick) on 1 in. Honeycomb Substrates on Final Testing.	56

LIST OF TABLES (cont'd)

	<u>PAGE</u>
Table XIII. Flat-Wise Tensile Strength of Zircon Foams at Room Temperature	61
Table XIV. Water Solubility of Castable Zircon Foams	63
Table XV. Thermal Conductivity of Zircon Foam Z-67	66
Table XVI. Thermal Conductivity of Zircon Foam Z-90	66
Table XVII. Specific Heat of Zircon Foam Z-90	68
Table B-I. Mechanical Properties of Zirconia Foams at Room Temperature	B-17
Table B-II. Typical Properties of Foamed Fireclay	B-23
Table B-III. Thermal Conductivity of Micro-Quartz Fibrous Silica	B-25
Table B-IV. Recipients of Technical Survey Questionnaire	B-28
Table B-V. Property Data on Ceramic Foams	B-31

LIST OF ILLUSTRATIONS

	<u>PAGE</u>
Figure 1 Insulation Weight as a Function of Thermal Properties	72
Figure 2 Surface Temperature as a Function of Thermal Properties	73
Figures 3a,b Dependence of Insulation Weight Requirement upon Absorptance	74
Figure 4 Minimum Volumetric Specific Heat Requirement as a Function of Thermal Conductivity	76
Figures 5a,b Minimum Volumetric Specific Heat Requirement as a Function of Absorptance	77
Figure 6 Influence of Substrate Upon Insulation Performance	79
Figure 7 Insulation Weight Requirement with Conductivity as a Function of Density	80
Figure 8 Insulation Thickness Requirement with Conductivity as a Function of Density	81
Figure 9 Photomicrograph of Zircon Foam, Z-40	82
Figure 10 Photomicrograph of Zircon Foam, Z-35-1	82
Figure 11 Photomicrograph of Zircon Based Foam Containing Fiberfrax, Z-43	83
Figure 12 Photomicrograph of Optimized Zircon Foam Z-90	83
Figure 13 Test Set-Up for Subjecting Foams to Heat Flux with Simultaneous Vibration and Acceleration	84
Figure 14 The Back Face Temperature (T_s) of $\frac{1}{2}$ in. Foams on Steel Panels After 150 sec Exposure to a Heat Flux of 24 Btu/ft ² -sec	85

LIST OF ILLUSTRATIONS (cont'd)

	<u>PAGE</u>
Figure 15 The Back Face Temperature (T_s) of $\frac{1}{2}$ in. Foams on Steel Panels After 150 sec ² Exposure to a Heat Flux of 40 Btu/ft ² -sec	86
Figure 16 The Effect of Surface Conditioning on the Back-Face Temperature of Zircon Foam, Z-87 ($\frac{1}{2}$ in. Thick), After 5 Minutes	87
Figure 17 Effect on Foam Thickness on Insulative Characteristics of Rigid Heat Shields	88
Figure 18 Thermal Conductivity of Ceramic Foams	89
Figure 19 Specific Heat of Zircon Foam Z-90	90
Figure 20 Absolute Reflectance of Zircon Foams	91
Figure B-1 Compressive Strength of Alumina Foams at Room Temperature	B-32
Figure B-2 Flexural Strength of Alumina Foams at Room Temperature	B-33
Figure B-3 Effect of Temperature on Flexural Strength of Alumina Foams of Various Densities	B-34
Figure B-4 Effect of Temperature on the Thermal Conductivity of Alumina Foams of Various Densities	B-35
Figure B-5 Emittance of Various Alumina-Based Foams	B-36
Figure B-6 Effect of Temperature on Thermal Conductivity of Zirconia Foams of Various Densities	B-37
Figure B-7 The Effect of Density on the Thermal Conductivity of Foamed Zirconia	B-38
Figure B-8 The Thermal Conductivities of Foamed and Fibrous Materials	B-39

DEVELOPMENT OF LIGHTWEIGHT
THERMAL INSULATION MATERIALS
FOR RIGID HEAT SHIELDS

I. INTRODUCTION

This is the annual summary report under NASA contract NAS8-11333, for the development of lightweight thermal insulation materials for rigid heat shields.

The severity of radiation and convection heating from the engine plumes of high-thrust rocket engines requires the use of inorganic insulation materials that must meet certain specific requirements. Mechanical integrity is also a critical factor because of the acceleration and high vibrational forces that are present during the lift-off and powered stages of flight. Therefore, the optimum insulation required for such applications should display certain characteristics such as low density, low thermal conductivity, good mechanical strength, thermal shock resistance, and good adhesion to metal substrates. Further, since the insulation is required primarily for applications in a radiant heating environment, the insulation material should have desirable reflective properties over the wavelength range of 1.0 to 2.4 microns.

Foamed ceramic composites, containing dispersed phases and fibers, as well as in the form of layered structures have demonstrated a potential for use in rigid heat shields.

Specifically, the foamed ceramics developed under this program have a bulk density not greater than 60 lb/ft³. Further, the foam insulations that have been developed are such that the structures to be shielded do not exceed 400°F in 150 sec when subjected to a heat flux of 40 Btu/ft²-sec and simultaneous vibrations of 60 cps with a double amplitude displacement of ½ in. and an acceleration level of up to 90 g's.

IIT RESEARCH INSTITUTE

Chemically bonded, castable-type zircon, mullite, and calcium aluminate foams were prepared and their mechanical and insulative characteristics investigated. These foams were prepared by mechanical whipping, using egg albumin as the foaming agent. Optimization to meet the program requirements was carried out on composite zircon foams, cast onto honeycomb structures.

A comprehensive literature and technical survey on foamed ceramics was carried out. This includes information gathered from technical journals, reports, and patent literature, together with data gathered from some prominent manufacturers by way of a technical questionnaire.

A computer program for predicting the performance of foamed ceramics as thermal insulators, as a function of certain parameters, was also carried out, and is presented in this report.

II. THERMAL ANALYSIS OF FOAMED CERAMIC INSULATORS

A. Introduction

The ability of a material to perform as a thermal insulator is dependent upon its thermal properties and the application in which it is used. Since the roles of thermal conductivity, specific heat, density, emittance, and absorptivity in determining the effectiveness of an insulator are not evident, a thermal analysis to determine the influence of these properties in the present application was undertaken.

The computer program for predicting the performance of foamed ceramics as insulators has been developed in the Fortran II language for use on the IBM 7090 computer. This program has been used to carry out a comprehensive parametric study of the heat-transfer system. The insulation performance has been evaluated over a broad range of thermal properties, and the influence of the various thermal properties upon performance has been determined.

IIT RESEARCH INSTITUTE

B. Thermal Analysis

The numerical analysis of the thermal properties of foamed insulation is shown in Appendix A. In this analysis, a one-dimensional steady-state equation was set up, together with the radiation boundary condition at the insulation-substrate interface. The nonsteady, radiant heating of a material has been analytically treated to determine the temperature distribution in an infinite plate subjected to a radiant heat flux. An insulation-substrate boundary condition has been assumed, wherein the substrate is uniform in temperature throughout. This is undoubtedly true since the substrate conductivity and diffusivity will be large in comparison to that of the insulation.

The functional variations of thermal conductivity, rate of change of thermal conductivity with temperature, and emittance and specific heat with temperature have been incorporated into four subroutines so that the functional relationships can be altered with ease for a particular material.

By non-dimensionalizing the differential equation and the boundary conditions for the case of constant thermal properties the pertinent groups of problem parameters are obtained. This procedure yields the following expression which relates insulation weight, density (ρ), specific heat (C_p), thermal conductivity (k), absorptance (α), incident heat flux (q), and emittance (ϵ).

$$\frac{W''}{p} = (\rho C_p k, \alpha q'', \epsilon)$$

where W'' = weight per unit area of insulation ($W'' = \rho L$)
 L = insulation thickness.

A parametric study has been performed employing the computer program by allowing $\rho C_p k$, $\alpha q''$, and ϵ to vary over suitable ranges and calculating the corresponding values of W''/k . Thus, for a given material with known density and thermal properties the

thickness of insulation (and therefore its weight) required to yield the desired interface temperature after the prescribed heating time can be determined from this study. Alternately, for a prescribed thickness the values of absorptance, emittance, density, specific heat, and thermal conductivity required to provide the desired performance are delineated.

The parametric study was performed for the following conditions:

Initial temperature = $540^{\circ}\text{R} = 80^{\circ}\text{F}$

Heating time = 150 sec

Interface temperature (at $t = 150$ sec) = $960^{\circ}\text{R} = 500^{\circ}\text{F}$

Substrate parameter ($M''C_{p,s}$) = $0.0662 \text{ Btu/ft}^2\text{-}^{\circ}\text{F}$

The results of the parametric study are presented in the following section.

C. Results of the Analysis

The results of the analysis have yielded a set of curves that indicate the dependence of the pertinent parameters involved in the thermal performance of foamed ceramic insulation. The parameters that have been considered are the thermal conductivity, specific heat, density, emissivity, absorptance, thickness, and the front- and back-face temperatures of the ceramic insulation for various heat fluxes.

In Figure 1 the insulation on weight parameter ($W''/\rho k$) is shown as a function of $\rho C_p k$ for various values of the absorbed heat flux ($\alpha q''$) and emittance (ϵ). The most obvious conclusion that can be made from Figure 1 is that the surface emittance has very little influence in the determination of the required insulation thickness. However, the emittance is of some consequence for very low values of $\alpha C_p k$. It should be noted, however, since this study was performed for constant thermal properties, that the dependence of thermal conductivity of a foamed material upon emittance at high temperatures was not considered. Should the thermal conductivity of foam materials

be greatly dependent upon emittance, a low-emittance material can be employed without suffering any significant weight penalties. The savings in weight that can be obtained for a given heat flux by employing a material with low absorptance is shown clearly in this figure. Given a material with known thermal properties the thickness of insulation required can be determined from this figure.

Figure 2 shows the insulation surface temperature as a function of $\alpha C_p k$ for various values of emittance and absorbed heat flux. Emittance plays a larger role in determining the magnitude of the surface temperature. Here again, for a given heat flux, a low absorptance is desirable to maintain lower surface temperatures.

In Figures 3a and 3b the data have been replotted for the two pertinent heating rates to make the influence of absorptance upon the required insulation weight (or thickness) clear. Great savings in weight or reductions in the other thermal property requirements can be obtained by employing a material with low absorptance.

The minimum volumetric specific heat (ρC_p) required to produce the desired performance is shown in Figure 4 as a function of thermal conductivity for an insulation thickness of 1 in. For the lower values of absorbed heat flux little reduction in the specific heat requirement is obtained by reducing thermal conductivity until very low values of conductivity are approached. If the reductions in thermal conductivity are obtained by decreasing the insulation density, it is possible that no savings will occur; a penalty may be incurred since the volumetric specific heat of a material decreases with density. To fully investigate the role of conductivity an analytical relationship between thermal conductivity and density is required.

The data of Figure 4 are replotted in Figures 5a and 5b to show the reductions in the volumetric specific heat require-

ment that are obtained by reducing the absorptance of the two pertinent heating rates. For all values of thermal conductivity significant savings in the volumetric specific heat requirements can be obtained by reducing the absorptance.

To investigate the influence of the substrate upon the insulation performance the insulation weight parameter was calculated for various values of $\rho_p C_p k$ and the substrate parameter. The results of these calculations are shown on Figure 6.

To investigate the merits of reducing thermal conductivity by decreasing the foam density (i.e., increasing porosity) the dependence of thermal conductivity on density was taken as

$$\frac{k}{k_s} = A \left(\frac{\rho}{\rho_s}\right)^n$$

where A = Constant
 ρ_s = Density of the solid material
 k_s = Thermal conductivity of the solid material
 n = Constant

The above expression has been used in conjunction with the parametric study results to yield the influence of decreasing density (hence, decreasing thermal conductivity). In Figure 7 an insulation weight parameter ($W''C_p$) is shown as a function of density $\rho_s C_p k_s A (\rho/\rho_s)^{n+1}$. The weight of insulation required decreases with decreasing density--with the rate of this decrease depending upon the absorbed heat flux. It should be noted that for the form of conductivity-density variation assumed, the weight requirement is independent of n. An insulation thickness parameter ($L^2 \rho_s C_p / k_s A$) is shown as a function of density in Figure 8 for the case n = 1. The thickness of insulation required increases with decreasing density, with the rate of increase again depending upon the absorbed heat flux. Figure 8 was plotted for n = 1 since this value is a fair approximation of the true variation.

The thermal analysis is useful in understanding the effects of various parameters on the performance of an insulator and permits us to achieve property interchanges. By knowing some of the basic properties of the foamed material, it is then possible to determine what other characteristics are of importance for the insulator to perform under a particular heat flux. For instance, from Figure 1, we know that the emittance does not have any significant effect on the thickness of insulation required. Therefore, in preparing the ceramic foams for our application, it is not necessary to coat the surface with a material of high emittance. The thickness required and the surface temperature at the insulation can also be determined for materials of various densities and thermal conductivities by the use of Figures 1 and 2.

Several important conclusions can be made from the results of the parameter study:

1. The surface emittance of the insulation has only a slight effect upon the thickness of insulation required; however, surface temperature increases significantly with decreasing emittance. If the higher temperatures can be tolerated, a low emittance material should be employed so that radiant heat exchange within the foam will be lowered.
2. The surface absorptance is by far the most important parameter problem. Efforts should be made to reduce the absorptance as much as possible.
3. For a constant density, reductions in thermal conductivity will lead to savings in insulation weight or in the volumetric specific heat requirement. The relative merits of reducing thermal conductivity depends upon the manner in which it is reduced, the range over which it can be altered, and the absorptance.

The results obtained from the parameter study have been used as guidelines in the preparation of composite foams with optimized insulative properties. The experimental program is presented in the subsequent sections.

III PREPARATION OF CERAMIC FOAMS

A. General Procedure

A number of techniques are available for preparing ceramic foams. However, on the basis of previous work carried out at IITRI, the method of mechanical whipping using an air-entraining agent was selected for preparing zircon, mullite, and calcium aluminate foams. A major part of the experimental effort has been in the preparation of chemically bonded, castable-type foams that can be effectively cured at temperatures not exceeding 400° - 500°F. Such a curing process is essential for use with large size structural members. Some preliminary work was also done on fired foams; however, the results presented in this report pertain to castable potassium silicate-bonded zircon and mullite foams and self-bonded calcium aluminate foams.

1. Mechanical Whipping Technique

A weighed amount of the foaming agent, albumin, is dissolved in water. When the albumin is fairly well dispersed in the water, the potassium silicate binder (PS-7) is added.

Solid materials such as zircon, Na_2SiF_6 , and clay are ball-milled together for a short time (approximately $\frac{1}{2}$ hr). Longer periods of milling are not recommended as this causes the mix to cake up.

The foaming, on a laboratory scale, has been carried out with a Sunbeam Mixmaster. When the albumin is dissolved and the PS-7 added to the solution, the mixer is turned to the lowest speed (approximately 270 rpm). With the mixer at this

low speed, the solids previously ball-milled are added to the mix. This low speed is continued for 1 min after all the solids have been added to assure thorough wetting of the materials. The speed is then increased to the maximum (approximately 920 rpm). The speed is held for 2 to 3 min depending upon the solids used to give the desired foam structure. When Fiberfrax is included in the foam composition, this material is added to the water-albumin-PS-7 solution and wetted for 1 min before the addition of the ball-milled solids. The subsequent operations are similar to those described above.

Two types of foaming agents have been investigated; the first type consists of surface-active agents, while the second type consists of high protein materials. The surface agents such as "Mearl" SW 2336 are powerful foaming agents and generally form uniform foams with a low density. They yield a low viscosity mixture which can be poured into place. The high protein foaming agents such as egg albumin and gelatin produce foams with a very fine micropore structure. The mechanically whipped mixture with high protein foaming agents, especially albumin, is usually more viscous than that obtained from a surface-active foaming agent such as SW2336. The materials foamed with albumin have a lower shrinkage coefficient on drying. By combining both these types of foaming agents in various proportions, it has been possible to prepare foams with an intermediate micropore structure. The major portion of the experimental effort has been carried out using egg albumin as the foaming agent, as it forms foams with very fine micropore structure. Such a micropore structure is desirable for use in a radiant heating environment, as discussed in subsequent sections.

2. Preparation of Steel Substrates

Cold-rolled steel panels 3 x 6 x 1/8 in. and honeycomb structures 3 x 6 x 1 in. have been used as substrates for

the foam specimens. The surface of these panels was first washed with Alconox, followed by an acetone rinse to assure complete removal of water. Emery cloth (No. 100) was used to slightly roughen the surface in the case of the steel panels.

A thin layer of a base coat was applied twice to the surface, before casting the foam. A typical composition of the base coat is:

500 g of Al_2O_3 (-325 mesh)--T61 Alcoa alumina is used
150 cc PS-7
70 cc H_2O
1.5 g. gum tragacanth

The coatings are cured by placing the painted panels in an oven at 240°F for 30-60 min.

The foams were then cast directly onto the panels or honeycombs, which were surrounded by a wire mesh, and subsequently subjected to drying and curing.

3. Drying and Curing the Foam

Drying was done by infrared lamps. The coated panels were removed from the oven and while still hot the foam was cast. The foam was immediately placed in the infrared dryer using the bottom lamps only. Pre-heating the metal substrate at around 115°F decreases the amount of stress that the foam must overcome when they are cured at 240°F. As a consequence, well-bonded foams with minimum cracks were obtained. An alternate modification during the drying process entails the use of a plastic wrapping cover (such as Saran-wrap) in direct contact with the top surface of the foam during drying.

When a plastic wrapping is not used, a hard surface skin is formed on the foam, especially with zircon foams, due to the upward migration of the potassium silicate and zircon during drying. Consequently, insolubilization of the

potassium silicate is reduced and differential shrinkage is significant, giving rise to some surface cracks.

The plastic wrapping minimizes the formation of the hard surface skin by drastically reducing the rate of evaporation of moisture from the foam surface, thus permitting more complete insolubilization of the binder. This not only results in a stronger bonded foam body, but also prevents the formation of surface cracks. However, the top surface is not as hard as that obtained without the use of the plastic wrapper. By using the plastic-wrap cover for only part of the drying procedure, it was possible to prepare zircon foams with crack-free surface which retained considerable hardness at the surface.

B. Zircon Foams

1. Introduction

The major emphasis has been in the preparation of zircon foams because this material has certain properties that make it attractive for rigid heat shield applications. It has good resistance to thermal shock, a low coefficient of thermal expansion, a low thermal conductivity, and a density intermediate to that of alumina and zirconia. Besides, it offers a potential for tailoring the foam with second-phase additives to alter its radiation scattering characteristics.

2. Compositional Variations

Zircon powders of various particle sizes have been used for preparing the foams shown in Tables I-IV. The materials designated as "Zircon", "Zircon A", and "Superpax" were obtained from Titanium Alloy Manufacturing Corporation. The first has an average particle size less than 44 microns, 1% +200 mesh, and 10% +325 mesh; the second type of powder (Zircon A) has an average particle size less than 44 microns, 0.1% +325 mesh; and the Superpax has an average particle size less than 4 microns, 0.1% +325 mesh. The "Zircon U" material

was obtained from Metal and Thermit Corporation and is designated by the manufacturer as "Ultrox 100." This is an ultrafine grained powder of less than 1 micron.

Table I indicates the nominal compositions and characteristics of 1 in. thick zircon foams. The earlier specimens were not cast onto steel substrates but merely on paper mats, so as to evaluate the effects of drying and curing cycles on zircon foams with varying compositions. This is indicated for compositions Z-3 to Z-9. Cracking was apparent in the foam structure on drying. Examination of the foam structure indicated that migration of the potassium silicate binder (PS-7) to the outer surface was responsible for the cracking.

In foams Z-11 to Z-25 attempts were made to prevent the migration of the PS-7 by additions of zinc oxide, clay, and/or Na_2SiF_6 . These additives essentially form a complex gel with the potassium silicate, thereby preventing its migration. Foam Z-25, which contained Na_2SiF_6 , gave good results. It was still soft at the bottom after overnight air drying; however, after infrared drying, it showed less silicate migration than Z-25. Neither foam cracked on drying. Exposure in boiling water for 5 hr indicated that neither foam crumbled, but that Z-24 was stronger than Z-25. This indicates that more complete insolubilization of the PS-7 was obtained with ZnO than with Na_2SiF_6 . These results indicate that although ZnO is a slower acting insolubilizer of PS-7 than Na_2SiF_6 , it gives a foam that is more resistant to water. This is probably due to the ease of completion of the reaction with ZnO in comparison to Na_2SiF_6 and also because of the fact that ZnO dispersed more easily than Na_2SiF_6 in the mix.

The results shown in Table I also indicate that foaming agents Antaron FC-34, manufactured by the General Aniline Company, and Armeen-Z, manufactured by Armour and

TABLE I
 CHARACTERISTICS OF ZIRCON FOAMS (1 IN. THICK) PREPARED BY MECHANICAL WHIPPING

Foam No.	Nominal Composition								Foam Density (lb/ft ³)	Process	Comments
	Zircon (g)	Zircon A (g)	Water (cc)	Albumin (g)	PS-7 (cc)	Na ₂ SiF ₆ (g)	Clay (g)	Other Additives			
Z-3	300	-	100	8	70	-	-	-	32	Oven dried, RT-120°F, 5 hr; at 120°F - 15 hr.	Foam developed cracks.
Z-4	400	-	100	12	100	-	-	-	69	Oven dried, RT to 120°F - 5 hr; at 120°F - 15 hr.	No cracks.
Z-7	300	-	256	25	225	-	-	-	44	Oven dried, RT to 120°F - 5 hr; at 120°F - 15 hr, at 160°F	Foam cracked.
Z-8	900	-	256	25	225	-	-	-	44	Oven dried, RT to 120°F - 5 hr; at 120°F - 15 hrs. cured and fired slowly - 160°F to 2000°F (1/2 hr at T max).	Strong, fine-pore structure.
Z-9	450	-	200	12.5	-	-	-	-	-	-	No foam structure, collapse.
Z-11	450	-	135	15.8	-	-	-	Antaron 2.7 g	-	-	Poor, nonuniform foam.
Z-12	450	-	36	12.4	113	-	-	Antaron 2.3 g	-	-	Mix very viscous. Poor bubble structure obtained.
Z-13	650	-	119	12.4	113	-	-	-	40	Oven dried slowly to 140°F. At 190°F.	Foam bloated.
Z-14	900	-	140	-	-	-	-	Antaron 7 g Methocel 3.5 g	30	Oven dried at 155°F.	Weak foam structure.
Z-15	625	-	119	12	113	-	-	ZnO 25 g	57	Oven dried at 130°F.	Foam developed cracks.
Z-16	600	-	119	12	113	-	-	Plaster 50 g	-	-	No foam structure, instantaneous gelling.
Z-17	630	-	119	12	113	-	20	-	58	Oven dried, RT to 120°F, 5 hr; at 120°F - 15 hr. Cured and fired slowly - 160°F to 2000°F (1/2 hr. at T max).	Fine pore structure; developed fine cracks on firing.
Z-19	570	-	243	7	5	-	30	Antharon 14 g Plaster 50 g	-	-	Insufficient foaming.
Z-21	550	-	250	15	-	-	-	SW 2336 6 g Plaster 100 g	55	Air dried - 15 hr. Dried by infrared lamps at 175°F - 6 hr.	Weak green strength. Fine micropore structures but foam developed surface cracks.
Z-22	610	-	115	15	120	-	-	ZnO 40 g	65	Air dried - 15 hr. Dried by infrared lamps at 175°F - 6 hr. Cured at 500°F - 1 hr.	Fine micropore structure, no cracking, strong foam body. Foam bonded to stainless steel substrate with epoxy. (Epoxy cured at 300°F). Strong bond with substrate.
Z-23	650	-	119	15	120	6	-	-	69	Air dried - 15 hr. Dried by infrared lamps at 200°F.	Weak green strength. Foam developed cracks.
Z-24	585	-	93	15	150	-	-	ZnO 65 g	60	Air dried - 15 hr. Dried by infrared lamps at 200°F - 6 hr.	No cracking, strong foam. Cured at 500°F. Foam developed hairline crack over substrate.
Z-25	650	-	119	15	120	12	-	-	66	Air dried - 15 hr. Dried by infrared lamps at 200°F - 6 hr.	Fine micropore structure, no cracks.

TABLE I (Cont'd)

Foam No.	Nominal Composition								Foam Density (lb/ft ³)	Process	Comments
	Zircon (g)	Zircon A (g)	Water (cc)	Albumin (g)	PS-7 (cc)	Na ₂ SiF ₆ (g)	Clay (g)	Other Additives			
Z-26	650	-	125	15	120	13	-	-	70	Mix poured onto stainless steel substrate. Air dried 15 hr. Dried by infrared lamps at 170°F - 6 hr. Cured at 500°F - 1 hr.	Foam developed hairline cracks near foam-substrate interface due to warping of substrate plate. Good bonding between foam and stainless steel plate.
Z-27	650	-	120	50	120	12	6.5	-	71	Cast onto steel panel. Air dried - 15 hr. RT to 160°F - 8 hr.	Fine micropore structure. Foam separated from substrate.
Z-28	650	-	120	15	120	6	6.5	ZnO 32.5 g	80	Cast onto steel panel. Air dried - 15 hr. RT to 140°F - 4 hr.	Fine micropore structure. Minor surface cracks. Foam separated from substrate.
Z-29	650	-	120	15	125	14	6.5	ZnO 32.5 g	79	Cast onto steel panel. Air dried - 15 hr. RT to 150°F - 4 hr.	Fine micropore structure. Surface cracks. Foam separated from substrate.
Z-30	650	-	120	15	125	14	13	-	73	Cast onto steel panel. Air dried - 15 hr. RT to 150°F - 8 hr.	Fine micropore structure. Foam separated from substrate.
Z-31	650	-	120	15	120	13	-	-	96	Air dried - 60 hr.	Surface cracks.
Z-32	-	600	120	15	125	14	-	ZnO 25 g	61	Air dried - 15 hr. RT to 150°F - 4 hr. Cemented to steel panel with alumina base cement.	Fine micropore structure. Foam well bonded to substrate.
Z-33	325	325	120	15	125	14	-	-	59	Cast onto steel panel with intermediate alumina base coating. Air dried - 15 hr.	Foam cracked on curing.
Z-34	325	325	120	15	125	14	13	-	71	Cast onto steel panel with double base coat. Air dried - 15 hr. Oven dried at 240°F - 1 hr.	Fine micropore structure. Slight bloating at foam surface. Foam and foam-substrate interface intact.
Z-35	325	325	120	15	125	16	13	-	64	Cast onto steel panel with double base coat. Dried by infrared lamps at 100°F - 15 hr. 100°F - 180°F - 1 1/2 hr. Cured at 300°F - 1 hr.	Fine micropore structure. Foam and foam-substrate interface intact. No cracks.
Z-36	-	325	120	16	125	18	13	Superpax 325 g	77	Air dried - 15 hr.	Vertical cracks in foam body.
Z-37	-	325	140	20	150	18	-	Superpax 325 g ZnO 20 g	62	Air dried - 15 hr.	Vertical cracks in foam body.
Z-38	-	-	160	24	130	18	-	Superpax 600 g ZnO 20 g	-	Air dried - 15 hr.	Vertical cracks in foam body.
Z-39	350	300	120	16	125	16	13	-	57	Air dried - 15 hr. Dried by infrared lamps, top only; 130°F - 6 hr. Cemented to steel panel.	Fine micropore structure. Foam well bonded to substrate but has horizontal cracks in foam body.
Z-40	650	-	120	15	100	14	-	SW 2336 2 cc	59	Air dried - 15 hr. Ht. top surface - 125°F - 6 hr.	Med. size pore structure. Foam substrate well bonded. Well formed foam.

Company, are not suitable for our process. Egg albumin is a far superior foaming agent and offers close control of the foam micropore structure.

Zircon foams cast directly onto steel panels (1/8 in. thick), although well bonded, were subject to minor cracks at the foam-substrate interface on drying. This was especially predominant in 1/2 in. thick zircon foams. This difficulty was overcome by applying an intermediate base coat of fine powdered alumina in PS-7 on the steel panel, prior to casting the foam. This thin base coat minimizes the stresses set up between the zircon and the steel panel due to a mismatch in their thermal expansions on drying and curing. The use of longer air-drying cycles and the addition of 2 wt% clay to the foam mix also proved beneficial. The clay addition aids the binder in the film forming and acts as a stabilizer, thereby preventing collapse of the foam structure during drying. Foam Z-27 and those following it in Table I, with a few exceptions, have a double base coat along with the clay addition.

Z-40 is a foam that was prepared by using albumin along with SW 2336 as the foaming agent. As mentioned earlier, foams prepared with SW 2336 have larger pores than those obtained with albumin. By combining these two foaming agents, it has been possible to obtain a foam with medium size pore structure. Figure 9 is a photomicrograph of Z-40, and it has an average pore size of 0.020 in. Figure 10 shows the micropore structure of a foam, Z-35 prepared with albumin alone which has a uniform pore size of 0.005 in.

3. Fiberfrax Additions

Zircon foams, 1/2 in. thick, have also been prepared and are shown in Table II. All these foams were directly cast onto steel panels with a base coat of Al₂O₃ in PS-7. Foam Z-41A contains 10 wt% ceric oxide as an additional constituent. This was added so as to alter the emittance characteristics of the

TABLE II

CHARACTERISTICS OF CHEMICALLY BONDED CASTABLE ZIRCON FOAMS
(1/2 IN. THICK) ON STEEL PANELS

Foam No.	Nominal Composition										Foam Density (lb/ft ³)	Comments
	Zircon (g)	Zircon A (g)	Suprapax (g)	Water (cc)	Albumin (g)	PS-7 (cc)	Na ₂ SiF ₆ (g)	Clay (g)	Fiberfrax (g)	Other Additives		
Z-35	325	325	-	120	15	125	16	13	-	-	60	Vertical cracks; good bonding to substrate.
Z-41A	293	292	-	120	15	125	16	13	-	Ceric oxide 65 g	52	Cracks in foam body; well bonded to substrate.
Z-41B	293	292	-	120	15	125	16	13	178" thick layer over panel	Ceric oxide 65 g	52	Cracks in foam; well bonded to substrate.
Z-42	325	325	-	140	15	65	9	13	-	-	58	Foam cracked.
Z-43	325	325	-	120	15	125	16	13	19.5	-	48	Very fine surface cracks; foam-substrate interface intact.
Z-44	400	250	-	140	12	125	16	13	19.5	-	84	Cast in 1/4" thickness; five vertical cracks; good bonding.
Z-45	400	250	-	130	13	130	18	13	19.5	-	64	Vertical cracks; well bonded.
Z-47	400	250	-	120	14	130	18	13	19.5 bulk	-	68	Foam 1/4" thick; uniform small pore structure (No. 004"n)
Z-48	80	80	-	40	5	45	5	4	-	TiO ₂ 40 g	37	Large cracks; poor pore size uniformity.
Z-49	80	80	-	40	5	45	5	4	-	ZnS 40 g	43	Cracks; debonded at edges; large pore size distribution (0.002-0-010)
Z-50	80	80	-	40	5	45	5	4	-	SiC 40 g	41	Cracks and lamination; nonuniform pore structure.
Z-51	80	80	-	40	5	45	5	4	-	TiO ₂ 40 g	51	Surface cracks; good bonding; uniform pore structure (0.004-0.006")
Z-52	110	-	-	40	5	45	5	4	-	ZrO ₂ 110 g	75	Surface cracks formed during final curving; excellent bonding to substrate.
Z-53	325	325	-	120	15	125	16	13	19.5 bulk	-	46	Vertical cracks; well bonded.
Z-54	80	80	-	45	5	45	5	4	-	SiC 50 g	41	Surface cracks; poor substrate bond.
Z-55	70	70	-	40	5	45	5	5	-	ZrO ₂ 70 g	49	Surface cracks; poor substrate bond.
Z-56	325	325	-	120	15	125	16	13	19.5	Gr. Zircon 19.5	65	Fine surface cracks; well formed foam, good bonding.
Z-57A	325	325	-	120	15	125	16	13	19.5 fine	-	37	Fine cracks on hard surface skin, poor dispersal of uncut fibers.
Z-57B	325	325	-	120	15	125	16	13	19.5 fine	-	32	Plastic wrap cover used during drying. No hard surface skin; free of cracks.

TABLE II (Cont'd)

Foam No.	Nominal Composition										Foam Density (lb/ft ³)	Comments
	Zircon (g)	Zircon A (g)	Suprapax (g)	Water (cc)	Albumin (g)	PS-7 (cc)	Na ₂ SiF ₆ (g)	Clay (g)	Fiberfrax (g)	Other Additives		
Z-58A	325	165	160	120	15	125	16	13	-	-	59	Hard surface skin. Vertical cracks. Well bonded foam.
Z-58B	325	165	160	120	15	125	16	13	-	-	58	Plastic wrap cover used; soft surface. Free of cracks. Well bonded form.
Z-59	325	165	160	120	15	152	16	13	-	ZnO 16.5 g	-	Plastic wrap cover used; poor foam.
Z-60	50	50	100	37	5	55	5	4	-	-	-	Plastic wrap cover used; large surface cracks. poor foam; discard.
Z-61	325	325	-	90	16	160	17	13	-	-	53	Plastic wrap cover used; faint vertical cracks.
Z-62	60	100	40	37	5	55	6	-	-	-	38	Plastic wrap cover used; foam stronger than Z-58 but more cracks.
Z-63	325	325	-	80	16	195	21.5	13	-	-	44	Plastic wrap cover used; very faint surface cracks.
Z-64	200	120	40	37	5	132	18.5	8	-	-	42	Foam without plastic wrap cover has faint surface cracks; without wrap, surface cracks.
Z-65	325	165	160	120	15	152	16.5	13	-	-	50	No plastic wrap cover; faint vertical cracks.
Z-66	200	100	100	74	9.3	94	-	8	-	MgO 4.7 g	48	Large cracks on surface.
Z-67	200	100	100	80	8	100	12.8	8	12	-	60	Foams prepared with and without wrap. Well bonded.
Z-68	325	325	-	80	15	195	25	13	26	-	42	No wrap; faint cracks and separation from substrate. Fine long stable Fiberfrax used.
Z-69	200	200	-	60	8	120	15.4	8	16	-	47	Plastic wrap covered; good foam.
Z-70	200	200	-	60	8	120	15.4	8	16 Fine	-	34	Wrap used; soft in center; fine long stable Fiberfrax used.
Z-71	325	325	-	98	9.8	215	27.5	13	26	-	53	Foam without wrap has slight cracks and separation. Foam with wrap, well bonded, no cracks.

foam. Z-41B has a similar composition but contains a 1/8 in. thick Fiberfrax layer (long staple) at the foam-substrate interface. The foam was prepared by spreading out the Fiberfrax on the base-coated steel panel and then casting the foam onto it. In both cases, these 1/2 in. thick foams developed minor cracks on drying. To minimize the internal stresses due to shrinkage in the foam during drying, three different approaches were investigated. First, the amount of liquid binder, PS-7, was decreased as shown in Z-42. This did not prove successful, for the foam still developed cracks. Next, as in Z-35-2, the steel panel was preheated to 100°F prior to casting the foam. The foam was heated at 100°F for 15 hr from the bottom only, and no cracks developed. Minor cracks did develop on heating to 240°F, but the foam was still bonded to the substrate. The third approach was to add 3 wt%, 1/8 in. long Fiberfrax fibers (medium diameter) to the original mix. This proved to be very successful as shown in Z-43. Figure II is a photomicrograph of this foam. Note the Fiberfrax fibers within the foam body. The foam had no cracks after drying and final curing at 250°F, and the foam-substrate interface was intact. The Fiberfrax fibers obtained from Carborundum Company are designated as No. 3750-2 (medium). In compositions Z-68 through Z-71, foams were prepared with 4 wt% Fiberfrax instead of 3 wt%. The amount of Fiberfrax was increased to 10 wt% in the optimized foams, such as in compositions Z-87 to Z-90.

4. Incorporation of Opacifying Additives

A series of zircon foams were prepared with additions designed to opacify the foam by means of scattering or absorption of the radiation. Titanium dioxide, with a high refractive index of 2.6, and zinc sulfide with an index of 2.4, were employed in compositions Z-51 and Z-49, respectively, for scattering purposes.

Silicon carbide is highly absorptive of radiation and does not exhibit the high thermal conductivity of metals or carbon, and was incorporated in compositions Z-50 and Z-54. These foams were structurally poor although Z-54 was adequate for testing.

Zirconium oxide additions were made to decrease the thermal conductivity of the foams and to improve whiteness. A pure zirconium oxide was added to Z-52 and a lime-stabilized zirconium oxide was incorporated in composition Z-55.

5. Use of Superpax A

Improved whiteness and thermal efficiency can be expected by use of a finer zircon powder. However, the use of a material such as TAM Superpax A, with average particle size of 4 microns, resulted in increased drying shrinkage and, consequently, cracking of castable foams. A means of utilizing the fine particle sized zircon powder was developed by controlling the moisture evaporation in the foam while the binder established a bond by reaction with sodium silicofluoride. This was accomplished by covering the foam after casting with a plastic wrapper. The effects of this procedure were described in a preceding section. The elimination of most of the shrinkage permitted use of Superpax A.

Other compositions were prepared, such as Z-62, with increased binder. These although less fragile than Z-58, developed more cracks due to strains generated by increased stiffness. Other changes were made in binder and Na_2SiF_6 content; the most promising results were obtained with composition Z-87, where the use of Superpax A was combined with 10 wt% Fiberfrax. The use of Fiberfrax permits us to increase the binder content without subsequent surface cracking.

6. Application of Coatings

Table III indicates the characteristics of layered composite foams based on the zircon Z-61 composition. Attenuation

TABLE III
CHARACTERISTICS OF LAYERED COMPOSITE FOAMS
BASED ON ZIRCON Z-61 COMPOSITION (1/2 IN. THICK)

Foam No.	Coatings on Zircon Foam	Basic Foam Density, lb/ft ³	Areal Density of Coatings, lb/ft ²	Composite Foam Density, lb/ft ³
Z-61A	SiC/Zircon	52	0.49	60
Z-61B	Ni/Zircon	53	0.48	62
Z-61C	TiO ₂	51	0.38	57
Z-61D	Zircon	53	0.24	58

of radiation transfer through the insulative foam can be realized by absorptive or reflective mechanisms. Incorporation of additives in the foam mix which opacify the foam is one approach of attenuating radiation. Unfortunately, the blending of additional materials into the zircon mix often affects the ability to foam and to obtain reproducibility in its density and microstructural characteristics.

On the other hand, the use of surface coatings for attenuation of radiation permits the use of a standardized foam composition, and can be applied to a set of essentially identical specimens.

Layered composite foams were prepared by applying a coating of the additive suspended in a potassium silicate binder brushed on the surface of a Z-61 foam bonded to a steel panel. The foam was preheated to 250 °F prior to application of the coating. A zircon coating was applied over the dark, additive coatings. The zircon coating had the following composition:

Zircon	500 g
Water	75 cc
PS-7	150 cc
Gum tragacanth	2.0 g

Z-61A is a layered composite foam consisting of a zircon foam (Z-61) with a surface layer of SiC, and an overcoat of zircon (of the composition mentioned above). A slurry was prepared of PS-7 pigmented with silicon carbide (Norton Crystolon B) to produce an absorptive layer.

For maximum opacification of the zircon foam a metallic nickel layer was investigated. A nickel metal powder was suspended in PS-7 with some water added and applied to the preheated Z-61 foam.

A rutile coating was also evaluated for maximum scattering by utilizing the high refractive index of TiO_2 . Attempts to brush on a very white, finely divided rutile powder with PS-7 binder were unsuccessful. A coarser, not as white, grade designated TAM Titanox TG was readily applied to the preheated foam specimen.

In all these cases the total thickness of the additive layer, along with the zircon overcoat, does not exceed 1/32 in. These are very thin layers. However, as discussed in the next section, they can significantly affect the insulative characteristics of the foam.

7. Optimization of Foam Compositions

On the basis of a large number of zircon foams prepared and subsequently evaluated for their insulative and mechanical characteristics (see Section IV), nearly optimized $\frac{1}{2}$ in. thick zircon foams were cast directly onto honeycomb structures. The nominal compositions and characteristics of these foams are shown in Table IV.

The optimized foams are based on a composition which contains Superpax A with no granular zircon (Z-87) and compositions which contain no Superpax with or without granular zircon (Z-88 to Z-90). These foams are approximately 55-60 lb/ft³ in density, and all contain 10 wt% Fiberfrax (medium diameter) based on the zircon powders with the exception of Z-90, which contains fine diameter Fiberfrax. Figure 12 is a photomicrograph of foam Z-90. In all cases it has been possible to prepare a foam specimen with either a hard surface skin, partial skin, or no surface skin. This is possible by controlling the time during curing when a plastic wrapping cover is used. The least skin effect is obtained when such a wrap is used for the longest time. The insulative and mechanical properties of these nearly optimized foams as a function of its surface properties have been discussed in subsequent sections.

TABLE IV

CHARACTERISTICS OF CHEMICALLY BONDED CASTABLE ZIRCON FOAMS
(1/2 IN. THICK) ON HONEYCOMB SUBSTRATES

Foam No.	Nominal Composition										Foam Density (lb/ft ³)	Comments
	Zircon (g)	Zircon A (g)	Superspax (g)	Water (cc)	Albumin (g)	PS-7 (cc)	Na ₂ SiF ₆ (g)	Clay (g)	Fiberfrax (g)	Other Additives		
Z-67	200	100	100	80	8	100	12.8	8	12	-	52	Specimens prepared with and without plastic wrap. Good foams.
Z-72	300	100	150	70	12	198	25.4	12	18	-	48	Plastic wrap covered, no skin, good bonding. Painted with nickel subcoat and zircon surface coat.
Z-73	200	200	-	74	4	80	10.3	8	28	Gr. Zircon 12 g	67	Plastic wrap only after 1 hr. drying. Good bonding.
Z-74	200	200	-	74	4	80	10.3	8	40	-	51	Plastic wrap only after 1/2 hr. drying. Very little skin formation.
Z-75	300	200	150	80	6	198	25.4	12	60	-	42	Plastic wrap only after 1/2 hr. drying. Partial skin formed. No cracks.
Z-77	200	150	150	90	6	198	25.4	12	60	Gr. Zircon 12 g	45	Plastic wrap not used; surface skin; faint cracks.
Z-77	200	100	100	70	2	132	16.9	8	40	Gr. Zircon 12 g	57	Skin type, faint vertical cracks.
Z-82	200	100	100	75	2	132	16.9	8	40	-	48	Plastic wrap after 1/2 hr. drying. Partial skin, no surface cracks.
Z-85	200	100	100	75	1.5	132	16.9	8	40	-	56	Plastic wrap after 1 hr. drying. Partial skin, very faint surface cracks.
Z-87	200	100	200	75	1.4	132	16.9	8	40	-	60	Several specimens prepared with and without plastic wrap cover. Good foam, well bonded.
Z-88	200	200	-	70	1.2	132	16.9	8	40	Gr. Zircon 12 g	57	Foam prepared with and without plastic wrap cover.
Z-89	200	200	-	60	1.2	132	16.9	8	40	-	52	Foam prepared with plastic wrap cover. No surface cracks. Well bonded.
Z-90	200	200	-	60	1.2	132	16.9	8	40 (+fine)	-	59	Foam prepared with partial use and without plastic wrap. No cracks, well bonded.

8. Discussion

The foams optimized for rigid heat shields are essentially castable zircon foams, chemically-bonded with potassium silicate and containing certain additives. In concept they may be considered as "composite" ceramic foams. A typical optimized foam contains the following nominal constituents: zircon, albumin, potassium silicate, clay, Na_2SiF_6 , and dispersed "Fiberfrax" fibers. Although the functional characteristics of the various additives are known, the exact reactions involved can at best be speculated upon.

The foaming action is obtained by mechanical whipping of the mix, using albumin as the foaming agent. The albumin, which is a surface-active-protein-based agent, stabilizes the entrained air structure.

The binder system is potassium silicate. The commercial potassium silicate binders usually range in composition from $\text{K}_2\text{O} \cdot 3.9\text{SiO}_2$ to $\text{K}_2\text{O} \cdot 3\text{SiO}_2$. On appropriate drying and curing, the binder is essentially in the form of a highly polymerized potassium silicate. Its adhesion properties are caused by the reactivity of the Si-O-K groups.

Now for the adhesive to perform its function it must undergo a large increase in viscosity and maintain its integrity in the form of a thin film across the interconnecting pores of the foamed material. The clay added to the mix acts as an extender and stabilizes the foamed body. It also aids in the retention of the solids in suspension. The clay maintains a suitable viscosity when added to silicate solutions. The addition of clay could also contribute to the integrity of the silicate viscous film across the pores by promoting the easy release of water and preventing the foaming or disruption of the binder film.

The beneficial effect observed on adding the Na_2SiF_6 along with the clay to the mix, was that it prevented the excessive migration of the binder on curing. The migration of the binder results in a weakened foam. We can speculate on the beneficial roles of the Na_2SiF_6 addition. The Na_2SiF_6 increases the rate of gellation, thereby preventing the excessive migration of the binder. It probably acts as a deflocculant further extending the clay. The deflocculation produces a homogeneous mass with less water, thus facilitating the drying with a minimum of cracks. The Na_2SiF_6 can also be considered as a "placement" material, i.e., it affects the placement of the silicate bonds thereby keeping the silicate uniformly distributed. The clay also adds a thixotropic quality which aids in the placement of the silicate binder.

Zinc oxide was also used to insolubilize the binder and prevent migration. However, the Na_2SiF_6 was preferred in the optimized foams. With a potassium silicate binder the ZnO may react to form some zinc silicate leaving an amorphous siliceous precipitate or a hard gel, depending upon the amount of water in the mix. However, no definite evidence exists that this is the primary reaction.

The use of chopped "Fiberfrax" fibers enhances the mechanical properties of the foam by reinforcing it. Not only is the structural integrity maintained during curing and drying, but also during subsequent vibrational testing. Additions of 3-10 wt% Fiberfrax permitted us to increase the binder content without surface cracking during the curing cycle.

Therefore, what is actually happening in the preparation of our chemically-bonded castable foam is that a thixotropic potassium silicate gel is foamed in the presence of a zircon mix which is aerated with the aid of albumin (foaming agent) and further stabilized and reinforced by adding clay (Ajax P), Na_2SiF_6 and Fiberfrax fibers.

C. Mullite Foams

Mullite powders from two different sources were used in preparing the foams listed in Table V.

The mullite powder used in preparing the foams M-3 to M-13 was -325 mesh, manufactured by H. R. Porter and Company. It contains small quantities of a silica phase.

Mullite foams M-20 to M-23 were prepared with a mullite powder obtained from the Norton Company and designated as "Mullite B, 325F." This mullite product has no silica phase, but a very slight excess of alumina, and is lighter in color than other mullite materials investigated.

All these foams were prepared by mechanical whipping. The nominal compositions of the starting materials are given for each of these foams. These results indicate that, for mullite foams, the albumin is the preferred foaming agent, as it forms foams with a fine uniform micropore structure. All these foams, with the exception of M-8 and M-11, are castable. Foam M-8, which is a mullite foam without a binder, was fired at a high temperature (2330°F). The other foams have only been oven dried and not yet cured at higher temperatures. However, they indicated good bonding in spite of not being cured at high temperature. Foam M-22 was obtained with a minimum of fine surface cracks but was well bonded to the substrate. Further optimization is required to obtain crack-free mullite foam structures. This has been accomplished to a degree with composition M-23, which was covered with plastic wrap while drying.

D. Calcium Aluminate Foams

Preliminary work has been carried out on calcium aluminate foams. The starting material was calcium aluminate cement manufactured by Alcoa Chemicals. Alcoa calcium aluminate designated as "CA-25" is a high-purity, hydraulically setting refractory cement, and is composed of about 79% alumina, 18%

IIT RESEARCH INSTITUTE

TABLE V
CHARACTERISTICS OF MULLITE FOAMS (1/2 IN. THICK) PREPARED BY MECHANICAL WHIPPING

Foam No.	Nominal Composition										Foam Density (lb/ft ³)	Comments
	Mullite (g)	Water (cc)	PS-7 (cc)	Sw 2366 (cc)	Albumin (g)	Clay (g)	Other Additives					
M-3	200	30	60	20	-	-	Methanol HG 6g				-	Foam collapsed.
M-4	200	70	60	20	-	-	Baymal 20 g				-	Baymal incompatible with PS-7 binder; did not go into suspension.
M-6	200	35	75	20	-	60	Na ₂ SiF ₆ 20 cc				45	Large pores. Little shrinkage on drying.
M-7	200	46	75	-	10	60	-				50	Fine pore structure. Good strength and uniformity.
M-8	200	130	-	-	10	60	-				62	Fired to 2330°F. Strong foam body.
M-9	200	70	75	-	25	60	-				37	Very slow air drying needed to prevent rupture.
M-10	200	50	75	10	12	60	-				35	Medium size pores (between M-6 and M-7).
M-11	200	45	-	-	-	60	Gelatin 60 g				-	Fine pores, but larger than those obtained with Albumin.
M-13	95	75	-	-	25	60	-				25	Foam cast on aluminum plate. Well bonded to metal substrate.
M-20	150	70	70	-	6	50	-				37	Excessive shrinkage.
M-21	200	50	45	-	5	5	-				61	Large cracks, some debonding.
M-22	200	60	47	-	6	5	-				44	Fine cracks, well bonded.
M-23	200	60	50	-	6	4	Na ₂ SiF ₆ 4.5 g				37	Plastic wrap cover used during drying. Faint surface cracks. Foam well bonded.

NOTE: Foams M-3 through M-13 were prepared with mullite powder supplied by H. F. Porter and Co. and contains excess silica. Foams M-20 through M-23 were prepared with mullite powder supplied by Norton and Co. and contains slight excess alumina.

lime, and not more than 2% impurities. This composition conforms to the empirical molar formula $2\text{CaO} \cdot 5\text{Al}_2\text{O}_3$.

Table VI shows the compositions and densities of the calcium aluminate foams prepared by mechanical whipping. Although further optimization is required, this low thermal expansion material has shown considerable promise on preliminary investigation. Foam specimens were also tested by immersing them in boiling water for 3 hr and showed very little deterioration.

In the case of the calcium aluminate foam, an undercoat of calcium aluminate cement in 30 wt% water was found to give better adhesion to the steel substrates than the previously used aluminum oxide bonded with PS-7.

Composition CA-5 was prepared in two specimens, one cast on a steel plate and cured and the other fired to 2900°F. CA-6 and CA-7 were cast on bare panels. Due to the weakness of bonding to the steel panels of cast foams, no further work was conducted with cast calcium aluminate compositions. Composition CA-8 showed a density of approximately 60 lb/ft³ when this foam was fired to a temperature of 2900°F. This sample was cemented onto a steel panel with the silicate-bonded Al_2O_3 base coat.

IV. EFFECTS OF HEAT FLUX WITH SIMULTANEOUS VIBRATION AND ACCELERATION ON CERAMIC FOAMS

A. Screening Program

1. Introduction

A screening program was carried out to evaluate the effects of a specific heat flux along with simultaneous vibration and acceleration on the foams. This included subjecting all candidate materials to a radiant heat flux of 24 Btu/ft²-sec and simultaneous vibrations of 30 cps with a double amplitude displacement of $\frac{1}{2}$ in. and an acceleration level

TABLE VI

CHARACTERISTICS OF CALCIUM ALUMINATE CEMENT FOAMS (1/2 IN. THICK)
PREPARED BY MECHANICAL WHIPPING ON STEEL PANELS

Foam No.	Nominal Composition					Foam Density (lb/ft ³)	Comments
	Ca ₁ . Alum. (g)	Al ₂ O ₃ (g)	Water (cc)	Alumin (g)	Clay (g)		
CA-1	300	-	100	9	-	60	Crack free foam.
CA-2	400	-	130	13	8	67	Fine cracks, poor bond.
CA-3	300	-	110	10	6	60	Fine pore structure; pore size 0.002-0.005". Crack free, some debonding.
CA-4	300	-	110	10.5	7	55	Double base coat of CA + 30 WT % H ₂ O applied to substrate. Foam intact, well bonded.
CA-5	500	125	210	21.3	-	72	Density as cured. On firing to 2900°F density 82 lb/ft ³ .
CA-6	400	100	195	20	20	42	Faint vertical cracks, foam intact.
CA-7	550	-	225	22	27.5	45	Faint vertical cracks, foam intact.
CA-8	500	125	245	25	-	53	Fine pores, 0.002-0.004". No cracks.

of 11 g's. The objective of this screening program was to determine the ability of the prepared foams to withstand a back face surface temperature not exceeding 400°F after 150 sec exposure to the above test conditions.

2. Test Equipment

The chemically bonded foam on a stainless steel substrate with dimensions 6 x 3 x 1/8 in. was bolted to a rigid frame, which in turn was directly bolted onto the vibration pad. A set of five thermocouples was welded onto the top face of the stainless steel substrate plate, and the back face surface temperature at the foam-substrate interface monitored during the test. The entire fixture with the foam is shown in Figure 13.

A radiant heating facility was used to provide the radiant heat fluxes called for in the screening as well as the final tests. The heating equipment consists of a water-cooled aluminum reflector (Research, Inc. No. WC14-12) equipped with air-cooled ceramic lamp holders (Hi Shear Lux-Therm Dual Lamp Holders No. LT 1200). Six 3600-watt quartz lamps (General Electric No. 3600/T3/ICL/HT) with a lighted length of 10 in. are located on ½ in. centers to provide a lighted area of 10 x 3 in. The power supplied to the lamps is regulated by a 220 volt, 100 ampere powerstat.

Test sample temperatures are monitored on a 12-channel Brown Recorder. The magnitude of the incident heat flux is measured by a slug calorimeter whose millivolt output is recorded on a Leeds and Northrup Type G Continuous Recorder.

The present equipment is capable of providing an incident heat flux to the sample in excess of 40 Btu/ft²-sec while operating the lamps slightly below rated voltage. A survey of the incident heat flux over the surface of the test specimen indicates negligible variation.

The vibration facility includes a fully integrated random vibration system, consisting of 6 kva electronic driver console and an MB C10E 1200-lb sinusoidal vector, 2550-lb peak random force electromagnetic exciter. The frequency spectrum can be manually shaped as desired or to compensate for mechanical resonances. A frequency spectrum display is provided for visually monitoring the response spectrum of the exciter at all times. Frequency response of the driver system is 5 to 2000 cps, 70 g acceleration or 1 in. total excursion. A second unit capable of 90 g acceleration with $\frac{1}{2}$ in. peak-to-peak displacement is also available and was used later in the optimization testing program.

3. Experimental Results

Results on the effects of simultaneous vibration and acceleration with a heat flux of 24 Btu/ft²-sec on zircon, mullite, and calcium aluminate foams 1 in. and $\frac{1}{2}$ in. thick have been obtained, and are shown in Tables VII and VIII.

These results indicate that zircon foams 1 in. and $\frac{1}{2}$ in. thick have been prepared that can successfully withstand a heat flux of 24 Btu/ft²-sec and simultaneous vibrations of 30 cps with double amplitude displacement of $\frac{1}{4}$ in. and an acceleration level of 11 g's without mechanical failure for as long as 5 min. All the 1 in. thick zircon foams listed in Table VII with the exception of Z-24 were intact at the end of the tests. The maximum back face temperature reached for the 1 in. thick foams was 238°F after 300 sec test exposure. This was for Z-40, which had a density of 39 lb/ft³. Z-39, which was $\frac{3}{4}$ in. thick and has a density of 57 lb/ft³, showed maximum back face temperature of 334°F after 300 sec exposure.

Table VIII summarizes the results obtained with $\frac{1}{2}$ in. thick zircon foams. Foams Z-35-2, Z-41A, and Z-41B were subjected to a heat flux of 24 Btu/ft²-sec without any simultaneous

TABLE VII
SCREENING TEST RESULTS ON ZIRCON-BASED FOAMS,
1 IN. THICK

Foam No.	Foam Density, lb/ft ³	t, (a) sec	Avg. T _s , (b) °F	Comments
Z-24	60	60	107	Failure due to fracture at foam-substrate interface.
Z-32	61	60 120 150 180 240	109 159 173 189 230	Foam and foam-substrate interface were absolutely intact at end of 4 min. Minor hairline cracks on foam surface.
Z-34	70	60 120 150 180	92 122 133 145	Test discontinued at the end of 3 min due to electrical failure. Foam and foam-substrate interface intact at the end of 3 min.
Z-35	64	60 120 150 180 240 300	100 135 155 170 207 235	Foam and foam-substrate interface intact. Minor cracks developed in foam.
Z-39 (3/4 in. thick)	57	60 120 150 180 240 300	120 171 195 215 287 334	Foam and foam-substrate interface intact.

TABLE VII (Cont'd)

Foam No.	Foam Density, lb/ft ³	t, (a) sec	Avg. T _s , (b) °F	Comments
Z-40	39	60	100	Foam and foam-substrate interface were absolutely intact at the end of 5 min.
		120	135	
		150	147	
		180	165	
		240	185	
		300	238	

The screening tests were carried out at a heat flux of Btu/ft²-sec and simultaneous vibrations of 30 cps with a double amplitude displacement of ¼ in. and an acceleration level of 11g's.

(a) t is the time duration to which the foam was exposed to the above test conditions.

(b) T_s is the back face surface temperature at the end of time t.

TABLE VIII
SCREENING TEST RESULTS ON ZIRCON-BASED FOAMS,
1/2 IN. THICK

Foam No.	Foam Density, lb/ft ³	t, (a) sec	Avg. T _s , (b) °F	Comments
Z-35-2	64	60	120	Foam was subjected to heat flux but no simultaneous vibration and acceleration. Test indicates that composition Z-35 is insulative after 5 min exposure to maintain T _s 500°F.
		120	190	
		150	220	
		180	270	
		240	350	
		300	410	
Z-41A	52	60	130	Foam was subjected to heat flux but no simultaneous vibration and acceleration. Foam contained 10 wt% ceric oxide. Test indicates that composition Z-41A is more thermally insulative than Z-35.
		120	190	
		150	218	
		180	270	
		240	335	
Z-41B	52	60	145	Foam was subjected to heat flux of 24 Btu/ft ² -sec but no simultaneous vibration and acceleration. Foam contained 10 wt% ceric oxide and 1/8 in. thick layer of Fiberfrax at foam-substrate interface.
		120	213	
		150	243	
		180	260	
		240	368	
Z-43-1	36	60	130	Foam subjected to heat flux and simultaneous vibration and acceleration. Foam contained 3 wt% chopped Fiberfrax in mix. Foam and foam-substrate interface intact during 4 min test. Cracks developed in foam on cooling but foam still intact.
		120	195	
		150	210	
		180	265	
		240	335	

TABLE VIII (Cont'd)

Foam No.	Foam Density lb/ft ³	t, (a) sec	Avg. T _s , (b) °F	Comments
Z-43-2	36	60	135	Foam subjected to heat flux and simultaneous vibration and acceleration. Foam identical in composition to Z-43(1) but top surface of binder migrated layer was removed. Foam and foam-substrate interface intact at end of test.
		120	216	
		150	250	
		180	275	
		240	351	
Z-43-3 (3/8 in. thick)	36	60	145	Foam subjected to heat flux and simultaneous vibration and acceleration. Foam identical in composition to Z-43(1) but 3/8 in. thick. Foam and foam-substrate interface intact during test but cracked on cooling.
		120	230	
		150	284	
		180	310	
		240	407	
		300	458	

The screening tests were carried out at a heat flux of 24 Btu/ft²-sec and simultaneous vibration where indicated of 30 cps with a double amplitude displacement of 1/4 in. and an acceleration level of 11 g's.

(a) t is the time duration to which the foam was exposed to the above test conditions.

(b) T_s is the back face surface temperature at the end of time t.

vibration and acceleration as they had minor cracks close to the foam-substrate interface on drying. The results obtained, nevertheless, indicate the effects of foam composition and density on the insulation characteristics. The addition of ceric oxide to zircon foams did improve the insulation characteristics slightly. It enables us to use a lighter density foam as indicated by Z-41A. The presence of Fiberfrax at the interface as shown in Z-41B did not prove to be significant.

The addition of 3 wt% of chopped Fiberfrax in the foam body proved to be advantageous as shown by zircon foams of composition Z-43. This is a lightweight foam of density 36 lb/ft³ which has good insulative characteristics. It showed a maximum back face temperature of 335°F at the end of the 250 sec of test exposure, and was mechanically stable to the vibration and acceleration. The back face temperature of this foam increases from 335°F to 407°F after 240 sec exposure, when the foam thickness is reduced from 1/2 in to 3/8 in.

The back face temperatures shown in Tables VII and VIII were measured at the bottom of the 1/8 in. stainless steel panel substrate. To obtain a more accurate measure of the insulative characteristics of these foams it was decided to weld the five thermocouples onto the top face of the stainless steel panel. This was done prior to applying the base-coat and casting the foam.

Table IX summarizes the results obtained on additional zircon, mullite, and calcium aluminate foams. In all cases, with the exception of foam Z-44, the average back surface temperature was measured at the foam-substrate interface and not at the bottom of the steel substrate, as was measured previously. The T_g measured at the interface is, of course, a more exact indication of the insulating characteristics of the foam.

TABLE IX
SCREENING TEST RESULTS ON FOAMS ON STEEL PANELS

Foam No.	Foam Density lb/ft ³	Foam Thickness in.	Vibration Applied	t, sec (a)	Avg T _s , °F (b)	Comments
Z-43-2	48	½	No	60 120 150 180 240 300	130 247 289 340 425 493	Slight enlarging of the fine cracks at surface. Foam body and interfacial bond intact.
Z-44	80	¼	Yes	60 120 150 180	185 360 440 505	Foam and interface absolutely intact.
Z-45	64	½	Yes	60 120 150 180 240	105 230 265 310 415	Foam body and interfacial bond intact.
Z-45	64	3/16	Yes	60 120	270 500	Foam body and interfacial bond intact.

IIT RESEARCH INSTITUTE

TABLE IX (Cont'd)

Foam No.	Foam Density lb/ft ³	Foam Thickness in.	Vibration Applied	t, sec (a)	Avg T _s , °F (b)	Comments
Z-47	68	¼	Yes	60 120 150	240 510 580	Foam body and interfacial bond intact.
Z-47	68	¼	No	60 90	580 840- 1000	Foam cast on 10 mil steel foil. Severe warpage on heating. Terminated at 90 sec.
Z-49	43	½	No	60 120 150 180 240 300	130 258 306 380 479 552	Enlargement of surface cracks. Some loss of bonding on edges.
Z-51	51	½	No	60 120 150 180 240 300	120 227 274 330 425 505	Enlargement of surface cracks; interfacial bond intact.
Z-52	75	½	No	60 120	115 202	Foam body and interfacial bond intact.

IIT RESEARCH INSTITUTE

TABLE IX (cont'd)

Foam No.	Foam Density lb/ft ³	Foam Thickness in.	Vibration Applied	(a)		Avg T _s , (b) °F	Comments
				t, sec			
Z-52	75	½	No	150		236	
				180		280	
				240		380	
				300		445	
				360		539	
Z-53	46	½	No	60		135	Enlargement of cracks. Some debonding on edges.
				120		245	
				150		307	
				180		350	
				240		450	
Z-54	41	½	No	60		115	Poor bonding with panel. Practically broken from base.
				120		210	
				150		257	
				180		310	
				240		400	
Z-55	49	½	No	60		105	Foam laminated through entire middle section.
				120		190	
				150		230	
				180		280	
				240		360	
300		420					

IIT RESEARCH INSTITUTE

TABLE IX (Cont'd)

Foam No.	Foam Density lb/ft ³	Foam Thickness in.	Vibration Applied	t, (a) sec	Avg T _s , °F (b)	Comments
Z-35-4	55	½	No	60	115	Enlargement of surface cracks. Interfacial bond intact.
				120	220	
				150	262	
				180	300	
				240	406	
300	470					
Z-35-5	62	½	No	60	115	Fine cracks developed in top zircon coating. Interfacial bond intact.
				120	230	
				150	254	
				180	285	
				240	360	
300	460					
Z-35-6	69	11/16	No	60	95	No cracks. A slight separation from panel.
				120	150	
				150	178	
				180	200	
				240	300	
300	365					
M-21	64	½	Yes	60	110	Enlargement of cracks.
				120	230	

IIT RESEARCH INSTITUTE

TABLE IX (Cont'd)

Foam No.	Foam Density lb/ft ³	Foam Thickness in.	Vibration Applied	t, sec	(a)	Avg T _s , °F	(b)	Comments
M-21	64	½	Yes	150 180 240 300		300 350 475 580		
M-22	46	½	Yes	60 120 150 180 250 270 300		110 200 285 320 430 460 490		Interfacial bond intact. Little further crack enlargement.
CA-1	52	9/16	Yes	60 120 150 180 240 255		100 160 190 217 240 Failure		Cemented to steel panel with potassium silicate bonded aluminum oxide adhesive. Top 1/8 in. layer of foam lost integrity and was partially removed by vibration. Adhesive failed at 255 sec.
CA-3	60	½	No	60 120		115 160		Interfacial gap increased due to heating. Foam became

IIT RESEARCH INSTITUTE

TABLE IX (Cont'd)

Foam No.	Foam Density lb/ft ³	Foam Thickness in.	Vibration Applied	t, sec (a)	Avg T _s , °F (b)	Comments
CA-3				150 180 240 300	201 215 280 360	very friable on handling.
CA-4	55	½	No	60 120 150 180 240 300	100 148 182 200 280 335	Foam became very friable on handling.

The screening tests were carried out at a heat flux of 24 Btu/ft²-sec and simultaneous vibration of 30 cps with a double amplitude displacement of ¼ in. and an acceleration level of 11 g's. Specimens not vibrated are so indicated.

- (a) t is the time duration to which the foam was exposed to the above test conditions.
- (b) T_s is the average surface temperature measured at the foam-substrate interface at the time t. Z-44 was the only specimen where the thermocouples were mounted on the back of the panel.

The results of screening tests summarized in Figure 14 can be correlated on the basis of density in the case of zircon and mullite foams. The $\frac{1}{2}$ in. thick foams with density less than 50 lb/ft³ are observed to develop an interface temperature (at the base of the foam) of approximately 300°F at 150 sec, and slightly over 500°F at 300 sec. Those foams in the density range of 50 to 65 lb/ft³ reach approximately 260°F at 150 sec and average approximately 470°F at 300 sec. A zircon foam with zirconia addition of 75 lb/ft³ density (Z-52) exhibited a temperature of 236°F at 150 sec and only 441°F at 300 sec.

The effects of additives were somewhat masked by this significant density correlation. The use of ZnS in Z-49 and TiO₂ in Z-51, did not appear to influence thermal performance. The effect of ZrO₂, as a low conductivity addition, in composition Z-52 may have been beneficial, although the high density of this specimen also tended to attenuate heat transfer. Another composition with ZrO₂ addition was prepared in lighter density, Z-55, with good results and displayed a temperature of 230°F at 150 sec. The low temperature displayed by Z-54, which contained a silicon carbide additive, may have been due to the very poor bonding at the substrate. A good quality foam was not obtained with this addition.

The calcium aluminate foams displayed lower interface temperatures than those of zircon or mullite. The foam of composition CA-3, density of 60 lb/ft³, attained only 201°F after 150 sec, 359°F after 300 sec. A deterioration of the structure was observed, probably due to dehydration. Testing at more severe vibration and acceleration levels is required to determine whether this loss of integrity proscribes its use in the as-cast state.

However, prior to the final testing some of the prepared foams were exposed to the final heat flux of 40 Btu/ft²-sec, but at an intermediate vibration and acceleration of 30 cps,

$\frac{1}{2}$ in. double amplitude displacement and 20 g's acceleration. These tests were carried out on $\frac{1}{2}$ in. thick foams cast onto stainless steel panels. In all cases, the average back face temperature was measured at the foam-substrate interface. Table X shows the results obtained on zircon and mullite foams.

The results are summarized in Figure 15. In this figure the back face temperature (T_s) of various castable foams of $\frac{1}{2}$ in. thickness on steel panels are shown after exposure to 150 sec of test conditions. The relationship of density and T_s is evident at 40 Btu/ft²-sec as observed in the screening tests at a lower heat flux of 24 Btu/ft²-sec for compositions without coatings. The back face temperature, T_s , ranges from 330°F for zircon and mullite foams of 37 lb/ft³ density to 250°F for a zircon foam of density 58 lb/ft³.

Compositions Z-58 and Z-65 contained Superpax A, a fine-grained zircon powder. Both foams were covered with a plastic wrapper during drying to eliminate surface cracks and displayed a lower T_s than Z-58A, dried without wrapping. Although Z-65 is only of 50 lb/ft³ density, it displayed a T_s of only 241°F after 150 sec, perhaps indicating that the Superpax addition opacifies the material in a manner similar to increasing density.

Composite foams of a zircon-based composition with subsurface layers of SiC and Ni are very effective in attenuating radiation. A zircon foam with a subsurface layer of nickel paste with a zircon paint overcoat (foam Z-61B) gave the lowest back face temperature, 220°F, when exposed to 40 Btu/ft²-sec.

B. Final Test Program

In the final test program the effects of 40 Btu/ft²-sec heat flux (primarily radiant) with a simultaneous vibration of 60 cps, a double amplitude displacement of $\frac{1}{2}$ in., and an

TABLE X
TEST* RESULTS ON FOAMS (1/2 IN. THICK)
ON STEEL PANEL SUBSTRATES
AT HEAT FLUX OF 40 Btu/ft²-sec

Foam No.	Foam Density, lb/ft ³	Vibration Applied	t, (a) sec	Avg. T _s , (b) °F	Comments
Z-57A	37	Yes	60	140	Foam and interface absolutely intact.
			120	300	
			150	330	
			180	400	
			240	515	
Z-57B	32	Yes	30	110	Test discontinued after 65 sec, due to collapse of protective screen. Foam intact.
			60	150	
Z-58A	59	Yes	60	115	Cracks on surface prominent. Interfacial bonding to steel substrate intact.
			120	235	
			150	280	
			180	340	
			240	440	
Z-58B	58	Yes	60	120	No prominent cracks on surface. Foam and interface absolutely intact.
			120	220	
			150	250	
			180	290	
			240	390	
M-23	37	Yes	60	131	Foam and interfacial bond with interface intact.
			120	280	
			150	335	
			180	385	
Z-35-7	55	No	60	133	Foam and interfacial bond with substrate intact.
			120	258	
			150	305	
			180	350	
			240	460	
Z-61A	60	No	60	130	Layered composite foam and interfacial bond with substrate intact.
			120	200	
			150	235	

IIT RESEARCH INSTITUTE

TABLE X (Cont'd)

Foam No.	Foam Density, lb/ft ³	Vibration Applied	t, (a) sec	Avg. T _s , (b) °F	Comments
Z-61B	62	No	60	125	Layered composite foam and interfacial bond with substrate intact.
			120	195	
			150	222	
			180	250	
Z-61C	57	No	60	120	Titania surface layer decolorized. Spalled on heating. Substrate bond intact.
			120	205	
			150	237	
			180	280	
Z-61D	58	No	60	125	Layered composite foam and interfacial bond with substrate intact.
			120	230	
			150	268	
			180	310	
Z-65	50	No	60	100	Surface cracks enlarged. Test halted because of lamp guard failure.
			120	185	
			150	241	
			180	290	

The tests were carried out at a heat flux of 40 Btu/ft²-sec and simultaneous vibration of 30 cps with a peak-to-peak displacement of ½ in. and an acceleration level of 20 g's. Specimens not vibrated are so indicated.

(a) t is the time duration to which the foam was exposed to the above test conditions.

(b) T_s is the average surface temperature measured at the foam-substrate interface at the time t.

acceleration level of 90 g's were evaluated on the nearly optimized castable, composite zircon foams.

The test evaluations were carried out for $\frac{1}{2}$ in. thick foams cast on a $\frac{1}{2}$ in. thick honeycomb substrate of areal dimensions 3 x 6 in., with open face metal reinforcements of the design developed for the Saturn-V heat shield. This honeycomb-sandwich construction consists of 10 mil-thick face sheets and a 1 in. thick honeycomb core having $\frac{1}{4}$ in. square cell openings and a wall thickness of 2 mils. The components were fabricated from a high-strength stainless steel and joined with a silver-brazing alloy. A 190 mil thick honeycomb reinforcement core, having $\frac{1}{2}$ in. square cell openings and a wall thickness of 2 mils, is brazed to one face of the basic honeycomb structure. About 45 mils of the upper portion of the core walls were crimped over by crushing or bending using a hydraulic press. The foam is cast on this core panel. A set of thermocouples were placed at the foam substrate interface and at the bottom of the honeycomb to monitor the interface (T_i) and back-face temperature (T_b) during testing.

The results of the final testing are shown in Table XI. The back-face and interface temperatures of some of the optimized foams after $2\frac{1}{2}$ and 5 min exposure to the final test conditions have been indicated in Table XII.

These results indicate that castable-type, chemically bonded zircon foams have been developed with densities not exceeding 60 lb/ft³, which in $\frac{1}{2}$ in. thicknesses have the ability to limit the back face temperature (T_b) of the specimen to far less than the 400°F requirement, after $2\frac{1}{2}$ min exposure to the final test conditions. In fact, these optimized foams, $\frac{1}{2}$ in. thick, are capable of limiting the back face temperature to no more than 400°F even after 5 min exposure to the final heat flux and vibrational conditions.

TABLE XI
FINAL TEST RESULTS ON ZIRCON FOAMS (1/2 IN. THICK)
ON 1 IN. THICK HONEYCOMB SUBSTRATES

Foam No.	Foam Type (a)	Foam Density lb/ft ³	Test Cycle No.	t, sec	Temperatures, °F		Comments
					T _b	T _i	
Z-67	NS	52	1	60	100	110	Foam interface intact. Very faint cracks developed on cooling.
					168	225	
					190	310	
					235	400	
Z-67	S	52	1	60	122	142	Vertical cracks. (Uncrimped open face honeycomb substrate.)
					215	345	
					260	455	
					308	555	
					392	665	
Z-73	PS	67	1	60	88	88	No cracks.
					130	230	
					175	318	
					215	400	
			2	60	125	105	First recycle. Sample remained intact, with hairline cracks.
					157	250	
					185	340	
					218	420	
					290	545	

IIT RESEARCH INSTITUTE

TABLE XI (Cont'd)

Foam No.	Foam Type (a)	Foam Density lb/ft ³	Test Cycle No.	t, sec	Temperatures, °F		Comments
					T _b	T _i	
Z-73 (Cont'd)	PS	67	3	60	98	98	Second rerun. Jigsaw type vertical cracks, but specimens intact
				120	140	225	
				150	168	305	
				180	193	387	
				240	250	510	
				300	300	600	
Z-75	PS	42	1	60	110	No cracks after testing: specimen intact.	
				120	155		
				150	180		
				180	210		
				240	270		
				330	340		685
Z-79	S	57	1	60	125	Faint vertical cracks on surface.	
				120	200		175
				150	250		400
				180	290		510
				240	375		605
				300	420		710
Z-79 (1/4 in. thick)	S	57	1	60	190	Faint vertical cracks.	
				120	450		550
				150	530		920

IIT RESEARCH INSTITUTE

TABLE XI (Cont'd)

Foam No.	Foam Type (a)	Foam Density lb/ft ³	Test Cycle No.	t, sec	Temperatures, °F		Comments					
					T _b	T _i						
Z-79 (1 in. thick)	S	57	1	60	90	90	Completely intact.					
				120	120	120						
				150	140	145						
				180	150	165						
				240	168	192						
				300	175	210						
Z-83	PS	49	1	60	120	120	No cracks appeared after 5 min testing.					
				120	160	198						
				150	175	260						
				180	193	328						
				240	228	445						
				300	270	535						
				2					60	130	105	No vibration and acceleration during this cycle. Very faint hairline cracks developed on surface of foam.
									120	175	188	
									150	200	260	
									180	230	330	
240	300	465										
300	358	570										
3				60	120	100	Some cracks developed on surface of foam. Foam and interface bond absolutely intact.					
				120	155	208						
				150	180	275						
				180	200	340						
				240	243	450						
				300	280	535						

IIT RESEARCH INSTITUTE

TABLE XI (Cont'd)

Foam No.	Foam Type (a)	Foam Density lb/ft ³	Test Cycle No.	t, sec	Temperatures, °F		Comments
					T _b	T _i	
Z-85 (9/16- 5/8 in. thick)	PS	56	1	60	120	122	Very faint hairline cracks slightly enlarged on testing.
				120	160	205	
				150	180	270	
				180	208	330	
				240	265	448	
300	310	550					
Z-86	S	66	1	60	130	148	Faint cracks at surface.
				120	190	335	
				150	225	435	
				180	260	525	
				240	330	675	
300	385	770					
Z-87	S	60	1	60	125	140	Some vertical cracks.
				120	195	320	
				150	225	415	
				180	280	520	
				240	358	668	
300	395	750					
Z-87	PS	60	1	60	120	120	No cracks after 5 min testing.
				120	170	240	
				150	200	310	
				180	225	390	
				240	270	500	
300	315	590					

IIT RESEARCH INSTITUTE

TABLE XI (Cont'd)

Foam No.	Foam Type (a)	Foam Density lb/ft ³	Test Cycle No.	t, sec	Temperatures, °F		Comments
					T _b	T _i	
Z-87	NS	60	1	60	120	105	No cracks after 5 min testing.
					155	180	
					175	235	
					198	290	
					235	390	
					280	470	
Z-88	S	57	1	60	140	100	Faint hairline cracks developed.
					180	190	
					205	243	
					225	300	
					260	400	
					298	468	
Z-88	NS	57	1	60	115	150	Faint cracks
					170	300	
					205	390	
					240	475	
					305	615	
					355	715	
Z-88	NS	57	1	60	115	130	No cracks after 5 min testing.
					170	230	
					195	295	
					220	375	
					275	505	
					320	595	

IIT RESEARCH INSTITUTE

TABLE XI (Cont'd)

Foam No.	Foam Type (a)	Foam Density lb/ft ³	Test Cycle No.	t, sec	Temperatures, °F		Comments
					T _b	T _i	
Z-88 (Cont'd)	NS	57	2	60	115	138	Foam intact
				120	180	190	
				150	215	248	
				180	240	310	
				240	300	430	
300	345	520					
Z-89	NS	52	1	60	138	120	Foam intact
				120	190	215	
				150	220	300	
				180	253	375	
				240	310	515	
300	350	610					
Z-90	S	59	1	60	145	115	Foam intact after recycling test.
				120	190	215	
				150	225	300	
				180	253	375	
				240	310	515	
300	358	610					
360	385	685					
Z-90	S	59	1	60	120	150	Faint hairline cracks on heating.
				120	185	313	
				150	225	405	
				180	265	498	
				240	340	650	
300	385	730					

IIT RESEARCH INSTITUTE

TABLE XI (Cont'd)

Foam No.	Foam Type (a)	Density lb/ft ³	Test Cycle No.	t, sec	Temperatures, °F		Comments
					T _b	T _i	
Z-90	PS	59	1	60	90	100	Foam intact. No surface cracks. However, foam broke on recycling in less than 1 min.
					180	215	
					200	285	
					230	355	
					290	470	
					330	560	
Z-90	NS	59	1	60	125	125	Foam intact. No surface cracks. However, foam broke on recycling in less than 1 min.
					163	220	
					200	300	
					230	370	
					295	485	
					345	585	
Z-90 (Foam was soaked in water for 97 hr prior to testing)	PS	59	1	60	85	85	Foam intact.
					163	200	
					185	218	
					190	220	
					200	220	
					200	220	

IIT RESEARCH INSTITUTE

TABLE XI (Cont'd)

Foam No.	Foam Type (a)	Foam Density lb/ft ³	Test Cycle No.	t, sec	Temperatures, °F		Comments
					T _b	T _i	
Z-90 (Cont'd)	PS	59	2	60	100	120	Foam intact
				120	160	185	
				150	185	235	
				180	215	298	
				240	270	430	
			300	320	540		

The tests were carried out at a heat flux of 40 Btu/ft²-sec and simultaneous vibration of 60 cps with a double amplitude displacement of ½ in. and an acceleration level of 90 g's.

(a) The type denotes the foam surface: S indicates that foam has a hard surface skin, PS a partial skin, and NS no hard surface skin.

TABLE XII

BACK FACE TEMPERATURES OF SOME NEARLY OPTIMIZED
ZIRCON FOAMS ($\frac{1}{2}$ IN. THICK)
ON 1 IN. HONEYCOMB SUBSTRATES ON FINAL TESTING

Foam No.	Foam Type	Foam Density lb/ft ³	Back Face Temperatures °F			
			2½ min exposure		5 min exposure	
			T _b	T _i	T _b	T _i
Z-79	S	57	250	510	420	800
Z-87	S	60	225	415	395	750
	PS NS	60 60	200 175	310 235	315 280	590 470
Z-88	S	57	205	390	355	715
	NS	57	195	295	320	595
Z-89	NS	52	220	300	350	610
Z-90	S	59	225	405	385	730
	PS	59	200	285	330	560

All specimens were subjected to a heat flux of 40 Btu/ft²-sec with simultaneous vibration of 60 cps, acceleration of 90 g's, and ½ in. double amplitude displacement.

The surface texture of the foam significantly affects its insulative characteristics. As discussed in the preceding sections, we can control the surface texture of the foam, by the disuse, partial use or full use of a plastic wrapping such as "Saran-wrap" during the drying cycle, thus forming a hard skin, partial skin, or no skin, respectively on the surface. Foams without a hard skin have a lower back face (T_b) and interface (T_i) temperatures than those with a hard skin, the partial skin foams being intermediate in the insulative properties, as shown in Table XII. This difference is especially significant for test exposure of 5 min instead of $2\frac{1}{2}$ min, and is shown in Figure 16 for a zircon foam of composition Z-87. There is a back-face (T_b) difference of about 115°F and an interface (T_i) difference of 280°F , between two foams of identical densities and nominal compositions but differing in their surface textures.

This effect is probably due to the fact that the hard surface skin predominately consists of albumin which is yellowish, and would, therefore, have a lower reflectivity than that of a skin-free surface, which is whiter. A high reflectivity (i.e., low absorptivity) has been shown in our thermal analysis (see Section II) to be a critical parameter in limiting the back face temperature.

Further, the foams without a skin or with only a partial skin form fewer or no surface cracks when subjected to recycling of the final test conditions.

The most insulative zircon foam developed in the density range of $57\text{-}60\text{ lb/ft}^3$, and $\frac{1}{2}$ in. thickness, is Z-87 without a skin and which contains Superpax A as well as Fiberfrax. This foam gave back-face temperatures (T_b) as low as 175°F and 280°F after $2\frac{1}{2}$ and 5 min exposure, respectively, to the final test conditions. Further, it was able to withstand recycling under the final flux and simultaneous vibrational

and acceleration test conditions while maintaining its insulative properties and mechanical integrity.

The effect of foam thickness on the insulative properties has been investigated. The T_b and T_i values of three identical foams of $\frac{1}{4}$, $\frac{1}{2}$, and 1 in. thicknesses on a honeycomb, as a function of test time (under heat flux and vibrational conditions) are shown in Figure 17, for a nearly optimized composition (Z-79-2). The back-face (T_b) temperature of the $\frac{1}{4}$ in. thick foam was 530°F after 2½ in. exposure. This indicates that with an optimized composition such as Z-87 (no skin) it may be possible to use foams $\frac{1}{4}$ to 5/8 in. thickness and still meet the program requirements of a T_b value not exceeding 400°F after 2½ min exposure.

The use of 25 wt% Superpax A which is an ultra-grained (4) zircon powder in the zircon mix enhances the insulative characteristics of the foam, to an extent.

The addition of Fiberfrax to zircon foams is essential and improves the structural integrity of the foam, especially during drying and curing, and probably contributes to some amount of radiant scattering.

The recycling characteristics of these foams have also been evaluated. The foams were subjected to a full 5-min exposure under the final test conditions, allowed to cool down to room temperature, and then exposed to the final test conditions once again. The back-face and interface temperatures of some of the optimized foams on recycling are presented in Table XI. Zircon foams both with and without Superpax showed good recycling characteristics. However, foam Z-90 which contains 10 wt% fine diameter Fiberfrax (instead of 10 wt% medium diameter Fiberfrax as the other optimized foams contained) failed on recycling. This foam also has the highest flat-wise tensile strength of all the prepared foams, and its failure to

maintain its structural integrity or recycling may be due to its inability to strain relieve itself because of high rigidity of the foam structure compared to the other foams. Subjecting foam Z-90 to a 97 hr water soak did not impair its insulative or mechanical characteristics. The values of T_b and T_i obtained on subjecting a soaked foam to the final test conditions are shown in Table XI. In fact, the soaked Z-90 specimen withstood the recycling test without rupture.

The final test results indicate that the optimized zircon foams of $\frac{1}{2}$ in. thickness are not only able to meet the program requirements for a $2\frac{1}{2}$ min exposure to the test conditions, but have good insulative and mechanical properties when subjected to 5 min test exposure and even under recycling conditions.

V. CHARACTERISTICS OF OPTIMIZED ZIRCON FOAMS

A. Introduction

To be able to optimize ceramic foams for rigid heat shields, they must not only exhibit superior thermal efficiency and maintain mechanical integrity under the final test conditions (see Section IV-B) but must also possess certain other characteristics. These include desirable mechanical properties, especially a flat-wise tensile strength and an ability to resist water erosion. To achieve these objectives with the minimum acceptable foam thickness and density, castable-type, chemically bonded, composite zircon foams were developed and evaluated. Fiber reinforced foams, dispersed two-phase ceramic foams, layered or sandwich foams, are all examples of composite zircon foams.

The zircon foam compositions considered for optimization, on the basis of the final testing program are Z-87, Z-88, Z-89, and Z-90. All four foams have a density

not exceeding 60 lb/ft³. Foam Z-87 contains 25 wt% Superpax, while Z-88, Z-89, and Z-90 contain none. All the foams contain 10 wt% Fiberfrax. The nominal compositions of these foams are shown in Table IV.

B. Flat-Wise Tensile Strength

The zircon foams were cast onto 2 x 2 x $\frac{1}{4}$ in. 304 stainless steel plates in order to obtain flat-wise tensile strength data. The cured foam slightly more than $\frac{1}{2}$ in. in height, was ground parallel to a height of $\frac{1}{2}$ in. and the fixtures were attached to the foam and substrate with epoxy resin. The skin, partial skin, and no-skin types were tested on an Instron machine. The results have been shown in Table XIII. The results indicate that in all cases the skin-type foams are the weakest. Observation of the fractured specimens indicated that the "partial skin" and "no skin" type foams fractured in the middle of the foam specimen or close to the upper surface, while the "skin-type" failed at the interface (on which the foam was cast) or very close to the interface. This is in concurrence with the fact that the formation of a hard surface skin is due to the rapid migration of the albumin along with the potassium silicate binder material to the surface during curing, thus causing a depletion of the binder within the foam body and at the interface. The Superpax containing foams were found to have a lower flat-wise tensile strength than those without. A maximum tensile strength of 78 psi was obtained with foam Z-90, no-skin type. This foam contains the fine-diameter Fiberfrax instead of the medium-diameter Fiberfrax used in the other foams.

C. Water Effect

The effect of water on the properties of the optimized zircon foams was evaluated by a water boiling and a cold water soak test. Specimens were weighed and then immersed in boiling distilled water for 3 hr. The specimens were placed in wire

TABLE XIII
FLAT-WISE TENSILE STRENGTH
OF ZIRCON FOAMS AT ROOM TEMPERATURE

Foam No.	Foam Type	Density, lb/ft ³	Average Tensile Strength, psi
Z-87	S	60	33
	PS	60	40
	NS	60	42
Z-88	S	57	49
	PS	57	54
	NS	57	65
Z-89	NS	52	70
Z-90	S	58	55
	PS	58	60
	NS	58	78

baskets and suspended in the container. After boiling, the specimens were dried in an electric oven and weighed again. Weighed specimens were also subjected to a 24 hr cold water soak test. The per cent weight losses are shown in Table XIV. All these foams lose about 4 wt% when subjected to a water environment. The water loss is largely due to the presence of water-soluble silicates which were added to the zircon foam.

The effect of water on the flat-wise tensile strength of foam Z-89 was determined after a 24 hr soak test. There was a reduction in the tensile strength from 70 psi to 40 psi.

However, soaking these foams for a time period as long as 97 hr did not affect the mechanical integrity of the foam when subjected to the final test conditions of 60 cps vibration and 90 g's acceleration, as shown for Z-90 in Table XI. In fact, this foam was successfully subjected to a second 5 min recycle under the final test conditions.

D. Thermal Conductivity

The thermal conductivities of two zircon foams, Z-67 and Z-90 (having densities of 52 lb/ft³ and 60 lb/ft³, respectively) were determined from room temperature to 2500°F. In both cases a radial heat flow technique was used to measure the thermal conductivity.

The basic requirements for the radial heat flow technique are: uniform temperature along the axial direction, a means of limiting axial heat flow to negligible quantities, and a method for measuring temperatures and heat flow at steady state conditions. Axial thermal gradients are minimized by using stacked disks rather than a long cylinder. The poor thermal contact between adjacent disks limits the axial heat flow. Also top and bottom guard heaters were provided at each end of the stack to reduce the axial gradients.

TABLE XIV
WATER SOLUBILITY OF CASTABLE
ZIRCON FOAMS

Foam No.	Type	<u>Percent Weight Loss</u>	
		3 hr Boil	24 hr Soak
Z-87	PS	5.5	5.3
Z-88	PS	4.7	6.0
	NS	3.9	5.7
Z-89	NS	4.3	5.9
Z-90	PS	6.0	4.7
	NS	4.6	6.2

The samples consist of a stack of 5 disks, each disk having dimensions of $\frac{1}{2}$ in. thickness by $2 \frac{5}{8}$ in. outside diameter and $\frac{5}{16}$ in. inside diameter. Also, four holes 0.060 in. in diameter were located in each disk to permit insertion of thermocouples. A 0.3125 in. diameter hole was drilled in each disk to accommodate the central heater which controls the radial thermal gradient through the specimen. Four platinum/platinum-10% rhodium thermocouples were properly located in the test specimen. Two thermocouples were placed in the center of the stack of two different radii. Measured temperatures at those locations were used in the determination of thermal conductivity. A third thermocouple was placed $\frac{1}{2}$ in. from the bottom of the stack, and a fourth thermocouple was placed $\frac{1}{2}$ in. from the top of the stack. The temperatures measured at those locations, indicated the axial temperature distribution and this information was used to adjust top and bottom guard heaters.

Before the beginning of the test, the system was purged with helium gas, to provide an inert atmosphere. The inert atmosphere was maintained throughout the measurement of thermal conductivity. The system was heated to a desired temperature level by an outer heater, and when steady-state conditions existed, the heat flow through the specimen was determined by measuring the power dissipated across a known length of the center heater. The current supplied to the center heater was measured with an ammeter, having an accuracy of 0.25%. The voltage drop was measured across a 2 in. length of the center heater with a voltmeter having an accuracy of 0.25%. This was accomplished by attaching two leads of 0.10 in. molybdenum wire to the 2 in. test section of the center heater. The radial heat flow equation below is used to determine the thermal conductivity values.

$$K = \frac{Q \ln r_2/r_1}{2\pi L(T_1 - T_2)}$$

where

- k = thermal conductivity, Btu/hr-ft-°F
- Q = heat flow, Btu/hr
- r₂ = radius of outer temperature hole, ft
- r₁ = radius of inner temperature hole, ft
- L = distance between voltage leads, ft
- T₁ = temperature at r₁, °F
- T₂ = temperature at r₂, °F

The apparatus was tested by measuring the thermal conductivity of Armco iron. Errors in measurement may result from misalignment of the inner heater, variation in the resistance of the inner heater wire, location of the thermocouples, etc. Because of the close agreement with standardized data on Armco iron and the very small spread in experimental data, it is felt that accuracy of the results is $\pm 5\%$.

The thermal conductivity values obtained for the Z-90 "partial skin" foam along with a Z-67 foam are tabulated in Tables XV and XVI. Figure 18 compares the thermal conductivity of our composite zircon foams with other insulative foams. Z-67, which is a Superpax-containing foam, has a lower thermal conductivity than the non-Superpax containing Z-90 foam. The effect of radiation transparency is evidenced by the sharp increase in conductivity above 1100°F. The conductivity of these castable zircon foams was found to be very low, lower than that of a fired stabilized zirconia foam of similar density. Measurement was made to 2300°F.

E. Specific Heat

The enthalpy of zircon foam Z-90 was measured from room temperature to 2300°F by the drop calorimeter technique. In this method, the sample of the material is heated to a

TABLE XV
THERMAL CONDUCTIVITY OF ZIRCON FOAM Z-67

Temperature °F	Thermal Conductivity, Btu/hr-ft-°F
240	.094
460	.084
655	.076
900	.076
1085	.080
1305	.097
1560	.124
1835	.166
2130	.236
2300	.290

TABLE XVI
THERMAL CONDUCTIVITY OF ZIRCON FOAM Z-90

Temperature °F	Thermal Conductivity, Btu/hr-ft-°F
298	0.125
651	0.136
984	0.157
1293	0.185
1602	0.240
1839	0.285
2048	0.336
2295	0.397

desired temperature in a furnace and then dropped in a modified Parr calorimeter. The enthalpy of the material is calculated from the weight and temperature rise of the water in the calorimeter. The process is repeated at a series of temperatures at approximately 200°F intervals. An equation is fitted to the enthalpy curve and specific heat is obtained by differentiation of the enthalpy equation with respect to temperature at constant pressure.

The specific heat of zircon foam Z-90 as function of temperature is presented in Table XVII and in Figure 19.

The sudden change in specific heat around 1800°F, as can be seen from Figure 19, is due probably to the melting of cementing agent potassium silicate.

F. Reflectance

Reflectance measurements were made at room temperature on foams Z-67, Z-88, Z-89, and Z-90 in the range of 0.7 to 2.7 microns. The results are shown in Figure 20.

Reflectance measurements were made employing a Beckman DK2-A spectroreflectometer. This instrument measures hemispherical reflectance with normal illumination in the wavelength range 0.20 to 2.7 microns.

The results indicate that the reflectance of these foams prepared without a surface skin (NS type) is very high--above 90% in the important region of 0.75 to 1.85 microns. Considerable loss of reflectance occurs at higher wavelengths. The presence of a surface skin on this foam reduces the reflectance considerably as indicated by Z-90 with partial skin (PS type). This reduction in reflectance is probably due to the presence of the yellowish albumin in the skin layers.

TABLE XVII
SPECIFIC HEAT OF ZIRCON FOAM Z-90

Temperature °F	C _p , Btu/lb-°F
200	0.167
400	0.172
600	0.185
800	0.205
1000	0.224
1200	0.239
1400	0.264
1600	0.283
1700	0.291
1950	0.146
2200	0.146

VI. SUMMARY

The major emphasis in this investigation has been in the development of chemically bonded castable-type zircon foams for use in rigid heat shields. Work was also carried out in preparing and evaluating castable mullite and calcium aluminate foams; however, the optimization and final evaluations were confined to the zircon foams.

To be able to develop castable zircon foams, which would exhibit good insulative properties and maintain their structural integrity when subjected simultaneously to high heat fluxes and severe vibrational and acceleration levels, the concept of composite foams was studied. Fiber reinforced foams, dispersed multi-phase ceramic foams, layered or sandwich foams, are all examples of composite foams.

The surface texture of the foams was also found to be of major significance. By the use, partial use or disuse of a plastic wrapping on the foam surface during the drying cycle, it was possible to control the migration of the silicate binder as well as the albumin to the surface. The use of a plastic wrapper resulted in a foam free of a hard surface skin consisting primarily of unreacted binder and albumin. Foams prepared with this type of a texture and denoted as "no skin" types (NS) have a far higher reflectance and, consequently, more efficient insulative properties in a primarily radiant heating environment, than those prepared with a skin ("S" type). The "no-skin" type foams were also found to have a higher flat-wise tensile strength than the skin type foams. This is due to the fact that the formation of a hard skin is accompanied by the rapid migration of the albumin and potassium silicate binder material to the surface during curing, this causing depletion of the binder within the body of the foam and at the substrate interface.

The use of "Superpax" which is a fine particle (-4 microns) zircon powder along with the 44-micron size zircon powders resulted in a foam with good insulative characteristics. However, the Superpax containing, castable zircon foams had considerably lower flat-wise tensile strength. It is conceivable that the presence of Superpax in fired zircon foams will lead to both good insulative and mechanical properties.

The use of fibers, of stabilizing second-phase materials, along with the close control of microstructure, and in particular the surface texture have enabled us to develop castable-type, chemically bonded composite zircon foams which can be cured at low temperatures (not exceeding 250°F), and still possess excellent insulative structural properties for use in rigid heat shields.

VII. LOGBOOK RECORDS

All data pertaining to work done in this period are recorded in IITRI logbooks:

C 14965	C 15130	C15676	C 15127	C 15135
C 15677	C 15129	C15675	C 15681	

VIII. PERSONNEL

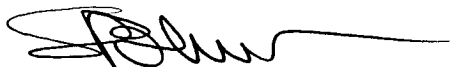
Contributions to this report were made by S. L. Blum, S. A. Bortz, A. J. Mountvala, H. Nakamura, H. L. Rechter, and L. Wolf, Jr.

Respectfully submitted,
IIT RESEARCH INSTITUTE

A. J. Mountvala

A. J. Mountvala
Research Scientist
Ceramics Research

APPROVED:



S. L. Blum
Director,
Ceramics Research

IIT RESEARCH INSTITUTE

ACKNOWLEDGMENTS

This work was sponsored by the National Aeronautics and Space Administration, George C. Marshall Space Flight Center, Huntsville, Alabama, under NASA Contract NAS8-11333. The advice of Mr. V. Seitzinger of the NASA Marshall Space Flight Center is gratefully acknowledged.

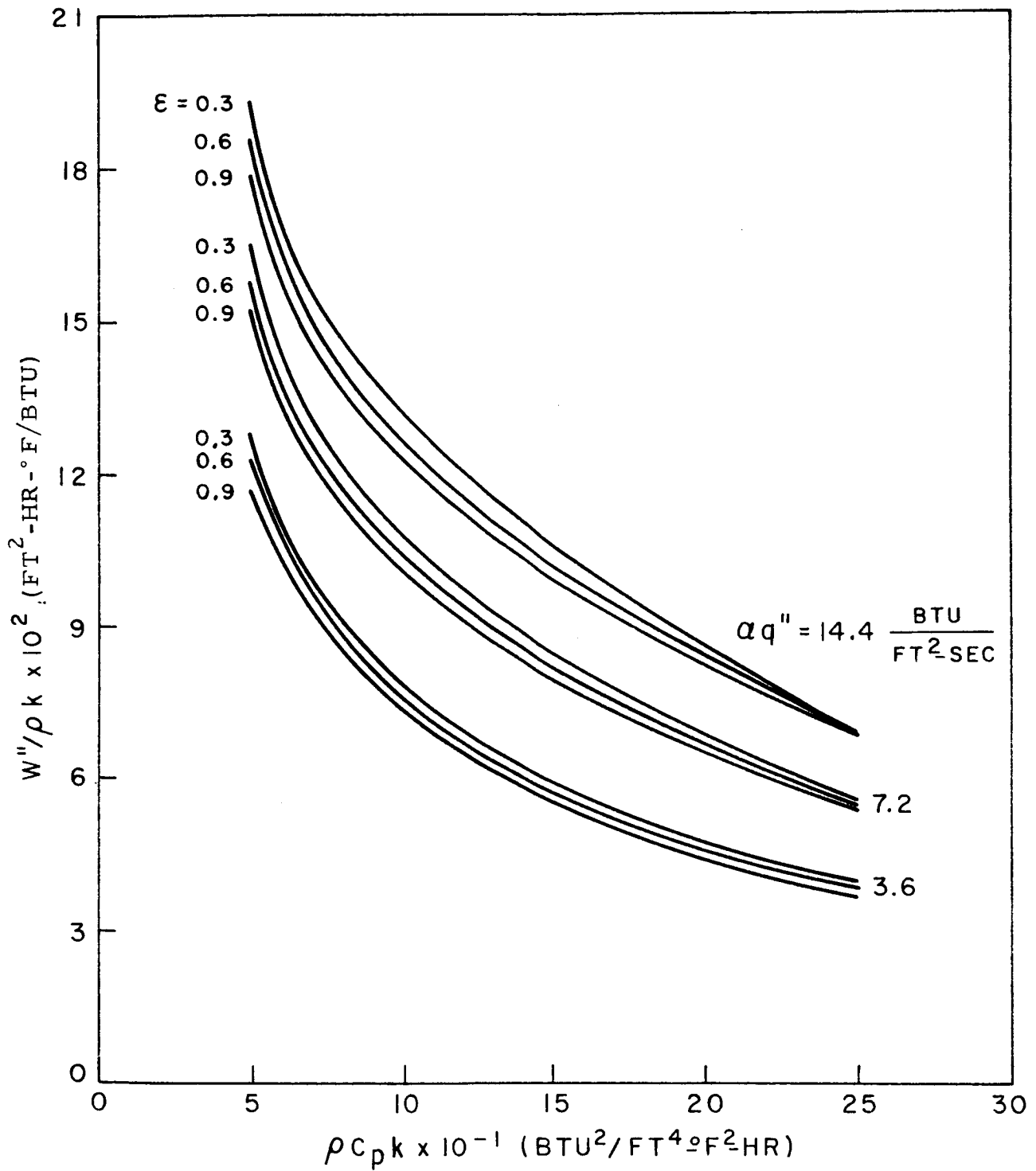


FIG. 1 INSULATION WEIGHT REQUIREMENT AS A FUNCTION OF THERMAL PROPERTIES

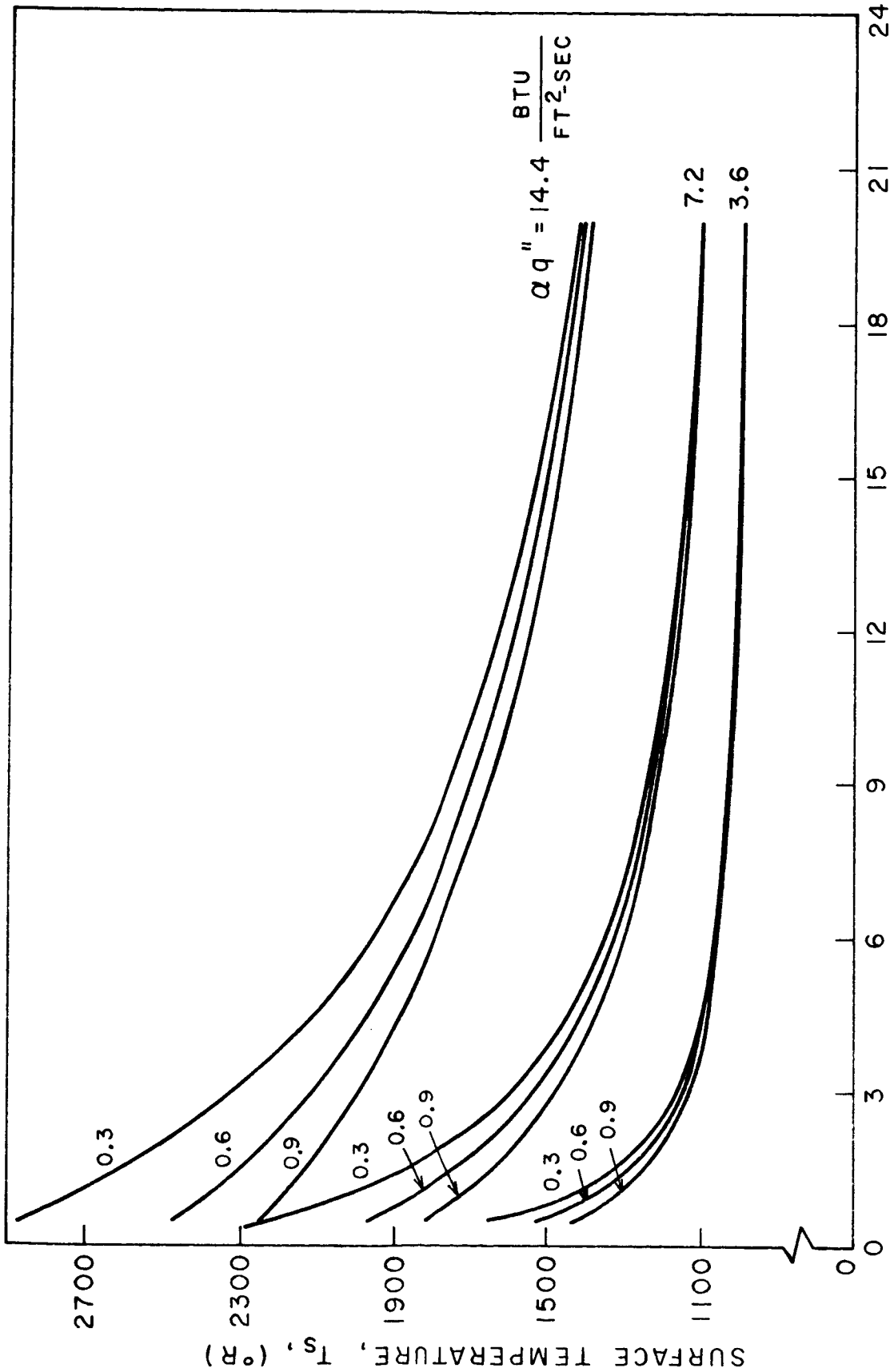


FIG. 2 SURFACE TEMPERATURE AS A FUNCTION OF THERMAL PROPERTIES

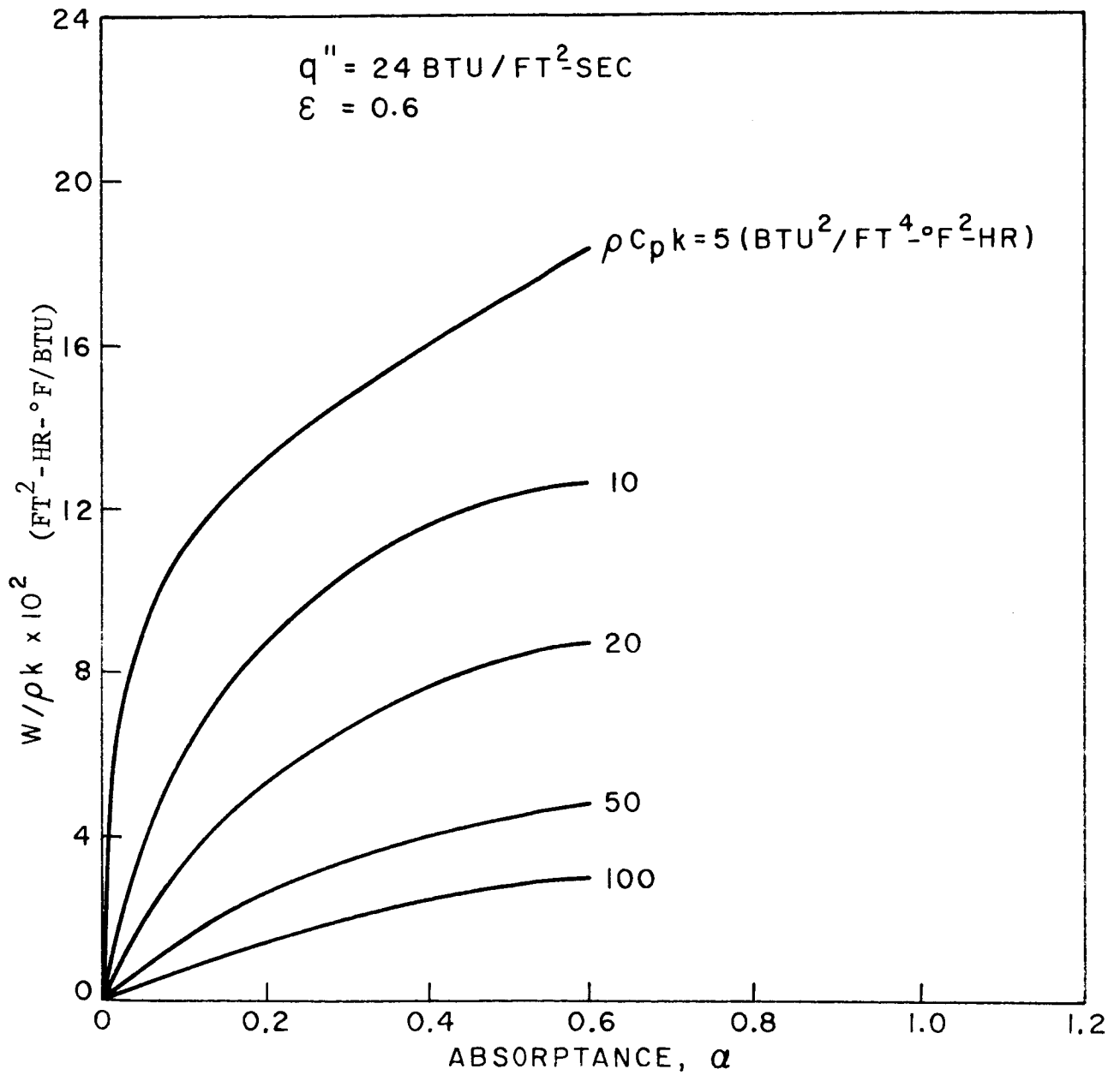


FIG. 3a DEPENDENCE OF INSULATION WEIGHT REQUIREMENT UPON ABSORPTANCE

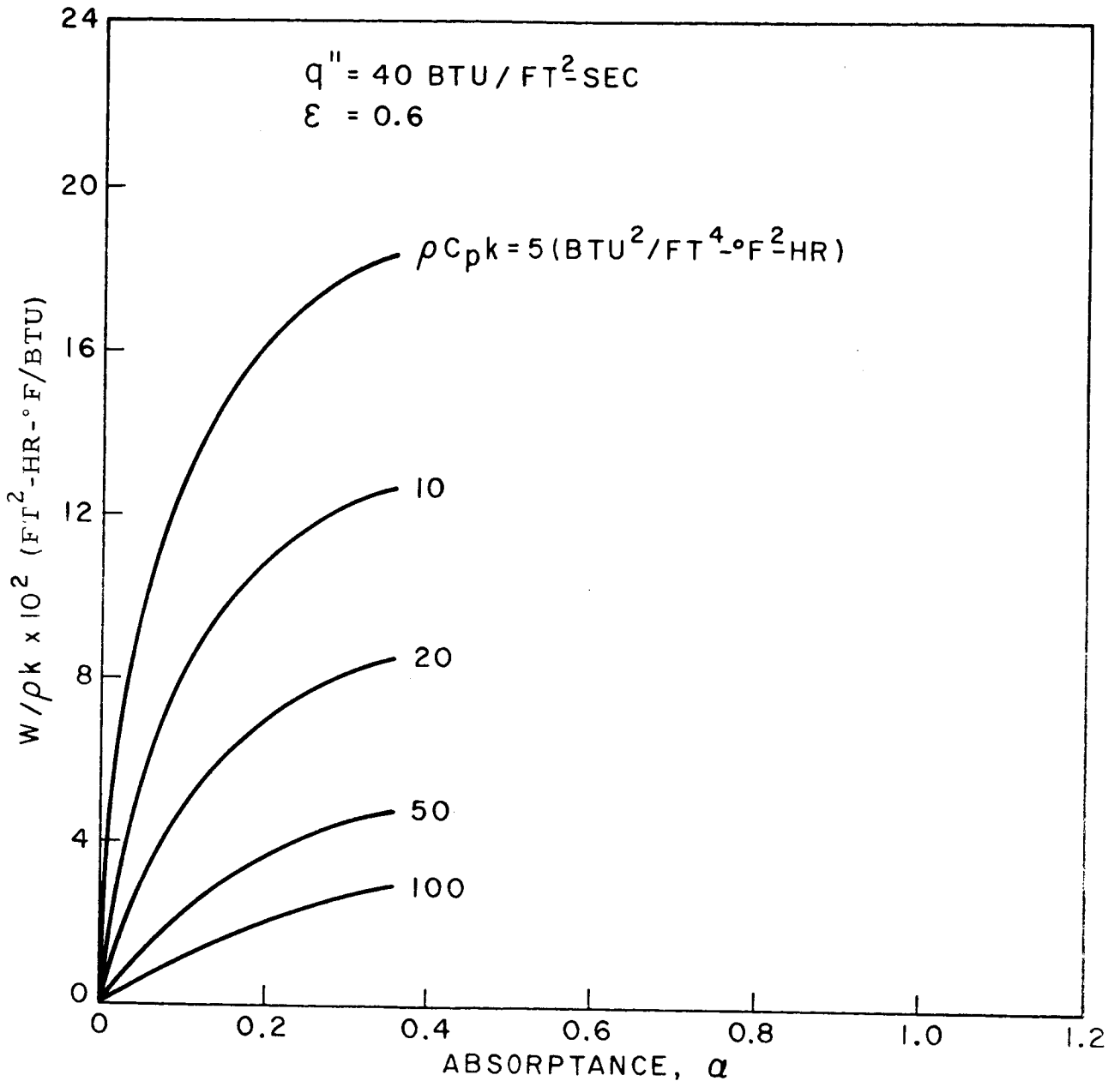


FIG. 3b DEPENDENCE OF INSULATION WEIGHT REQUIREMENT UPON ABSORPTANCE

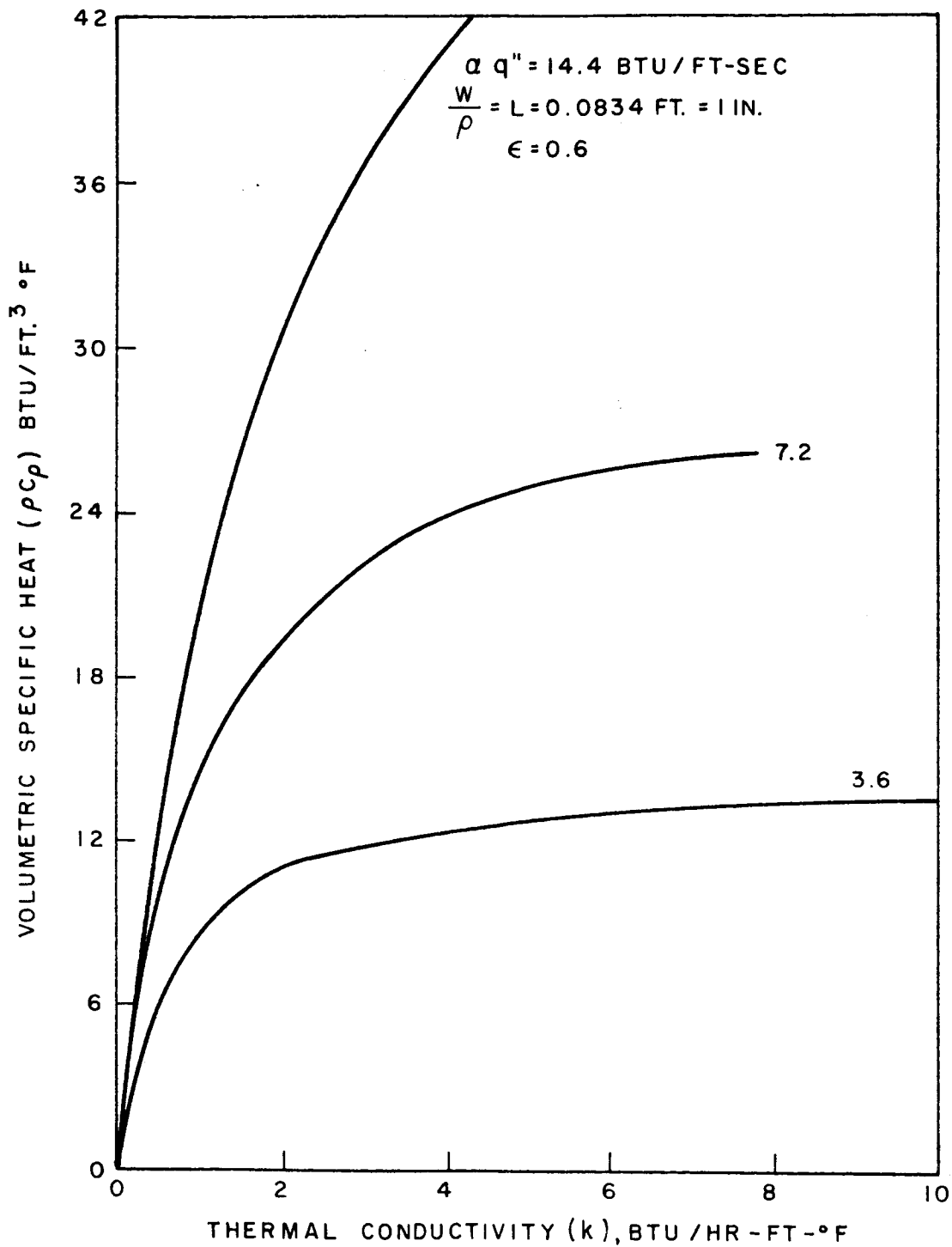


FIG. 4 MINIMUM VOLUMETRIC SPECIFIC HEAT REQUIREMENT AS A FUNCTION OF THERMAL CONDUCTIVITY

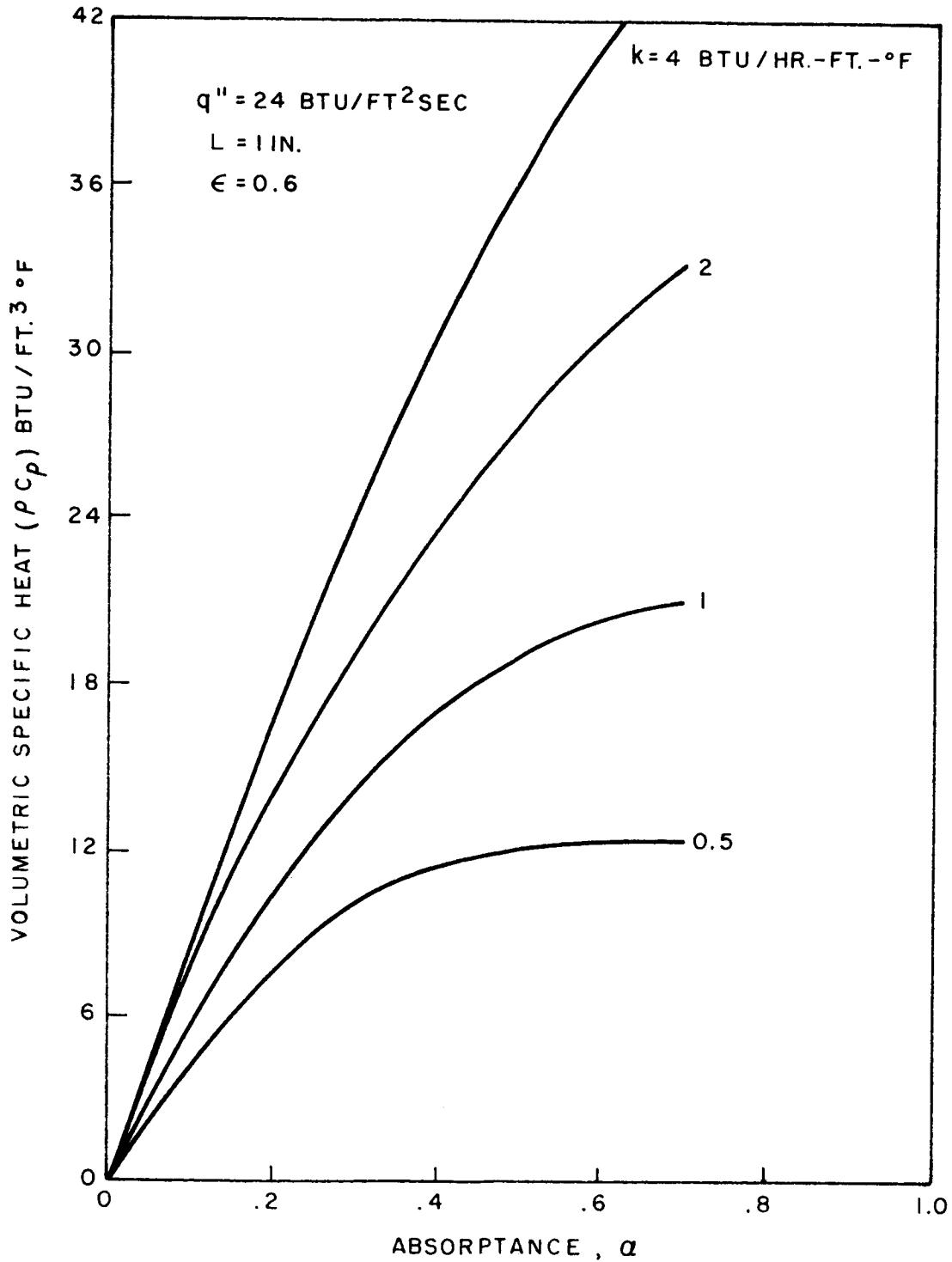


FIG. 5a MINIMUM VOLUMETRIC SPECIFIC HEAT REQUIREMENT AS A FUNCTION OF ABSORPTANCE

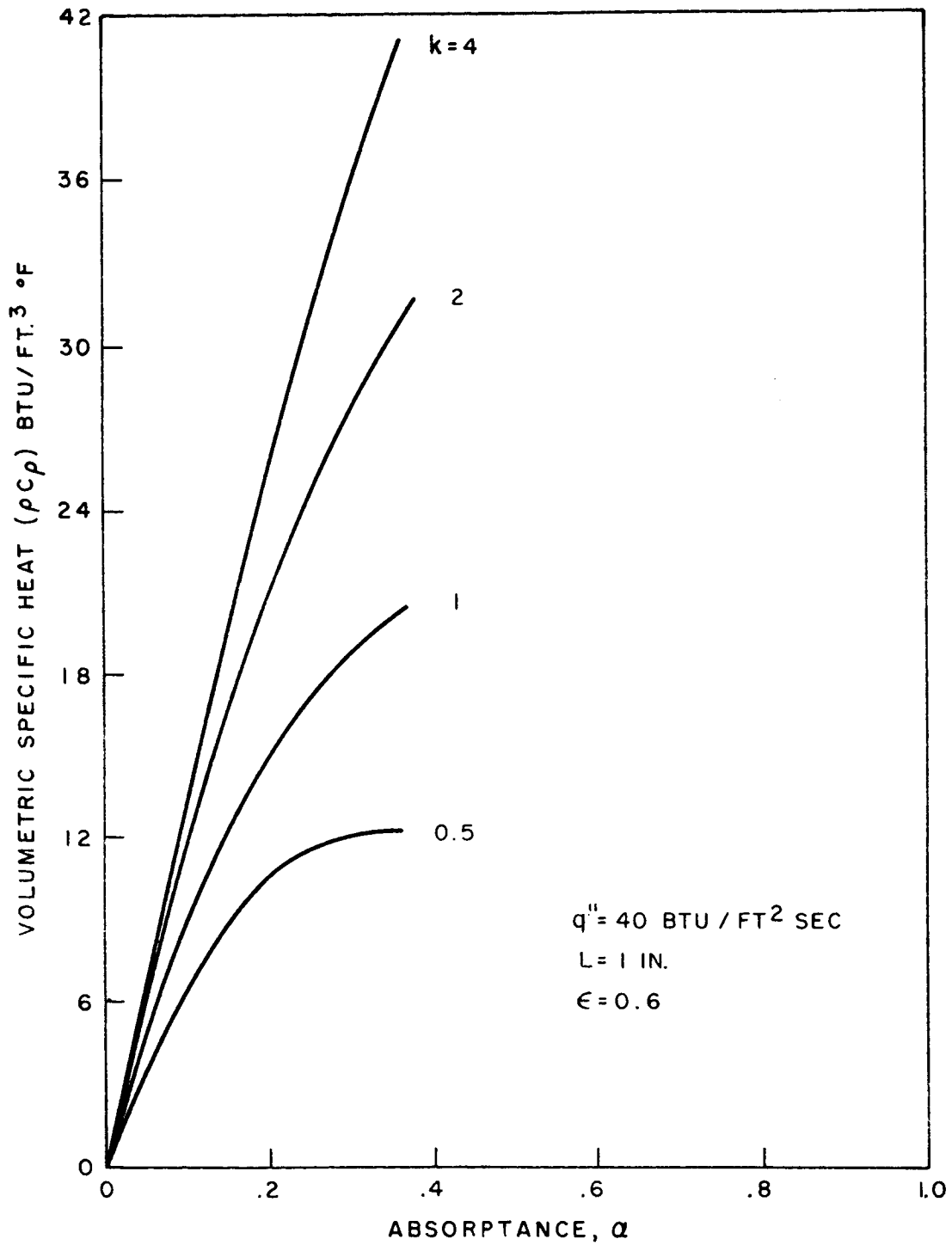


FIG. 5b MINIMUM VOLUMETRIC SPECIFIC HEAT REQUIREMENT AS A FUNCTION OF ABSORPTANCE

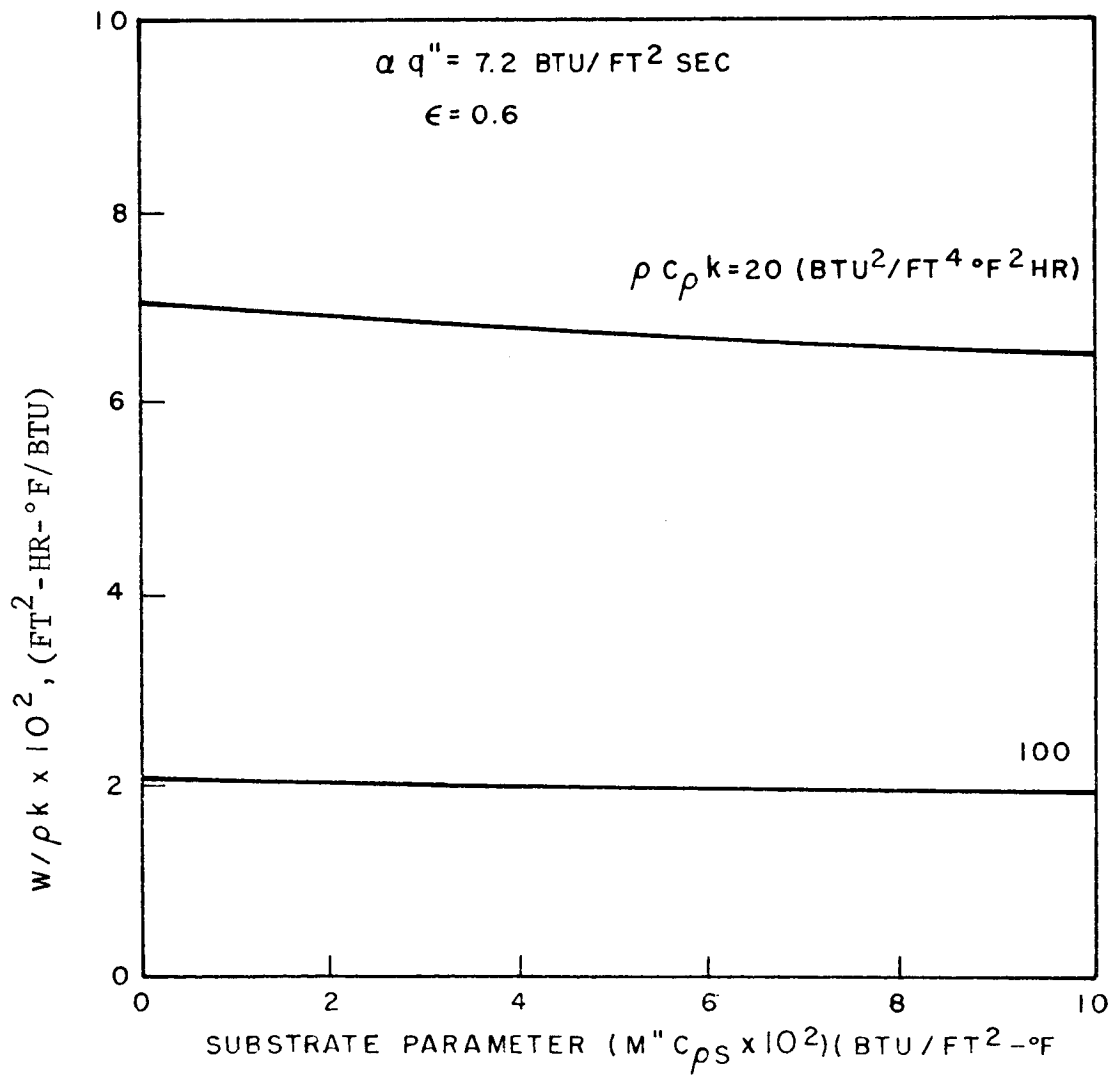


FIG. 6 INFLUENCE OF SUBSTRATE UPON INSULATION PERFORMANCE

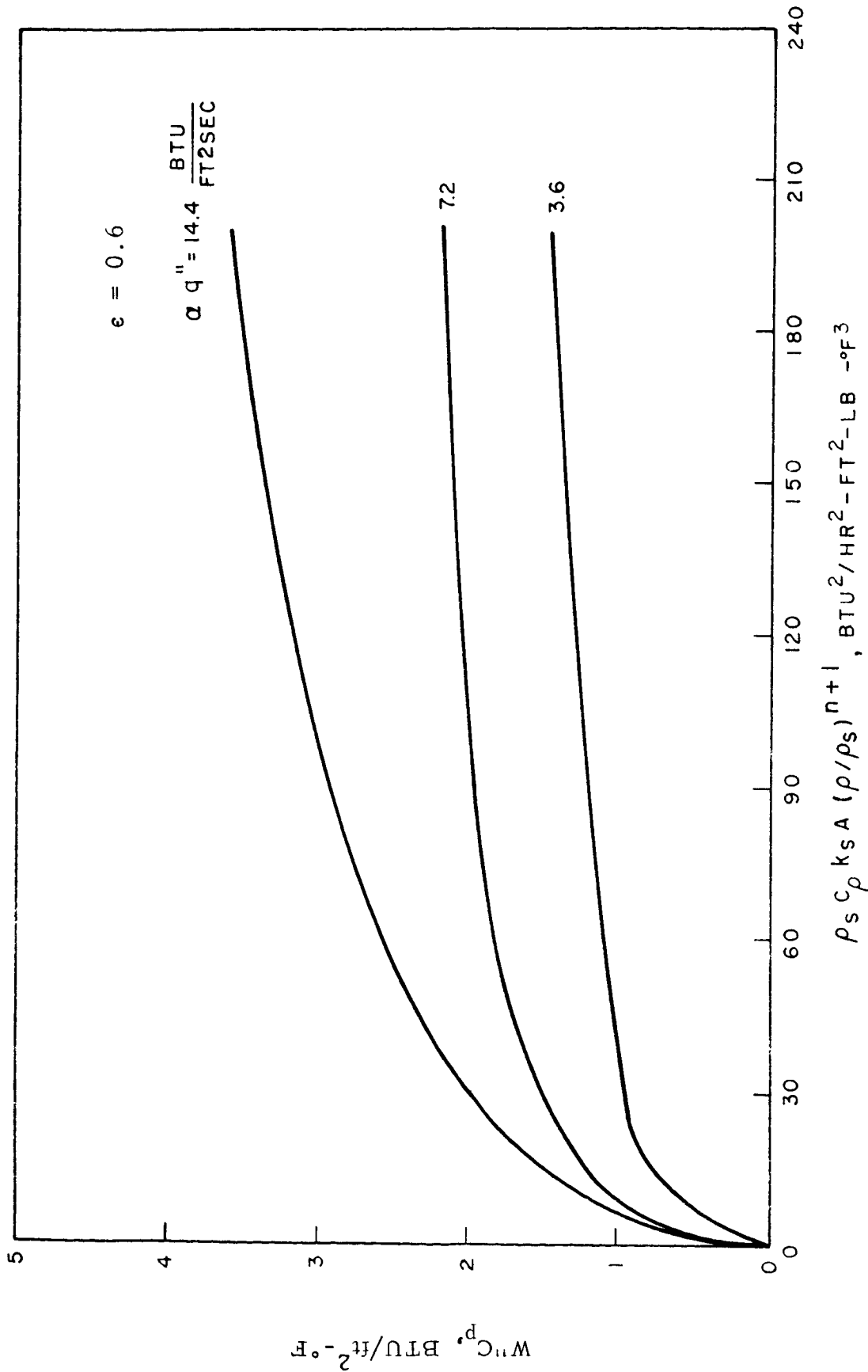


FIG. 7 INSULATION WEIGHT REQUIREMENT WITH CONDUCTIVITY AS A FUNCTION OF DENSITY

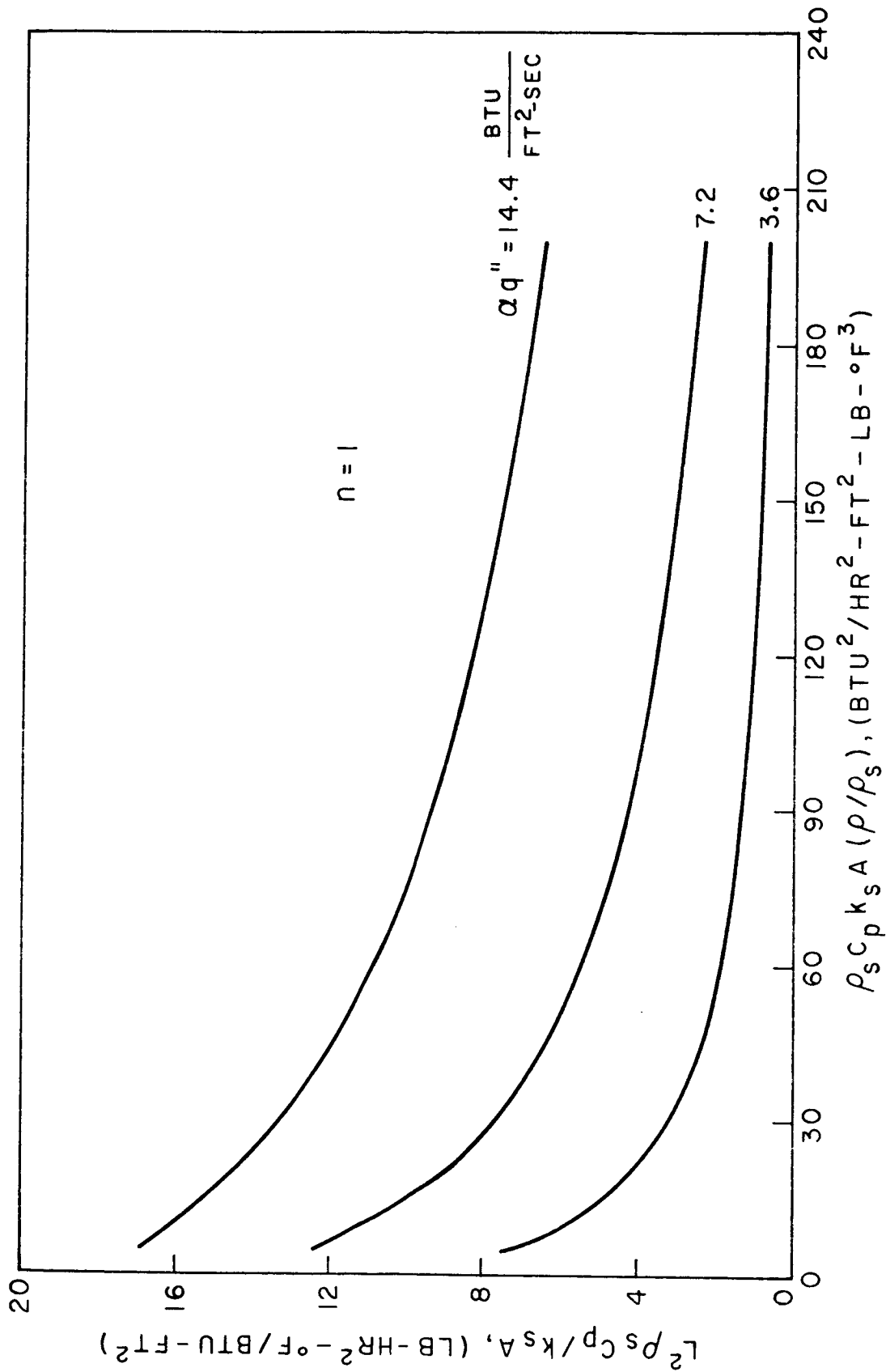
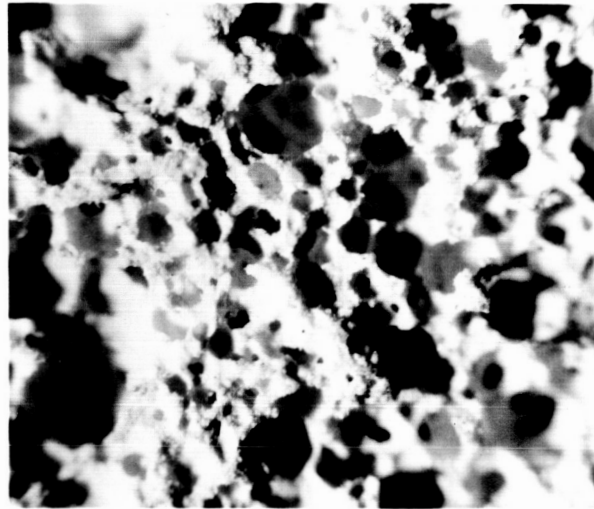
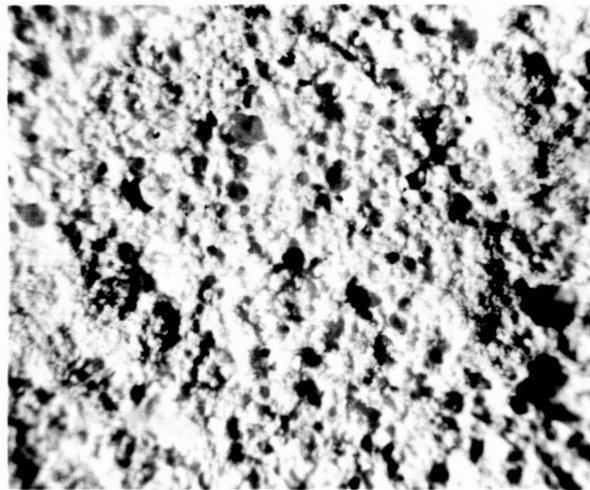


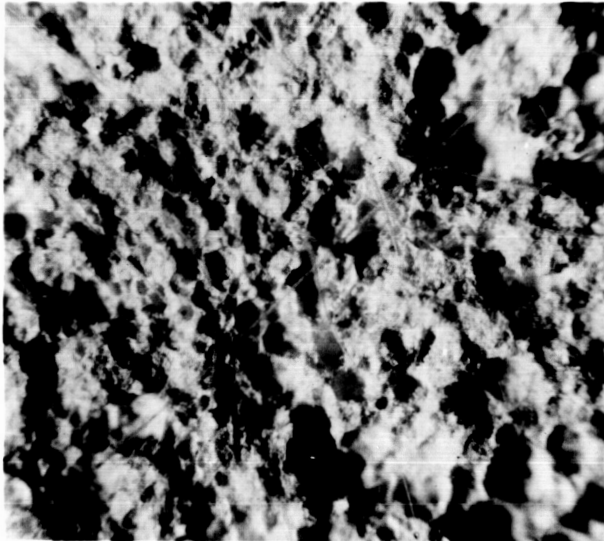
FIG. 8 INSULATION THICKNESS REQUIREMENT WITH CONDUCTIVITY AS A FUNCTION OF DENSITY



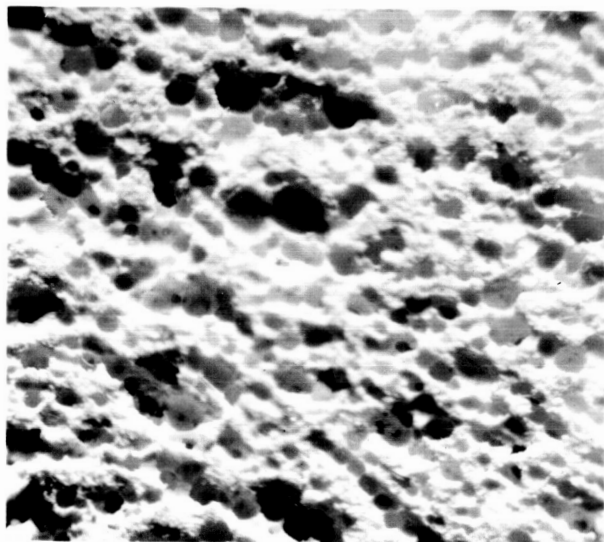
24X
FIG.9 PHOTOMICROGRAPH OF ZIRCON
FOAM, Z-40



24X
FIG.10 PHOTOMICROGRAPH OF ZIRCON
FOAM, Z-35



24X
FIG.11 PHOTOMICROGRAPH OF
ZIRCON BASED FOAM CON-
TAINING FIBERFAX, Z-43



24X
FIG.12 PHOTOMICROGRAPH OF OPTI-
MIZED ZIRCON FOAM, Z-90

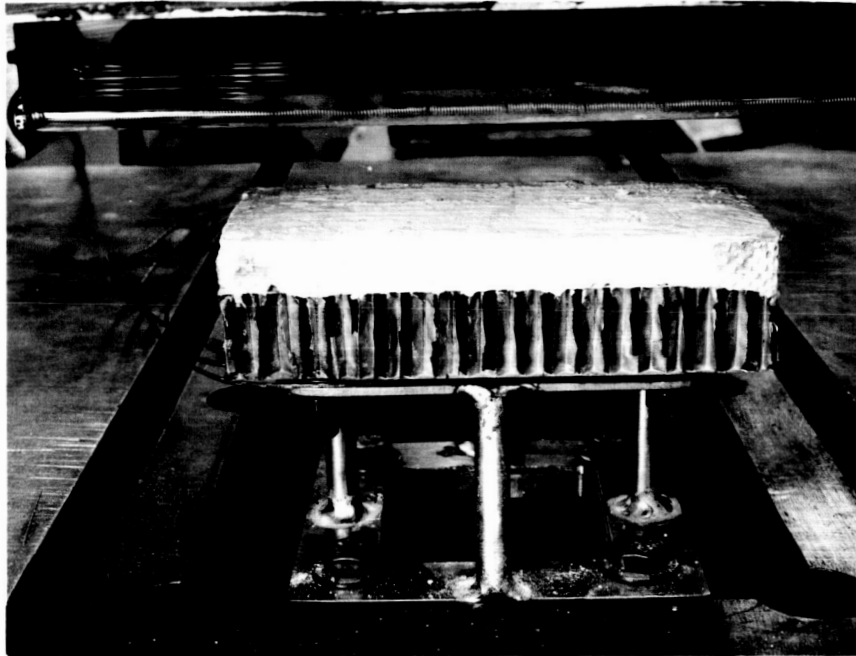


FIG. 13 TEST SETUP FOR SUBJECTING FOAMS TO
HEAT FLUX WITH SIMULTANEOUS
VIBRATION AND ACCELERATION

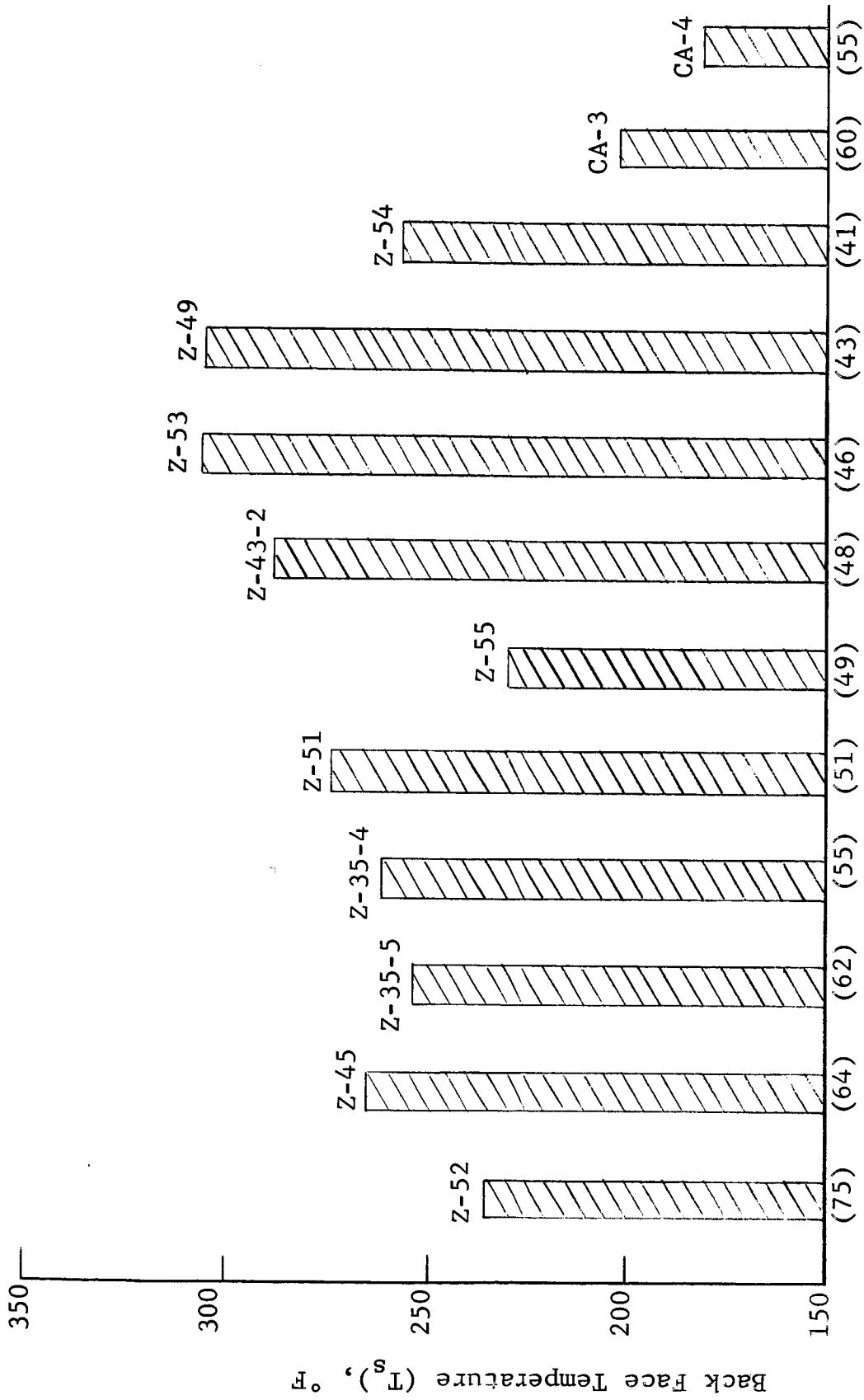


FIG. 14 - THE BACK FACE TEMPERATURE (T_s) OF ½ IN. FOAMS ON STEEL PANELS AFTER 150-SEC EXPOSURE TO A HEAT FLUX OF 24 Btu/ft²-sec.
(Numbers in parentheses indicate foam density in lb/ft³)

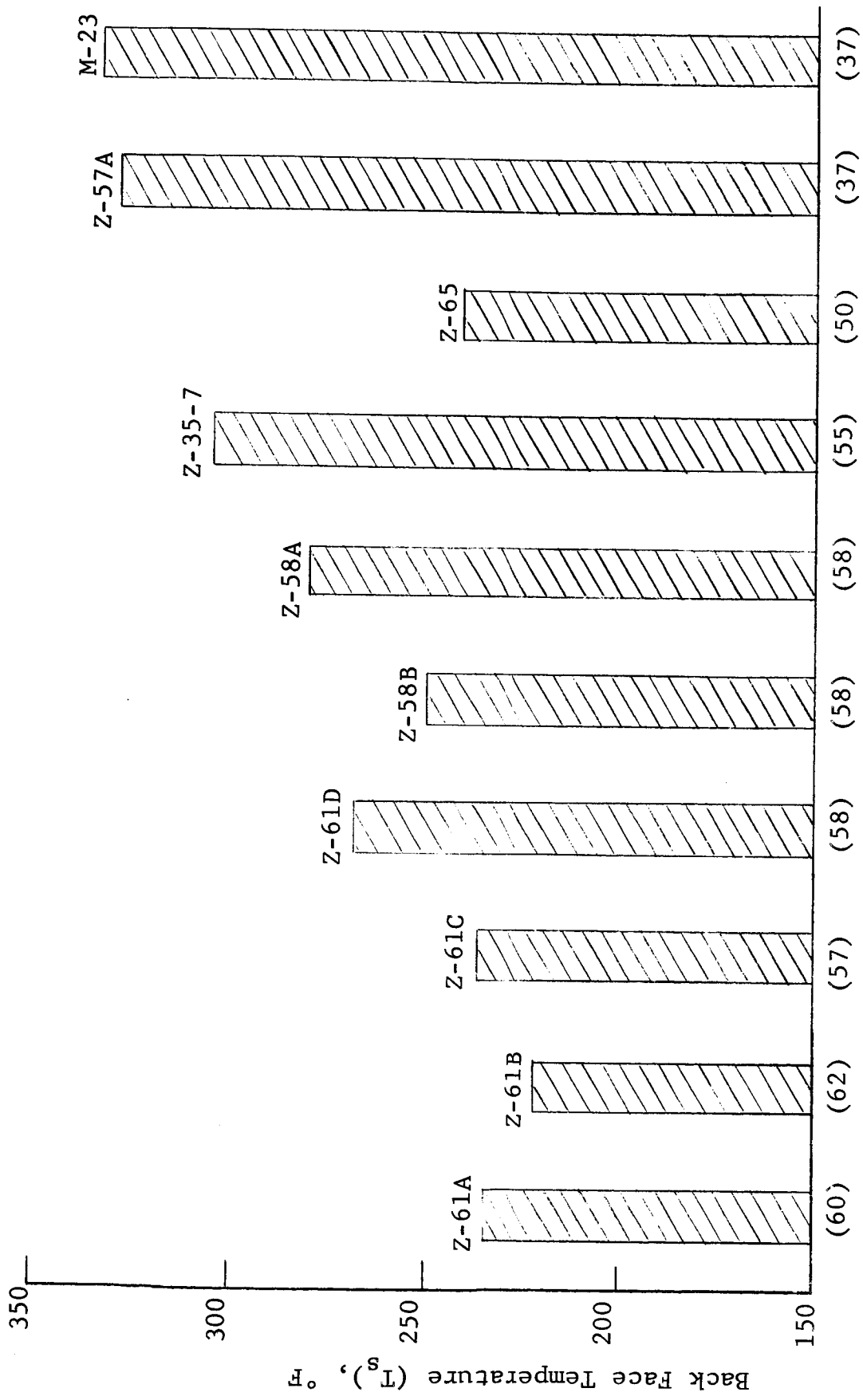


FIG. 15 - THE BACK FACE TEMPERATURE (T_s) OF ½ IN. FOAMS ON STEEL PANELS AFTER 150-SEC EXPOSURE TO A HEAT FLUX OF 40 Btu/ft²-sec. (Numbers in parentheses indicate foam density in lb/ft³)

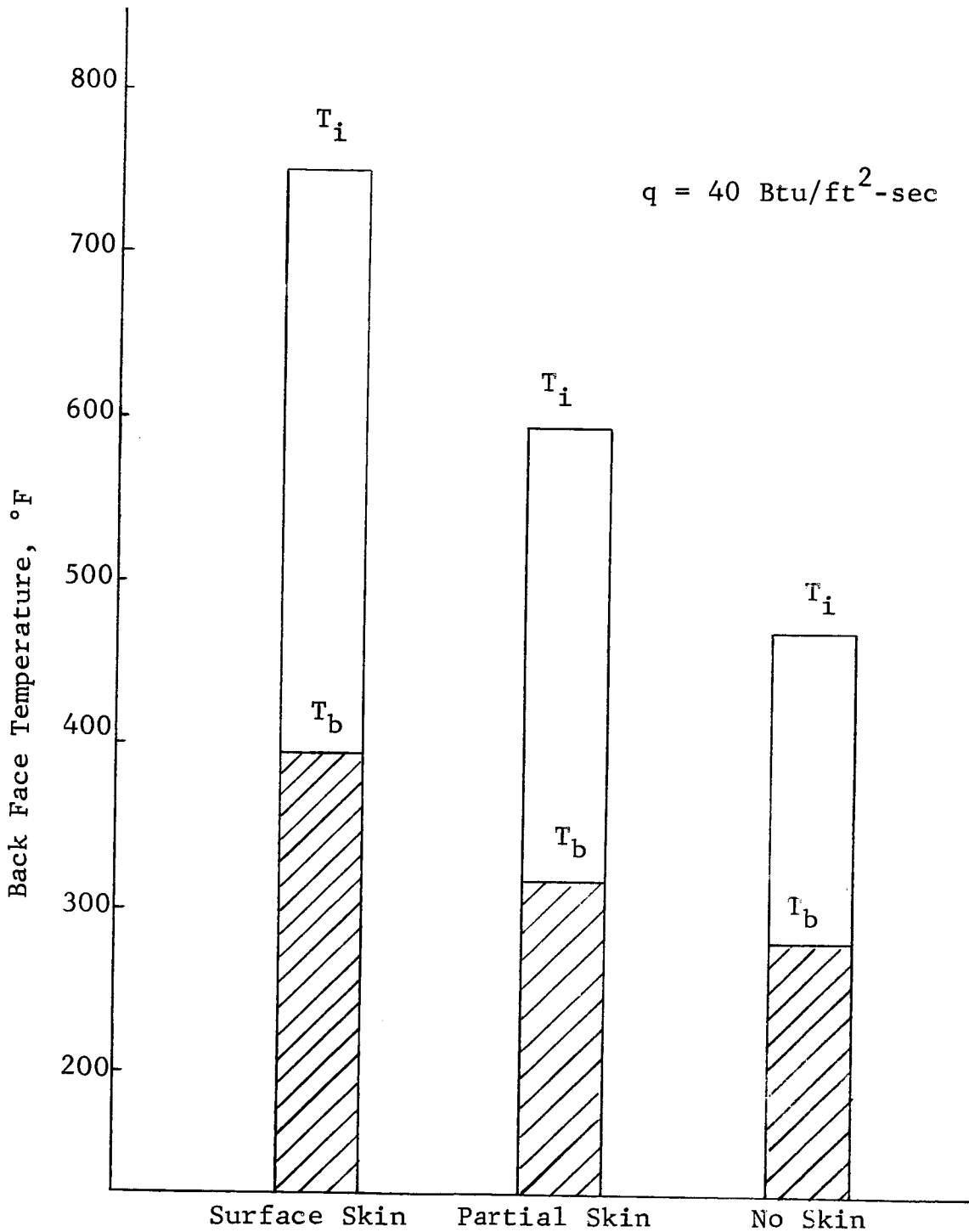


FIG 16 - THE EFFECT OF SURFACE CONDITIONING ON THE BACK-FACE TEMPERATURE OF ZIRCON FOAM Z-87 ($\frac{1}{2}$ IN. THICK), AFTER 5 MINUTES.

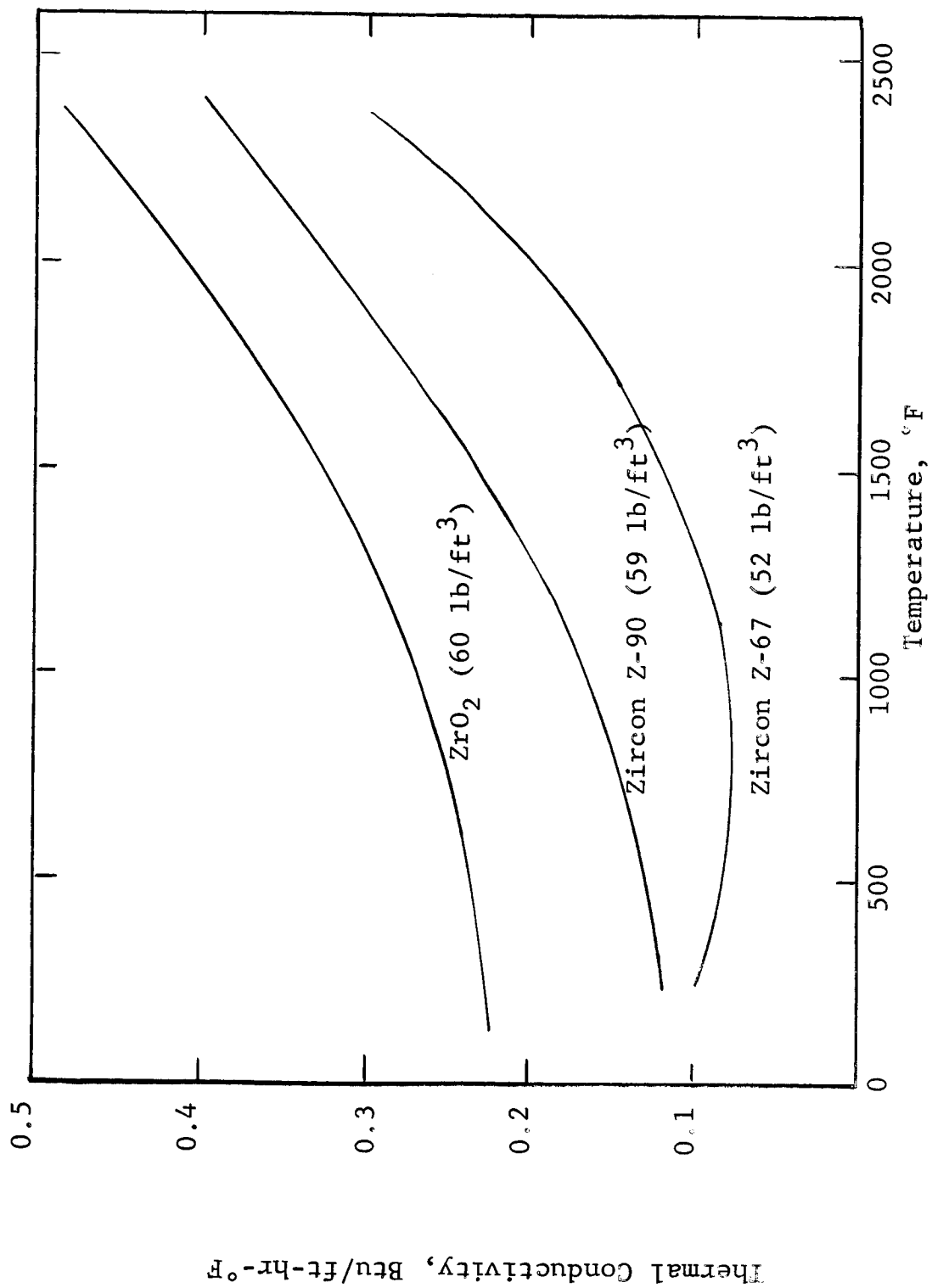


FIG. 18 - THERMAL CONDUCTIVITY OF CERAMIC FOAMS.

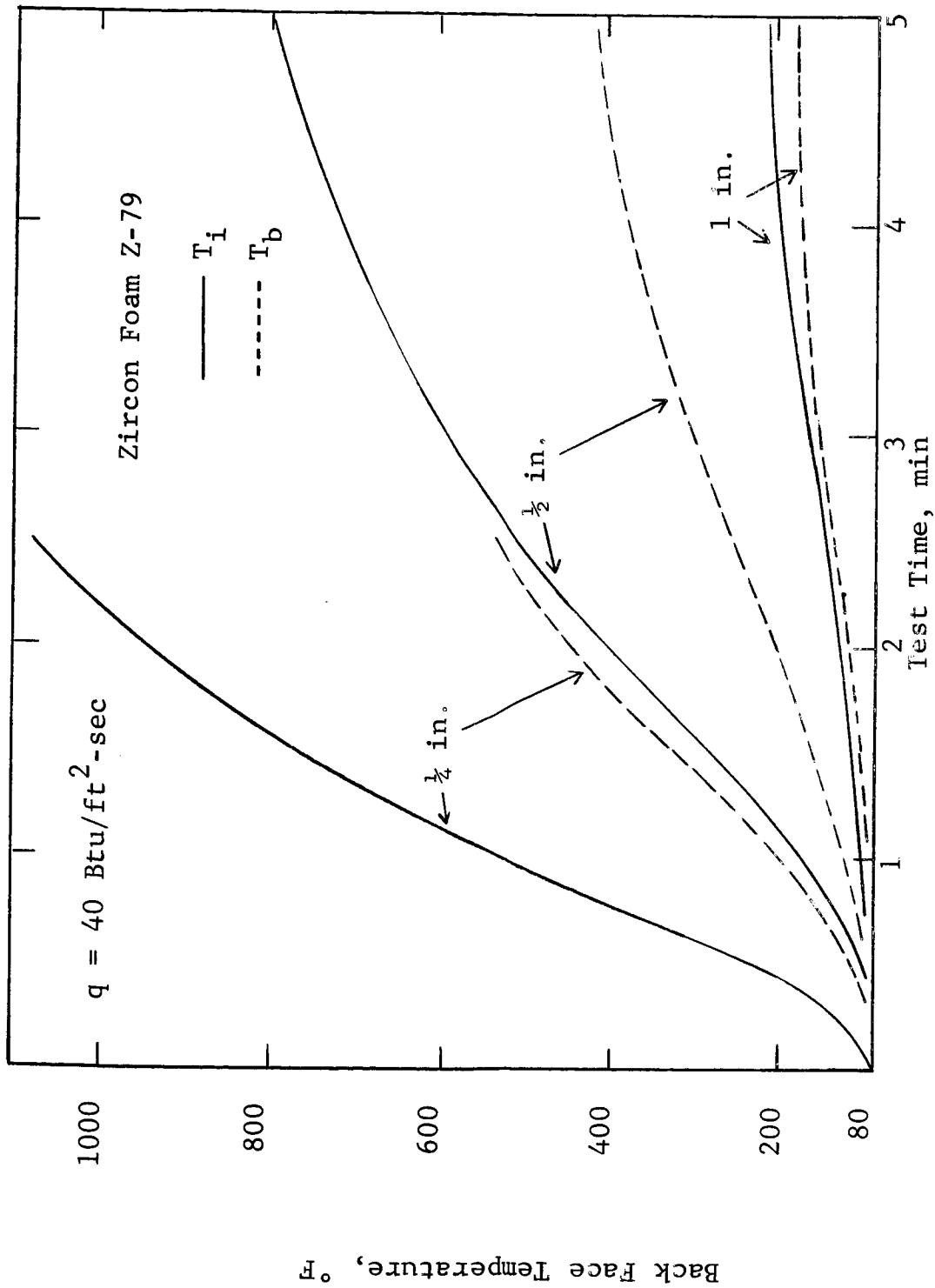


FIG. 17 - EFFECT OF FOAM THICKNESS ON INSULATIVE CHARACTERISTICS OF RIGID HEAT SHIELDS.

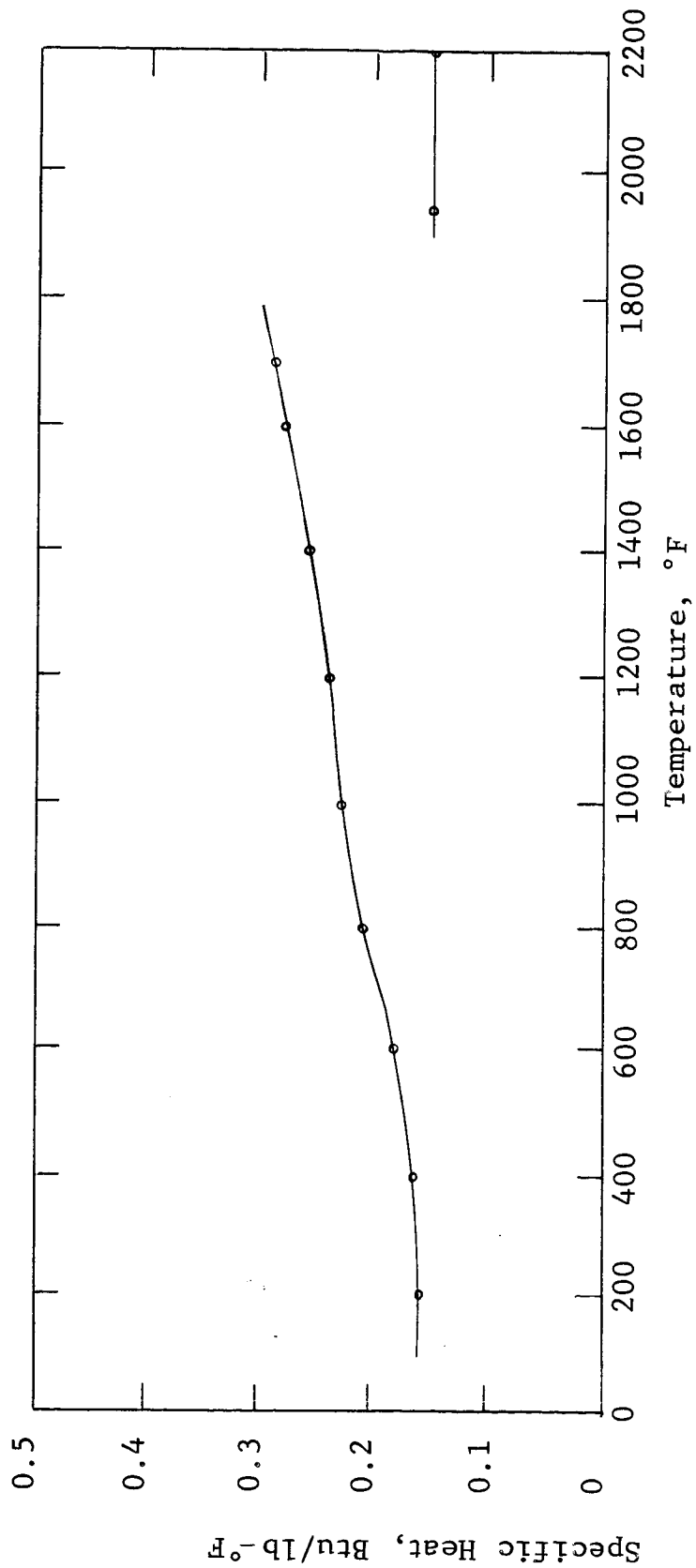


FIG. 19 - SPECIFIC HEAT OF ZIRCON FOAM Z-90

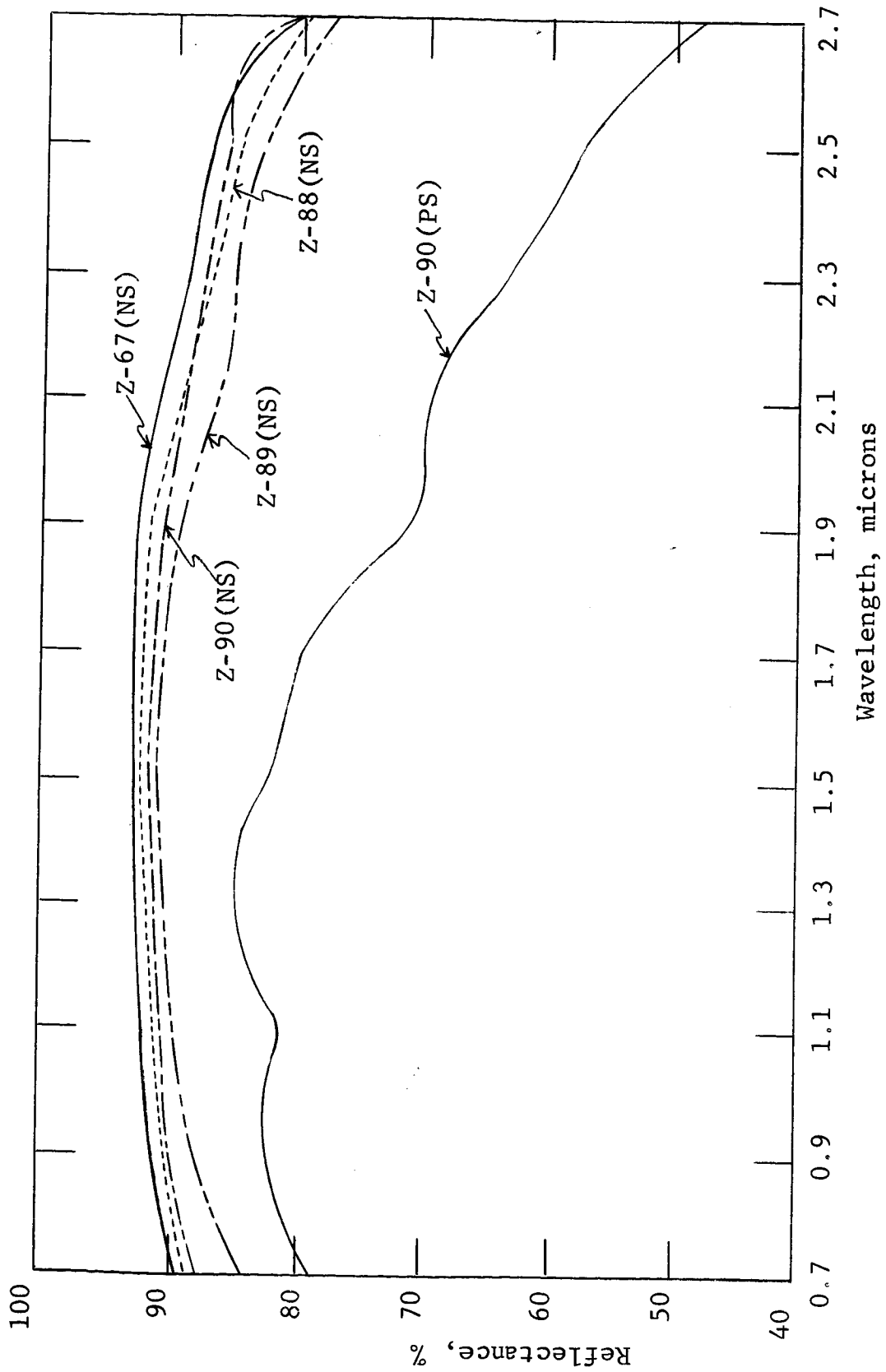


FIG. 20 - ABSOLUTE REFLECTANCE OF ZIRCON FOAMS

APPENDIX A
NUMERICAL ANALYSIS OF THE
THERMAL PROPERTIES OF FOAMS

The differential equation covering the nonsteady heat conduction in an infinite slab of the insulation is:

$$\rho C_p \frac{\delta T}{\delta t} = \frac{\delta}{\delta x} \left(k \frac{\delta T}{\delta x} \right) \quad (A-1)$$

where

T = Temperature

t = Time

ρ = Density

k = Thermal conductivity

C_p = Specific heat

For a homogeneous material

$$\frac{\delta k}{\delta x} = \frac{dk}{dT} \frac{\delta T}{\delta x}$$

Thus, the differential equation becomes

$$\rho C_p \frac{\delta T}{\delta t} = k \frac{\delta^2 T}{\delta x^2} + \frac{dk}{dT} \left(\frac{\delta T}{\delta x} \right)^2$$

The boundary condition at the surface of the insulation ($x = 0$) is:

$$-k \frac{\delta T}{\delta x} \Big|_0 = \alpha q'' - \epsilon \sigma T_o^4 \quad (A-2)$$

where

α = Absorptivity

q'' = Incident radiant heat flux

ϵ = Emittance

σ = Stefan-Boltzmann constant

To obtain this boundary condition, the assumption is made that

the insulation surface is opaque to the incident radiant heat flux.

The boundary condition at the insulation-substrate interface ($x = L$) is:

$$-k \left. \frac{\delta T}{\delta x} \right|_L = M'' C_{p,s} \left. \frac{\delta T}{\delta t} \right|_L \quad (A-3)$$

where

M'' = Mass per unit area of the substrate

$C_{p,s}$ = Substrate specific heat

L = Insulation thickness

In this boundary condition the assumption is made that the substrate is uniform in temperature throughout. It can be shown that this assumption is valid when:

$$\frac{M'' C_{p,s} L_s}{k_s} \left. \frac{\delta T}{\delta t} \right|_L \ll T_L \quad (A-4)$$

where

L_s = Substrate thickness

k_s = Substrate thermal conductivity

Because of the complexity of the boundary conditions and the dependence of thermal properties upon temperature, the solution of equations A-1, 2, and 3 must be performed numerically. Employing a forward finite difference in time and a central difference in space the differential equation (A-1) takes the so called explicit form

$$T_{m+1,n} = \frac{\Delta t}{(\rho C_p)_n (\Delta x)^2} \left[k_n (T_{m,n+1} + T_{m,n-1} - 2T_{m,n}) + \frac{dk}{dT} \right]_n \left(\frac{T_{m,n+1} - T_{m,n-1}}{2} \right)^2 + T_{m,n} \quad (A-5)$$

where

Δx = Length increment

Δt = Time increment

$x = n\Delta x$

$t = m\Delta t$

This expression yields the temperature at any interior point at any time in terms of the temperatures and thermal properties at the preceding increment of time.

The temperature at the insulation surface is determined by the difference equation for that point which is obtained from Eq. A-2 as

$$T_{m+1,0} = \frac{\Delta t}{(\rho C_p)_n (\Delta x)^2} \left[2k_o (T_{m,1} - T_{m,0}) + 2(\alpha q'' - \epsilon_o \sigma T_{m,0}^4) \Delta x + \frac{dk}{dT} \Big|_o \left(\frac{\alpha q'' - \epsilon_o \sigma T_{m,0}^4}{k_o} \right)^2 (\Delta x)^2 \right] + T_{m,0} \quad (A-6)$$

Similarly, the temperature at the insulation-substrate interface is obtained from (3) as

$$T_{m+1,L} = \Delta t \left\{ D \pm \left[D^2 - \frac{2k_L^3}{(\Delta x M'' C_{p,s})^2} \frac{T_{m,L-1} - T_{m,L}}{\frac{dk}{dT} \Big|_L} \right]^{\frac{1}{2}} \right\} + T_{m,L} \quad (A-7)$$

where

$$D = \frac{(\rho C_p)_L + \frac{2M'' C_{p,s}}{\Delta x}}{2 \left(\frac{M'' C_{p,s}}{k_L} \right)^2 \frac{dk}{dT} \Big|_L}$$

The positive sign is taken in the above expression when dk/dT is negative.

The three preceding differential equations A-5, 6, and 7 were programmed for solution on the IBM 7090 computer. The language used was Fortran II. An integration procedure employing

a linear interpolation scheme was used to obtain the thickness of insulation required to give a desired interface temperature at a particular time.

The functional variation of thermal conductivity, rate of change of thermal conductivity with temperature, emittance and specific heat with temperature were incorporated into four sub-routines so that the functional relationships could be altered with ease should the need arise for a particular material.

By non-dimensionalizing the differential equation and the boundary conditions for the case of constant thermal properties the pertinent groups of problem parameters are obtained. This procedure yields the following expression which relates insulation weight, density, specific heat, thermal conductivity, absorptance, incident heat flux, and emittance.

$$\frac{W''}{\rho k} = \int (\rho C_p k, \alpha q'', \epsilon) \quad (A-8)$$

where

W'' = Weight per unit area of insulation ($W'' = \rho L$)

L = Insulation thickness

A parametric study has been performed employing the computer program by allowing $\rho C_p k$, $\alpha q''$, and ϵ to vary over suitable ranges and calculating the corresponding values of $W''/\rho k$. Thus, for a given material with known density and thermal properties the thickness of insulation (and therefore its weight) required to yield the desired interface temperature after the prescribed heating time can be determined from this study. Alternately, for a prescribed thickness the values of absorptance, emittance, density, specific heat, and thermal conductivity required to provide the desired performance are delineated.

The parametric study was performed for the following conditions:

Initial temperature = $540^\circ R = 80^\circ F$

Heating time = 150 sec

Interface temperature (at $t = 150$ sec) = $960^{\circ}\text{R} = 500^{\circ}\text{F}$
Substrate Parameter ($M''C_{p,s}$) = $0.0662 \text{ Btu/sec-ft}^2\text{-}^{\circ}\text{F}$

The results of the parametric study have been discussed in Section II of this report.

APPENDIX B
LITERATURE AND TECHNICAL SURVEY

I. INTRODUCTION

This survey on the preparation and properties of "foamed" ceramic thermal insulation was part of a broader program whose ultimate objective was the development of lightweight foamed ceramics in a modified or tailored form designed to withstand the thermal radiation and vibrations encountered in the launching of space vehicles. A literature survey was conducted to determine the current state-of-the art and the performance characteristics of currently available foamed ceramics having a melting point in excess of 2500°F. The primary purpose of the survey was to integrate all available data on foamed ceramics and to critically evaluate this information in light of the program's current and future needs.

This survey includes information gathered from technical journals, reports, and patent literature together with information gathered from prominent manufacturers by way of a technical questionnaire.

The literature survey indicated that a significant amount of the work carried out on foamed ceramics has been for higher temperature refractory foams than the range required for our application. These are mainly resin-impregnated ablation foams which, in most cases, have a density exceeding 60 lb/ft³ and, therefore, do not meet our requirements. Comparatively, very little information was available on foams having the desirable reflective and emissive properties. The compiled data in our survey has emphasized foaming techniques and their correlation with micropore structure, measured mechanical the thermo-physical properties, and the influence of pore structure on the properties of the foamed ceramic.

The state of commercially available materials being developed by industry as well as through government sponsorship has also been evaluated, as a result of a technical questionnaire sent to some twenty-nine organizations, prominent commercial manufacturers, universities, and other research institutions. The information obtained from this questionnaire has been presented separately in a subsequent section.

This survey not only reviews the state-of-the-art of foam ceramics, but also shows the gaps in the available information, thereby indicating technical areas where further research and development effort would be justified.

II. METHOD OF PRESENTATION OF DATA

The property data are given wherever possible in a graphical form. The arrangement of these graphs is primarily by material class and then by property within each class. The source of the information has been indexed, and a complete reference is given in the bibliography.

In cases where there was disagreement between the data of different investigators, an attempt has been made to correlate this divergence. To be able to successfully correlate property data on foamed ceramics, it is essential that the data be characterized with regard to chemical composition, density, and pore structure. However, it is not always possible to do this due to the lack of details of the method of preparation as well as the mode of testing.

III. METHODS OF PREPARING CERAMIC FOAMS

A number of techniques are available for preparing foams. These essentially fall into one of four categories:

1. Mechanical foaming
2. Chemical foaming
3. Burnout of organic additives
4. Bloating

A number of comprehensive reviews are available (1,2) on the details involved in the various methods of preparing foams. Therefore, no attempt will be made in this discussion to describe the foaming techniques in great detail, but rather to point out the salient features in each technique.

Each of the listed techniques has both advantages and disadvantages which have been well reviewed by Kummer.⁽¹⁾ It was concluded that the mechanical foaming method was most compatible with fine-grained structures and capable of yielding low-density foams with uniform pores. The burnout process appeared best suited to coarse grained structures, while the chemical foaming method seemed difficult to control and reproduce because of its reliance on the rate and uniformity of a chemical reaction. However, various investigators have reported success with a particular technique, where some have reported otherwise.

A. Mechanical Foaming

The method of foaming by mechanical whipping of a slurry containing a surface-active agent has been employed for most of the commercially available foamed oxides. One advantage in this method over other techniques, especially where gas evolution is involved, is that in mechanical foaming the cellulation is completed before the body is cast and no secondary reactions take place.⁽³⁾ The effects of whipping speed and time, as well as of the slurry content on the structure of magnesia foams, have been reported.⁽⁴⁾ It was shown that pouring the whipped foam through a strainer prevented laminations.

In general, mechanical foaming has been the most commonly used method. Lindell⁽⁵⁾ reports an ability to control the fired density of lime-stabilized zirconia foams to about 0.5% by variation in foaming agent. Density was increased from 14.5 to 41.0% of theoretical by decreasing the "proportion of foaming agent" from 1.90 to 0.23% for a body containing 71% of -325 mesh

material. On plotting the data of Lindell, it was found that a nearly straight line was obtained of the logarithm of foaming agent content vs. density. A body of increased -325 mesh material displayed lower density at low levels of foaming agent, but the semilogarithmic relationship was still valid.

Lindell does not disclose the means of stabilizing the green foam from collapse, other than the necessity of critical control in each manufacturing step. Fused silica (Glasrock) foams appear to require no stabilizer. A -325 mesh slip with colloidal silica binder is foamed with "any available foaming agent." (6) Plaster of Paris or lime was employed for stabilization in the green state of foamed clays, (3) foamed alumina, (7,8) zirconia, magnesia, mullite, spinel, and zircon. (9) DuPont colloidal monohydrated alumina (Baymal) has also been used to stabilize a variety of high-alumina foam products (10,11) and low-expansion lithium aluminum silicate foams. (12)

B. Chemical Foaming

The most commonly used method of chemical foaming is of the type used to prepare foamed Al_2O_3 by the reaction of aluminum with phosphoric acid. (13) The phosphoric acid also acts as a binder when cured. The reaction takes place at room temperature and the product is cured at a higher temperature (185°F).

Zimmerman (14) describes a similar alumina product which is bonded by phosphoric acid and expanded at room temperature by reaction with aluminum powder. A wide variety of stabilizers are reported in the literature and include cornstarch, carboxymethyl cellulose, egg albumen, and even dried blood. The stabilizer serves to increase viscosity, to disperse the solid evenly, and to prevent slumping. Starch appears to be the preferred stabilizer. (15) Control of density of the foamed alumina product obtained from the aluminum-phosphoric acid reaction was obtained (16) by placing the mold in a restraining pressure fixture.

Zirconia foams have also been prepared by the metal-acid reaction using zirconium metal and phosphoric acid. ⁽⁴⁾ Magnesia foams cannot be prepared easily by this technique because of the reactivity of magnesia with acids.

Foaming in organic resin systems has been employed mainly with nonoxide materials. Silicon nitride has been foamed by blending a -325 mesh powder in a foamable silicone resin containing a cyanidine foaming agent and heating above the decomposition temperature of the resin. ⁽¹⁷⁾ Nickel metal foams were similarly prepared. ⁽¹⁸⁾ Copper foams utilized a catalyzed foamable phenolic resin with sodium bicarbonate as a foaming agent. ⁽¹⁹⁾ Logan ⁽²⁰⁾ used this technique for preparation of a variety of nonoxide foam materials, using phenol-formaldehyde and epoxy resins with an isocyanate resin foaming agent. The foaming occurred at room temperature due to a gasification reaction between the resins. Several boride, silicide, and carbide foams have been prepared. Efforts to produce nitrides proved unsuccessful.

The use of a blowing agent in a catalyzed foamable silicone resin has also been employed to produce aluminum oxide foams. ⁽²¹⁾ The final foam density was controlled by the amount of alumina filler in the blend.

C. Burnout Technique

This method essentially involves the pyrolysis of a mixture containing the material to be foamed with combustible organic materials.

An example of this technique is the preparation of lightweight foamed bricks prepared ⁽²²⁾ by pyrolysis of a starting mixture of clay and spherical foamed polystyrene bubbles. The foamed bricks could be made to float on water for a considerable length of time, thereby indicating that the foam had a closed cell structure.

A variation of the burnout technique is the use of polyurethane sponges, saturated with the oxide slurry, and fired. This offers excellent control over pore structure. Schwartzwalder ⁽²³⁾ describes the cellular alumina, zircon, and other bodies bonded with calcium aluminate cement and phosphoric acid prepared in this manner. Holland ⁽²⁴⁾ prepared alumina and beryllia foams in an acid slurry by an identical method.

D. Bloating

Another means of obtaining a cellular product through gas expansion is by a technique called "bloating." This method essentially entails the use of a gas-evolving melt which is incorporated with a material which becomes viscous at the gas-producing temperature and thereby causes bloating of the melt on solidification. This technique is useful for production of noncommunicating pore structures. Glass was bloated to form a closed pore material by a gaseous reaction of carbon and a refractory metal oxide, such as molybdenum trioxide. ⁽²⁵⁾ A coating of the refractory metal is produced on the cell walls. Clay bodies may also be bloated by the use of gas-forming constituents such as carbonates. A list of suitable gas-formers has been provided by Riley. ⁽²⁶⁾ Reaction of dolomite with dilute acid has been employed to bloat a clay body, which was then dried and fired. ⁽²⁷⁾

This review of foaming techniques indicates that a number of methods are available for preparing ceramic foams. Although a wide variety of techniques have been utilized, no attempt has been made in the past to characterize the processes that occur during foaming, nor has any serious correlation been attempted between the technique and the micropore structure. This has been a serious drawback in the development of foams, as it has affected the ability to prepare foams with reproducible properties. The lack of reproducibility is borne out by the wide scatter in the reported properties as shown in Section V of this appendix. An understanding of

the micropore structure and the ability to prepare foams with controlled microstructure is mandatory, especially for the development of foams having "tailored" reflective and emissive properties.

IV. CHARACTERIZATION OF THE PROPERTIES OF CERAMIC FOAMS

The use of lightweight ceramic foams in thermal heat shields for high-thrust rocket engines demands certain stringent requirements. The optimum insulation required for such applications must have a low density, low thermal conductivity, thermal-shock resistance, and desirable reflective and emissive properties.

Therefore, it is important to characterize some of these fundamental properties of ceramic foams for thermal heat-shield applications, especially in reference to their microstructures.

A. Mechanical Properties

The effect of density on the mechanical properties of the foam is important. Although a low density is desirable, certain minimum mechanical properties must also be met. Therefore, the effect of porosity on the mechanical strength of a foam must be evaluated.

The relationship of porosity and strength has been the subject of several reviews and analyses. Ryshkewitch⁽²⁸⁾ found a linear relationship between the logarithm of the compressive strength and the porosity in experiments with foamed alumina and zirconia bodies of from 3% to about 60% porosity.

Duckworth⁽²⁹⁾ noted that Ryshkewitch's data can be presented in the form:

$$S = S_0 e^{-bP} \quad (B-1)$$

where S = strength of porous body
 S_0 = strength of dense body
 b = constant
 P = volume pore fraction

The experimental constant, b , was found to be equal to 7, the slope of the logarithm of the strength vs. porosity curve for all experimental data and was apparently independent of material and pore size. On dividing both sides of Eq. B-1 by density, and assuming a value of 7 for b , the strength-to-density ratio reaches a minimum of $P = 1 - 1b$ or at 86% porosity. Above this the ratio is expected to increase.

Equation B-1 has been confirmed by several investigators. Experiments on foamed fine-grain zirconia bodies with a porosity of 90%,⁽³⁰⁾ gave a value for the constant b of 6.4. Coarser grain alumina foamed bodies did not display the semi-logarithmic relationship above 80% porosity, presumably because the continuous film structure could no longer be obtained with larger particles.

A theoretical study has been reported⁽³¹⁾ recently, relating pore shape and orientation to the strength of porous bodies. An equation satisfying the boundary conditions of zero and 100% porosity for i kinds of pores is given:

$$S = S_0 \left\{ 1 - \sum_i [(x_i a_i / V_i) P_i] \right\} \quad (B-2)$$

where x = characteristic length of pore
 V = pore volume
 a = projected maximum cross-sectional area of an intersected pore

The values of x , a , V , and a dimensionless constant α ($\alpha_i = x_i a_i / V_i$) are given for sphere, oblate spheroid, ellipsoid, cube, and cylinder pore shapes in various orientations.

In tests involving a large number of specimens of alumina, prepared by several ways and having a density range of 2.85 to 3.98 g/cm³, the elastic and shear moduli were found to decrease linearly with density. (32)

The response of highly porous materials to thermal stresses as related to pore geometry and grain size has not been systematically investigated. Factors affecting fracture initiation and propagation, and the role of pore size and cell voids in arresting cracks should be considered.

B. Thermal Properties

To be able to effectively use foamed ceramics for insulation applications it is mandatory to understand the effect of foam microstructure on the over-all thermal characteristics, and the effect of the various mechanisms of heat transfer which are important in high-temperature ceramic insulation systems.

The heat transfer through a foamed ceramic essentially takes place by processes of conduction, convection, and radiation. The geometry of the pores in the foamed ceramic, the emittance and transmissivity of the material, and the type of heat flux the material is subjected to will determine the contribution of each of the mechanisms to the over-all conductivity.

Several relationships have been derived for the thermal conductivity of porous materials. The resulting equations have been reviewed and compared. (33,34) At temperatures below which radiation becomes important the equations reduce to the form:

$$k_p = k_s (1 - P) + Pk_g \quad (B-3)$$

where k_p = conductivity of porous material
 k_s = conductivity of dense solid
 k_g = conductivity within pores of gas phase
 P = volume pore fraction

For rigid heat-shield applications with high-thrust rocket engines, the thermal environment is primarily radiant, and gas convection can be neglected. Loeb⁽³⁵⁾ considered the anisotropy in pore distribution and orientation, and also radiation as well as solid conduction in his derivation, but neglected gas conduction. His equation is:

$$k_p = k_s \left[(1 - P_c) + \frac{P_c}{\frac{P_L k_s}{4\sigma e \gamma d T_m^3} + (1 - P_L)} \right] \quad (B-4)$$

where P_c = cross-sectional pore fraction
 P_L = longitudinal pore fraction
 σ = Stefan-Boltzmann constant
 γ = geometrical pore factor
 e = emittance or pores
 d = dimension of pore in direction of heat flow
 T_m = mean of absolute temperature

The general applicability of the Loeb equation to anisotropic pore structures (such as oriented cylindrical pores) was confirmed experimentally⁽³³⁾ to a cross-sectional pore ratio of 0.5 (maximum tested). Materials with a high emittance were found to have a relatively higher increase in thermal conductivity above about 950°F because of the contribution from radiant heat transfer. This is in good agreement with the Loeb equation.

In order to evaluate the radiation transfer contribution to the total effective conductivity, one has to consider the equation relating the radiant thermal conductivity (k_r) with the temperature (T_m) and the materials parameter (M). The general form of this equation is:

$$k_r = 4M\sigma T_m^3$$

where σ = Stefan-Boltzmann constant

The term M includes the material emissivity, as well as the pore fraction and pore size.

In evaluating the effects of microstructure, emissivity, and transmissivity on the ceramic foam, all three modes of heat transfer--namely, conduction, convection, and radiation--must be considered. The conduction term is initially the controlling factor. If for a constant density, the pore size of the foam is increased, there will be a decrease in the solid conduction. However, at higher temperatures, the solid conduction tends to decrease while the contribution to the conductivity from the radiation transfer becomes significant and the effective conductivity increases. This increase is sharp if the material is not opaque to radiation. The temperature at which radiation becomes the controlling mechanism is different for various materials and is also dependent on the microstructure of the material.

V. MATERIALS AND PROPERTIES

A. Introduction

A review of the technical literature on foamed ceramic insulation indicates that the major effort in the development of foamed ceramics has been directed to highly refractory, resin-impregnated ablation foams for reentry applications. As a result, many of the data available in the literature pertain to materials such as alumina, zirconia, and silicon carbide. A good deal of information is also available for fused silica foams, but substantially less on various other oxide foams.

The property measurements most often determined are thermal conductivity, compressive strength, and flexural strength. Response to thermal shock environment has been obtained mainly on resin-impregnated foams, which are of minor interest to this survey, but some data have also been reported on nonimpregnated materials. Data are also available on the expansion coefficient of ceramic foams. However, very little information is available

on reflective and emissive properties. The influence of microstructure on the properties has received only minor attention and, because of this, there is considerable scatter in the reported properties of foamed materials.

B. Alumina Foams

A considerable amount of property data has been reported for foamed alumina (Al_2O_3) prepared by a variety of foaming techniques over a wide density range. The scatter in the property measurements and the uncertainties and lack of precise details of the preparation procedures are typical of most foamed ceramics that have been reported in the literature.

1. Mechanical Properties

The room-temperature compressive strength of foamed alumina as a function of density is shown in Figure B-1. The data have been obtained from five different sources. (14,16,22,24,34) The variations in the compressive strength, due to different amounts of porosity, are considerable. The maximum compressive strength reported for an alumina foam of density 30 lb/ft^3 is 500 psi, while the maximum compressive strength for a foam of density 76 lb/ft^3 is 1300 psi. The compressive strength of a 99% dense alumina is around 427,000 psi. However, there is considerable scatter in values for a particular density, as indicated by Figure B-1. For instance, the room-temperature compressive strength of an alumina foam of density 76 lb/ft^3 has been reported to be from 450 psi to 1300 psi. The lack of information concerning the micropore structure of the foams prevents correlation or possible explanation of this scatter.

Room-temperature flexural strength data obtained from the literature for alumina foams are shown in Figure B-2. As in the case of the compressive strength, considerable scatter in data is obtained preventing any correlation with foaming techniques or with density. The highest flexural strength obtained for a foam of density 32 lb/ft^3 is 550 psi, while that for an

85 lb/ft³ density foam is about 2900 psi. These values were reported by the Virginia Polytechnic Institute in a survey conducted by Bell Aircraft Corporation in 1960.⁽²⁾ No information on the method of preparation or testing of these foams is available.

The flexural strength of alumina foams of various densities over a temperature range is shown in Figure B-3. The foamed aluminas show no drastic change in strength from room temperature to 3200°F. However, the shear strength of foamed alumina has been reported⁽²⁵⁾ to have a catastrophic drop in strength beyond 2800°F. These data were reported for a foam of density 33 lb/ft³. The shear strength dropped from an average value of 205 psi at room temperature to 100 to 200 psi between 2000° and 2800°F; beyond 2800°F there was a catastrophic drop in strength.

The elastic modulus of foamed aluminas is low as reported^(36,37) from stress-deflection data obtained in flexure.

2. Thermal Conductivity

Thermal conductivity data for alumina foams are shown in Figure B-4. The thermal conductivity of the foams is significantly lower than that of the dense ceramic. The higher the density, the greater is the thermal conductivity. There is also a slight increase in the conductivity with temperatures up to 3000°F. It is important to characterize the method of determining thermal conductivity when comparing such data. Precise measurements that take into consideration heat losses are essential to obtain a representative value for thermal conductivity. Considerable scatter in the reported values may be due to different measuring techniques. For instance, in Figure B-4⁽³⁷⁾ the four curves are for alumina foam specimens produced by an identical technique and of equal density, but measured by different investigators. The four different investigators were: (a) IIT Research Institute, using the stacked disk radial flow method,

(b) an "independent laboratory," (c) a theoretical prediction, and (d) the Martin Company, using a guarded hot plate.

Measurements of similar density material by means of a radial heat flow calorimeter⁽³⁴⁾ display lower conductivity than any of the measurements presented by Martin;⁽³⁷⁾ another measurement by a comparative axial heat flow method⁽³⁶⁾ gave higher values than that of Martin. As a consequence, conductivity values for alumina foams with a density of 30 to 33 lb/ft³ vary over a wide range from approximately 0.3 to 10 Btu-in./hr-ft²-°F at 700°F to 2 to 7.5 Btu-in./hr-ft²-°F at 2000°F.

3. Thermal Exposure

The thermal exposure tests determine the temperature gradients through a specimen, and characterize the mechanical response of the material to specific heating rates. Generally, an oxyacetylene or plasma torch is used to heat the specimens to be tested.

The survey indicates that alumina foams have been found to be more resistant to thermal shock than zirconia foams, when unimpregnated by resins.⁽³⁷⁾ Higher densities and fine grain structures, necessary for high flexural strength, are required for thermal shock resistance.⁽⁵⁾ The density of the foam is a factor in determining its thermal shock resistance. Densities of below 60 lb/ft³ have been reported^(1,5) unable to withstand heating rates of 50° to 70°F/sec. A material of 33 lb/ft³ density did withstand a rate of 30°F/sec, but not 70°F/sec,⁽³⁷⁾ to a temperature of 2600°F with a 3/4 in. thickness. When this material was bonded to a honeycomb by means of resins capable of withstanding 500°F, the bond remained intact with a front face temperature of 3500°F. High-fired dense ceramic facings on the material proved satisfactory, whereas phosphate-bonded dense coatings displayed inadequate resistance to thermal stresses.

The temperature drop through a 1/2 in. foam module with a density of 31 lb/ft³ faced with Astroceram coatings (chemically-bonded zirconia) was 700°F with a front-face temperature of 3200°F.⁽¹⁹⁾ A composite of 3/8 in. of foam with a density of 60 lb/ft³ on 3/8 in. of Fiberfrax (alumino-silicate fiber mat) displayed back-face temperatures varying from 850° to 1380°F with the front-face at 3000° to 3400°F for several specimens.⁽¹⁶⁾

4. Thermal Expansion

The thermal expansion of dense or single crystal alumina is generally found to be in the range of 45 to 50×10^{-7} in/in.-°F⁽³⁸⁾ from room temperature to about 2000°F. Higher expansion coefficients are reported for foamed materials. An over-all expansion of 78×10^{-7} in/in.-°F has been reported for a 58 lb/ft³ foam in the range of 700° to 1500°F⁽¹⁶⁾ with an expansion of 98×10^{-7} in the range of 700° to 1200°F (shrinkage due to aluminum phosphate occurred at about 500°F). A 33 lb/ft³ foam displayed an expansion of $54 \times 10^{-7}/^{\circ}\text{F}$ for room temperature to 2300°F, with approximately $75 \times 10^{-7}/^{\circ}\text{F}$ in the range of 1650° to 2300°F.⁽³⁷⁾ Virginia Polytechnic reports $100 \times 10^{-7}/^{\circ}\text{F}$ for their material in a density range of 20 to 80 lb/ft³.⁽²⁾

5. Emittance

Data have been reported⁽¹⁶⁾ on the total hemispherical emittance of an alumina foam having a density of 60 lb/ft³ and prepared by the aluminum-phosphoric acid reaction. The emittance measured over a temperature range of 1500° to 2700°F is shown in Figure B-5. The emittance of the alumina foam decreased from 0.40 to 0.35 in this temperature range. The addition of coloring oxides, such as NiO-Cr₂O₃, increases the emittance of the alumina. Figure B-5 indicates that a 15% addition of 80/20 NiO-Cr₂O₃ caused a 47% increase in the emittance of alumina, to give a value of about 0.65. The alumina foam with a coating of

oxidized Inconel X powder possessed the highest emittance of about 0.83.

In general, there is a lack of sufficient data on the emittance characteristics of ceramic foams. Such data would be particularly helpful for reentry applications, where in order to take full advantage from radiation cooling, a high surface emissivity is desirable.

C. Zirconia

Zirconia in foam structures has received much attention because of its superior performance in ablative composites when impregnated with resins. Structural stabilization is required to prevent a phase and an accompanying volume change of monoclinic to tetragonal at approximately 1800°F. Calcium oxide is generally employed--approximately 5 wt%--to impart a nontransforming cubic phase. Other stabilizers are also employed with zirconia, notably oxides of yttrium, magnesium, and cerium.

The advantages of stabilized zirconia in heat-shield applications include a melting point of approximately 4700°F and a very low thermal conductivity. However, its relatively high coefficient of thermal expansion, approximately 5×10^{-6} in./in./°F, produces severe thermal stresses on nonuniform heating, resulting in mechanical degradation and failure.⁽³⁸⁾ The thermal expansion is reduced in some zirconia materials by partial, rather than full stabilization, on the assumption that a small volume change on phase transformation will be less disruptive than the higher thermal expansion.⁽⁵⁾ As a consequence, the coefficient of expansion is a factor which must also be considered in correlating mechanical properties with density and microstructure.

1. Mechanical Properties

A summary of the mechanical properties of zirconia foams is given in Table B-I. This table shows the effect of

TABLE B-1
MECHANICAL PROPERTIES OF ZIRCONIA FOAMS

AT ROOM TEMPERATURE

Average Density, lb/ft ³	Average Open Cells	Average Porosity, % Closed Cells	Average Pore Size, microns	Average Flexural Strength, psi	Average Comp. Strength, psi	Average Mod. of Elas., psi	Coeff. of Thermal Expansion (70-1800°F), in/in/°F	Ref.
46	87.1	.03		76	137	980	4.80	39
50	86.0	.03		230	569	1190	4.54	39
99	72.0	.06		148	469	365	3.92	39
38	89.1	.35	Fine	285	566	3449	4.88	39
35	88.5	.43	Medium	342	596	3559	4.70	39
36	89.4	.49	Coarse	209	363	2473	4.35	39
61	81.9	.17		261	1953	4878	3.64	39
69	81.6	.03		17	195	2968	4.04	39
100				185	228		5.16	16
70				84			5.16	16
53			200	5167				9
47			300	4053				9
55			1000	1400				9

IIT RESEARCH INSTITUTE

foam density on the average room-temperature flexural and compressive strength and the modulus of elasticity. The data from Reference 39 were obtained on materials received from several manufacturers. All of the zirconia specimens represented in the table are presumed to be lime-stabilized except for those of Reference 16 which were ceria-stabilized. The lime-stabilized materials with expansion coefficients of less than $4.8 \times 10^{-6}/^{\circ}\text{F}$ are partially stabilized.

The data on the lime-stabilized zirconia foams indicate that for a specific density the distribution of closed and open pores is significant in determining the strength characteristics.

2. Thermal Conductivity

The thermal conductivities of lime-stabilized zirconia foams varying in density from 38 to 60 lb/ft³, are shown in Fig. B-6. These results indicate that the thermal conductivity of zirconia foams in the density range of 38 to 60 lb/ft³ vary from 1.1 to 2.9 Btu-in/hr-ft²-^oF at 500^oF and 2 to 10 Btu-in/hr-ft²-^oF at 3000^oF. Generally speaking, the higher the density, the higher is the thermal conductivity whenever solid conduction is predominant. However, at higher temperatures, where radiation heat transfer becomes significant, this relationship is not necessarily true. This is well illustrated in Fig. B-7. In the lower temperature range, the zirconia foam with the higher porosity has the lower thermal conductivity. However, at a temperature of around 1560^oF, in the foam with the lower density the contribution to the conductivity from the radiation transfer is far greater than in the denser foam and consequently, its thermal conductivity increases over that of the denser foam. The radiation transfer could be effectively attenuated at high temperatures by dispersions of metallic and carbonaceous materials in the zirconia foams.⁽⁴⁰⁾ Zirconia foams appear to exhibit

a larger radiation component to heat transfer than do alumina foams, which may be due in part to the higher emissivity of zirconia.

3. Thermal Exposure

In general, the unimpregnated zirconia foams are significantly weakened by thermal exposure, regardless of the method of manufacture or density.^(1,37) Foams of higher density and relatively large grain size (if fired to high temperature in manufacturing) were found to be thermal shock resistant in one investigation.⁽⁵⁾ In another,⁽³⁹⁾ void-free cell walls were found most necessary for good thermal performance, along with small cell size. The use of zirconia facings on the foam did not help the thermal performance.^(36,37) Greater thermal stresses were withstood in a direction parallel to the direction of foaming, due to the flattening of cells in lower portions of foamed bodies in processing.⁽³⁷⁾

With a hot face of 2550°F, the temperature at the back of a ½ in. zirconia foam module of a density of 51 lb/ft³ with a cemented facing, was 1290°F.⁽³⁶⁾ Placing a 100 lb/ft³ density foam of 3/8 in. thickness on 3/8 in. of Fiberfrax resulted in a range of 990°-1290°F at the back face with 3100°-3800°F on the front face.⁽¹⁶⁾

4. Thermal Expansion

The coefficient of thermal expansion of zirconia foams is shown in Table B-I. Expansion coefficients from 2.24 to 6.86 x 10⁻⁶/°F have been obtained by varying the composition of various stabilized zirconia foams. It has also been found⁽¹⁶⁾ that the first heating cycle produced different expansion rates than subsequent heating cycles. This may be due to curing or further densification.

5. Emittance

There is a lack of detailed information on the emittance of zirconia foams. The spectral emittance of foamed zirconia at 45 lb/ft^3 density has been reported to be 0.32 to 0.34 at 1800° to 2130°F , and 0.59 at 2770°F .⁽³⁷⁾ The total emittance of a 100 lb/ft^3 material was measured as approximately 0.62 over the range of 1600° to 2600°F .⁽¹⁶⁾

D. Silica

Silica is an especially useful material where thermal gradients are encountered due to its very low coefficient of thermal expansion which provides excellent thermal shock resistance. The use of visibly opaque fused silica attenuates radiant energy more effectively than the clear form, and most foaming work has been performed on the opaque fused silica.^(6,41) This form also resists devitrification (transformation to cristobalite) at 2000°F better than the clear form.⁽⁴¹⁾

1. Mechanical Properties

The average compressive strengths reported⁽⁴²⁾ at room temperature for foamed silica with a density of about 39 lb/ft^3 , which was foamed by gas release in the molten silica, were about 500 psi. Comparable strengths were also obtained for an identical density foam prepared by organic burnout and cured at 600°F .⁽¹⁶⁾ The latter material displayed an average compressive strength of 825 psi at 1000°F .⁽¹⁶⁾ A commercial manufacturer⁽⁴³⁾ has reported a compressive strength of 500 psi for a silica foam with a density of 25 lb/ft^3 and a strength of 1000 psi for a similar foam of 50 lb/ft^3 density.

Room-temperature flexural strengths are reported in the range of 200-500 psi for a mechanically whipped and fired foam with density averaging 37 lb/ft^3 , while an organic burnout, inorganically-bonded product of 40 lb/ft^3 displayed flexural

strengths of 210 to 292 psi at room temperature and 302 to 425 psi at 1000°F. (16) The flexural strength of the above-mentioned silica foam, (43) was 100 psi for a material with a density of 25 lb/ft³ and 200 psi for material having a density of 50 lb/ft³.

The tensile strength measured indirectly by the brittle ring test also showed that the strength of dense fused silica increases with temperature, presumably due to reduced brittleness. (6) These measurements were not made on foams.

2. Thermal Properties

The thermal properties of silica foams have not been characterized to the same extent as alumina or zirconia foams. The thermal expansion of fused silica foams was found to be 0.30×10^{-6} in/in/°F. (6) Addition of quartz to the fused silica foam gave a body of coefficient $13.5 \times 10^{-6}/°F$ in the temperature range 200°-600°F and $1.86 \times 10^{-6}/°F$ from 800°-1500°F. (16)

Thermal conductivity values for foamed bodies of 31-44 lb/ft³ were 1.20 Btu-in/ft²-hr-°F at room temperature, 1.44 at 1000°F, and 2.40 at 2000°F. (21) A 45 lb/ft³ material was reported to have a thermal conductivity of 1.4 Btu-in/ft²-hr-°F at 1000°F. (44)

Composites of 3/8 in. thick foamed fused silica, 45 lb/ft², backed with 3/8 in. of Fiberfrax reached a back-face temperature of 1215°-1495°F with the front-face temperature at 2850°F. (16)

E. Aluminosilicate Materials

Clay and mineral products, high in aluminum and silicon oxides, are used extensively in the ceramic industry because of their low cost and ready availability. Aluminum-silicates are of special interest in applications of nonisothermal conditions because of their generally good thermal shock resistance, due to a low coefficient of expansion.

A series of mechanically whipped foams made of alumina and 10 to 40% clay, fired at 2700°F, and with a density of 60 lb/ft³ displayed compressive strengths of 1700-2100 psi.⁽⁷⁾ These were useful to 2900°F and showed a very good resistance to thermal shock.

A fireclay body foamed by mechanical whipping and fired at 2200°F, displayed typical properties as shown in Table B-II.⁽³⁾ The thermal conductivity for a 57 lb/ft³ density foam, at room temperature, was 1.41 Btu-in/ft²-hr-°F. Water absorption was 35-50% on a 24-hr cold soak and 70 to 85% on a 5-hr boil. Bloated fireclay bodies prepared by the same investigators displayed compressive strengths of over 4000 psi; however, they did not show the reproducibility that was obtained with the mechanically prepared foams. The impermeable bloated products absorbed only 0.4 to 4% of water after a 5-hr boil.⁽³⁾

Lithium-aluminum silicates have particularly low, sometimes negative, coefficients of thermal expansion. Mechanically whipped foams were produced by petalite and spodumene using kaolin for increased fired strength and colloidal boehmite for foam stabilization.⁽¹²⁾ Foams with densities in the range of 55 to 63 lb/ft³ were prepared which had crushing strengths varying from 400 to 4900 psi, depending upon the firing temperature and composition. Flexural strengths of up to approximately 1200 psi were obtained. Expansion coefficients ranged from approximately 0.1 to 0.4 x 10⁻⁶/°F, depending on composition and firing temperature. This is comparable to that of fused silica, with the additional advantage that devitrification is not a problem in this material.

F. Miscellaneous Foamed Materials

Some work has also been reported on other ceramic foamed materials. Data reported on silicon carbide foams include a thermal conductivity of 6.0 Btu-in/ft²-hr-°F at 1000°F

TABLE B-II
TYPICAL PROPERTIES OF FOAMED FIRECLAY⁽³⁾

Density, lb/ft ³	Compressive Strength, psi	Flexural Strength, psi	Modulus of Elasticity, psi
51	1177	376	355,000
55	1334	431	728,000
61	1507	524	868,000

(guarded hot plate)⁽⁴⁴⁾ and 6 to 8 Btu-in/ft²-hr-°F at 1900°F⁽⁴⁴⁾ for a 16 lb/ft³ material. This foam had a compressive strength of 85 psi. A material of 31-37 lb/ft³ displayed a compressive strength of 750 psi and a thermal conductivity of 11-14 Btu-in/ft²-hr-°F at 1900°F.⁽⁴⁴⁾ A coefficient of expansion of $2.91 \times 10^{-6}/^{\circ}\text{F}$ is reported at 2450°F.⁽³⁴⁾

Development work has also been performed on magnesia foams. Mechanically whipped foams, set with plaster, were prepared⁽⁴⁾ with a uniform structure, with compressive strengths of 650-1140 psi in the density range of 42-50 lb/ft³ after firing at 2850°F. Property measurements on the open cell foamed magnesia with an average density of 56 lb/ft³ showed an average flexural strength of 123 psi, and thermal expansion of $6.60 \times 10^{-6}/^{\circ}\text{F}$ to 1800°F.⁽³⁹⁾

Some information is also available on foamed metals. These, however, are not pertinent to our investigation and will not, therefore, be discussed.

G. Fibrous Insulation

It is interesting to compare the properties of refractory fibrous insulation with those of the foamed oxides. Both advantages and disadvantages are evident in a comparison of the properties of fibrous and foamed ceramic insulation. Fibrous materials have an advantage of low thermal conductivity as shown in Figure B-8; however, they are extremely weak mechanically.

The thermal conductivity of Johns-Manville Micro-Quartz Type II fibrous silica (density 4.58 lb/ft³) was measured in various environments by radial heat flow. Values obtained in ambient air are shown in Table B-III.⁽⁴⁵⁾ Thermal conductivity measurements in vacuum were about half of those reported in Table B-III. The radiation transfer becomes significant above 1700°F. Other measurements on the same material showed a thermal conductivity increase from 0.53 Btu-in/ft²-hr-°F at 600°F to 1.55

TABLE B-III
THERMAL CONDUCTIVITY OF MICRO-QUARTZ
FIBROUS SILICA*⁽⁴⁵⁾

Temperature, °F	Thermal Conductivity, Btu-in/ft ² -hr-°F
540	0.439
1057	0.640
1527	0.852
1575	0.880
2194	1.487
2542	2.360

*Reported ⁽⁴⁵⁾ density 4.58 lb/ft³.

at 2100°F for a 4.5 lb/ft³ density material, which is in good agreement with the data in Table B-III.⁽⁴⁶⁾ Heavier felts of 10 lb/ft³ display a lower conductivity of 1.17 Btu-in/ft²-hr-°F at 2100°F.

A fibrous ceramic insulation that has attractive properties has been prepared.⁽⁴⁷⁾ This is the "M-31" which is a colloidal silica-bonded potassium titanate fiber insulation with a density of 53-56 lb/ft³. The M-31 has anisotropic thermal conductivity. The conductivity with the heat flowing in the direction parallel to the plane of application is essentially constant at 1.7 Btu/ft²/hr/°F/in. in the temperature range 100° to 1500°F. With the heat flowing in the direction normal to the plane of application, the thermal conductivity is 0.85 Btu-in/ft²-hr-°F at 100°F and increases to 1.3 Btu-in/ft²-hr-°F at 730°F.

The coefficients of thermal expansion along the hard (exterior) and soft (interior) faces of the material were determined to be $9.2 \times 10^{-7}/^{\circ}\text{F}$ and $48.0 \times 10^{-7}/^{\circ}\text{F}$, respectively, in the 200° - 1500°F temperature range.

This material is also reported to have good reflective and emissive characteristics as well as good mechanical properties, especially to vibration and shock.

H. Summary

Although considerable data have been reported on the mechanical and thermal properties of foamed oxides, much of it is unreliable and very poorly characterized for microstructural variations. This is evident in the wide scatter of the reported properties, which makes correlation between the physical properties and its mechanical and thermal characteristics difficult.

The survey bears out some definite trends about the present state-of-the-art of foamed ceramic insulation materials.

First, much of the reported data are for far higher temperature refractory foams than the range required for our application. There are considerable data available for resin-impregnated ablation forms, most of them having a density greater than 60 lb/ft³. Secondly, there is a lack of useful information on the reflective and emissive properties of ceramic foams. Thirdly, very little attention has been paid to characterizing the properties of these foams as a function of their micropore structure. This is especially important if one is to understand the thermal radiation characteristics of semi-transparent materials such as polycrystalline ceramics, where radiant energy emission is a volume process and, therefore, influenced by the microstructure of the foamed material.

VI. ANALYSIS OF THE TECHNICAL QUESTIONNAIRE

A technical questionnaire was sent to 29 organizations. To date, 15 organizations answered the questionnaire. Of these only 11 companies are involved in developing, manufacturing or marketing ceramic foams. This is shown in Table B-IV.

A tabulation of the various types of ceramic foams that are being developed or manufactured by the organizations who responded to the technical questionnaire is shown in Table B-V.

Silica and alumina foams are the most commonly available materials. A stabilized-zirconia foam is also commercially available. One organization reported that they are developing magnesia and thoria foams.

Compressive strength, flexural strength, and thermal conductivity are the most easily available properties that have been measured by the manufacturers. A limited amount of information is available on the emittance values of some of the foams. No data were obtained on the reflectance of any of these foams.

TABLE B-IV

RECIPIENTS OF TECHNICAL SURVEY QUESTIONNAIRE

Low Density Refractory Foam:
Development, Property Evaluation and Marketing

Company Name and Address	Answered Inquiry	Not Applicable	Research and Development	Property Evaluation	Marketing	Government Sponsorship	Samples Received
1. Aeronca Manufacturing Co. Middleton, Ohio	X		X	X		X	
2. Aluminum Co. of America Pittsburgh, Pennsylvania							
3. American Lava Corporation Chattanooga, Tennessee	X		X	X	X		
4. Astro Met Associates Cincinnati, Ohio							
5. Boeing Company Seattle, Washington	X		X	X		X	
6. Carborundum Company Niagara Falls, New York	X		X	X	X		X
7. Emerson and Cuming, Inc. Canton, Massachusetts	X		X	X	X	X	
8. Foote Mineral Company Exton, Pennsylvania	X	X					
9. Ford Scientific Center Dearborn, Michigan							
10. General Dynamics Corp. Ft. Worth, Texas							
11. General Electric Company Central Research Laboratory Schenectady, New York							

IIT RESEARCH INSTITUTE

TABLE B-IV (Cont'd)

Company Name and Address	Answered Inquiry	Not Applicable	Research and Development	Property Evaluation	Marketing	Government Sponsorship	Samples Received
12. General Electric Company Chemical Materials Dept. Pittsfield, Massachusetts	X	X					
13. General Electric Company Materials Product Dev. Detroit, Michigan	X		X		X		X
14. General Motors Corp. Flint, Michigan							
15. Glasrock Corporation Atlanta, Georgia	X		X	X	X		X
16. International Pipe and Ceramic Corporation Los Angeles, California	X	X					
17. Ipsen Industries, Inc. Rockford, Illinois							
18. Kaiser Refractories Oakland, California	X		X	X	X	X	
19. Martin Company Space Systems Division Baltimore, Maryland	X		X	X			
20. McDonnell Aircraft Corp. St. Louis, Missouri	X		X	X		X	
21. Melpar, Incorporated Falls Church, Virginia	X		X	X	X	X	

IIT RESEARCH INSTITUTE

TABLE B-IV (Cont'd)

Company Name and Address	Answered Inquiry	Not Applicable	Research and Development	Property Evaluation	Marketing	Government Sponsorship	Samples Received
22. National Beryllia Corp. Haskell, New Jersey							
23. Northrop Corporation Ventura, California							
24. Norton Company Worcester, Massachusetts							
25. Simoniz Corporation Chicago, Illinois	X	X					
26. Titanium Alloy Mfg. Div. New York							
27. United Technology Center Sunnyvale, California							
28. Virginia Polytechnic Institute Blacksburg, Virginia							
29. Zirconium Corporation of America Cleveland, Ohio							

IIT RESEARCH INSTITUTE

PROPERTY DATA ON CERAMIC FOAMS

ORGANIZATION	COMPOSITION	MULTI-POINT % P	DENSITY LB./FT. ³	AVAILABILITY	PIRE SIZE	COMPRESSIVE STRENGTH, PSI	FLUTURAL STRENGTH, PSI	THERMAL CONDUCTIVITY BTU-IN./FT. ² °F-HR	SPECIFIC HEAT, BTU/LB. °F	COEFF. OF EXPANSION, 10 ⁻⁷ IN./IN. °F	EMITTANCE	REFLECTANCE	DIMENSIONS NORMALLY SUPPLIED, IN.	COST PER SHEET, \$
ANTONEX Mfg.	Silica	3000	40	d	44 μ	500-550 (RT)	275 (RT) 400 (1000F)	3-38		135 (200-600°F) 18.6 (600-1500°F)	0.30 (2600°F)		1x6x6	
	Alumina	1500	55	d	17/32-1/16 in.	400-500 (RT)	200-250 (RT)	2.5		70 (200-500°F) 98 (700-1200°F)	0.35 (2600°F)			
American Lava Corp.	Stabilized ZrO ₂ (ATSI Mag 766)	4000	27-53	p	.016 in.	120 (RT)		See Fig. 10		See Fig. 12				
	Alumina (ATSI Mag 761)	3200	19-40	p	.016	400 (RT)		See Fig. 11						
Baird Co.	Alumina (ATSI Mag 614)	3000	19-40	p	.016									
	Silica (98.5%)	3100	4.5-8.0	p		9.6-11.4 (RT) (ρ=6.2 lb./ft. ³)	1-3K (RT) 20-25 (2500°F)	1.7 (2500°F) (ρ=8.0 lb./ft. ³)						
Baird and Galt, Inc.	Silica (98.5%)	>4200	3-4	p										
	Alumina (99.5%)	>4000	3-4	p										
Emerald and Galt, Inc.	Alumina (99.5%)	>4000	4.5-8.0	p	<1/8 in.	500 (RT)	500 (RT) 150 (500°F) 12F	1.2 1.3-1.4 0.3					12x18x4 1/2 6x6x1/4 11x17x2-3	80 12 30-45
	Silica (99.5%)	>4000	4.5-8.0	p	<1/8 in.	500 (RT)	500 (RT)	1.2						
General Electric	Alumina (99.5%)	>4000	3-6	d	.03-.06 in.	500 (RT)	400 (RT)	1.0 (1000°F)						
	Silica (99.5%)	>4000	3-6	d	.03-.06 in.	1000 (RT)	300 (RT)	1.4 (1000°F)						
General Electric	Alumina (99.5%)	>4000	3-6	d	.03-.06 in.	500 (RT)	400 (RT)	1.0 (1000°F)						
	Silica (99.5%)	>4000	3-6	d	.03-.06 in.	1000 (RT)	300 (RT)	1.4 (1000°F)						
General Electric	Alumina (99.5%)	>4000	3-6	d	.03-.06 in.	500 (RT)	400 (RT)	1.0 (1000°F)						
	Silica (99.5%)	>4000	3-6	d	.03-.06 in.	1000 (RT)	300 (RT)	1.4 (1000°F)						
General Electric	Alumina (99.5%)	>4000	3-6	d	.03-.06 in.	500 (RT)	400 (RT)	1.0 (1000°F)						
	Silica (99.5%)	>4000	3-6	d	.03-.06 in.	1000 (RT)	300 (RT)	1.4 (1000°F)						
General Electric	Alumina (99.5%)	>4000	3-6	d	.03-.06 in.	500 (RT)	400 (RT)	1.0 (1000°F)						
	Silica (99.5%)	>4000	3-6	d	.03-.06 in.	1000 (RT)	300 (RT)	1.4 (1000°F)						
General Electric	Alumina (99.5%)	>4000	3-6	d	.03-.06 in.	500 (RT)	400 (RT)	1.0 (1000°F)						
	Silica (99.5%)	>4000	3-6	d	.03-.06 in.	1000 (RT)	300 (RT)	1.4 (1000°F)						
General Electric	Alumina (99.5%)	>4000	3-6	d	.03-.06 in.	500 (RT)	400 (RT)	1.0 (1000°F)						
	Silica (99.5%)	>4000	3-6	d	.03-.06 in.	1000 (RT)	300 (RT)	1.4 (1000°F)						
General Electric	Alumina (99.5%)	>4000	3-6	d	.03-.06 in.	500 (RT)	400 (RT)	1.0 (1000°F)						
	Silica (99.5%)	>4000	3-6	d	.03-.06 in.	1000 (RT)	300 (RT)	1.4 (1000°F)						
General Electric	Alumina (99.5%)	>4000	3-6	d	.03-.06 in.	500 (RT)	400 (RT)	1.0 (1000°F)						
	Silica (99.5%)	>4000	3-6	d	.03-.06 in.	1000 (RT)	300 (RT)	1.4 (1000°F)						
General Electric	Alumina (99.5%)	>4000	3-6	d	.03-.06 in.	500 (RT)	400 (RT)	1.0 (1000°F)						
	Silica (99.5%)	>4000	3-6	d	.03-.06 in.	1000 (RT)	300 (RT)	1.4 (1000°F)						
General Electric	Alumina (99.5%)	>4000	3-6	d	.03-.06 in.	500 (RT)	400 (RT)	1.0 (1000°F)						
	Silica (99.5%)	>4000	3-6	d	.03-.06 in.	1000 (RT)	300 (RT)	1.4 (1000°F)						
General Electric	Alumina (99.5%)	>4000	3-6	d	.03-.06 in.	500 (RT)	400 (RT)	1.0 (1000°F)						
	Silica (99.5%)	>4000	3-6	d	.03-.06 in.	1000 (RT)	300 (RT)	1.4 (1000°F)						
General Electric	Alumina (99.5%)	>4000	3-6	d	.03-.06 in.	500 (RT)	400 (RT)	1.0 (1000°F)						
	Silica (99.5%)	>4000	3-6	d	.03-.06 in.	1000 (RT)	300 (RT)	1.4 (1000°F)						
General Electric	Alumina (99.5%)	>4000	3-6	d	.03-.06 in.	500 (RT)	400 (RT)	1.0 (1000°F)						
	Silica (99.5%)	>4000	3-6	d	.03-.06 in.	1000 (RT)	300 (RT)	1.4 (1000°F)						
General Electric	Alumina (99.5%)	>4000	3-6	d	.03-.06 in.	500 (RT)	400 (RT)	1.0 (1000°F)						
	Silica (99.5%)	>4000	3-6	d	.03-.06 in.	1000 (RT)	300 (RT)	1.4 (1000°F)						
General Electric	Alumina (99.5%)	>4000	3-6	d	.03-.06 in.	500 (RT)	400 (RT)	1.0 (1000°F)						
	Silica (99.5%)	>4000	3-6	d	.03-.06 in.	1000 (RT)	300 (RT)	1.4 (1000°F)						
General Electric	Alumina (99.5%)	>4000	3-6	d	.03-.06 in.	500 (RT)	400 (RT)	1.0 (1000°F)						
	Silica (99.5%)	>4000	3-6	d	.03-.06 in.	1000 (RT)	300 (RT)	1.4 (1000°F)						
General Electric	Alumina (99.5%)	>4000	3-6	d	.03-.06 in.	500 (RT)	400 (RT)	1.0 (1000°F)						
	Silica (99.5%)	>4000	3-6	d	.03-.06 in.	1000 (RT)	300 (RT)	1.4 (1000°F)						
General Electric	Alumina (99.5%)	>4000	3-6	d	.03-.06 in.	500 (RT)	400 (RT)	1.0 (1000°F)						
	Silica (99.5%)	>4000	3-6	d	.03-.06 in.	1000 (RT)	300 (RT)	1.4 (1000°F)						
General Electric	Alumina (99.5%)	>4000	3-6	d	.03-.06 in.	500 (RT)	400 (RT)	1.0 (1000°F)						
	Silica (99.5%)	>4000	3-6	d	.03-.06 in.	1000 (RT)	300 (RT)	1.4 (1000°F)						
General Electric	Alumina (99.5%)	>4000	3-6	d	.03-.06 in.	500 (RT)	400 (RT)	1.0 (1000°F)						
	Silica (99.5%)	>4000	3-6	d	.03-.06 in.	1000 (RT)	300 (RT)	1.4 (1000°F)						
General Electric	Alumina (99.5%)	>4000	3-6	d	.03-.06 in.	500 (RT)	400 (RT)	1.0 (1000°F)						
	Silica (99.5%)	>4000	3-6	d	.03-.06 in.	1000 (RT)	300 (RT)	1.4 (1000°F)						
General Electric	Alumina (99.5%)	>4000	3-6	d	.03-.06 in.	500 (RT)	400 (RT)	1.0 (1000°F)						
	Silica (99.5%)	>4000	3-6	d	.03-.06 in.	1000 (RT)	300 (RT)	1.4 (1000°F)						
General Electric	Alumina (99.5%)	>4000	3-6	d	.03-.06 in.	500 (RT)	400 (RT)	1.0 (1000°F)						
	Silica (99.5%)	>4000	3-6	d	.03-.06 in.	1000 (RT)	300 (RT)	1.4 (1000°F)						
General Electric	Alumina (99.5%)	>4000	3-6	d	.03-.06 in.	500 (RT)	400 (RT)	1.0 (1000°F)						
	Silica (99.5%)	>4000	3-6	d	.03-.06 in.	1000 (RT)	300 (RT)	1.4 (1000°F)						
General Electric	Alumina (99.5%)	>4000	3-6	d	.03-.06 in.	500 (RT)	400 (RT)	1.0 (1000°F)						
	Silica (99.5%)	>4000	3-6	d	.03-.06 in.	1000 (RT)	300 (RT)	1.4 (1000°F)						
General Electric	Alumina (99.5%)	>4000	3-6	d	.03-.06 in.	500 (RT)	400 (RT)	1.0 (1000°F)						
	Silica (99.5%)	>4000	3-6	d	.03-.06 in.	1000 (RT)	300 (RT)	1.4 (1000°F)						
General Electric	Alumina (99.5%)	>4000	3-6	d	.03-.06 in.	500 (RT)	400 (RT)	1.0 (1000°F)						
	Silica (99.5%)	>4000	3-6	d	.03-.06 in.	1000 (RT)	300 (RT)	1.4 (1000°F)						
General Electric	Alumina (99.5%)	>4000	3-6	d	.03-.06 in.	500 (RT)	400 (RT)	1.0 (1000°F)						
	Silica (99.5%)	>4000	3-6	d	.03-.06 in.	1000 (RT)	300 (RT)	1.4 (1000°F)						
General Electric	Alumina (99.5%)	>4000	3-6	d	.03-.06 in.	500 (RT)	400 (RT)	1.0 (1000°F)						
	Silica (99.5%)	>4000	3-6	d	.03-.06 in.	1000 (RT)	300 (RT)	1.4 (1000°F)						
General Electric	Alumina (99.5%)	>4000	3-6	d	.03-.06 in.	500 (RT)	400 (RT)	1.0 (1000°F)						
	Silica (99.5%)	>4000	3-6	d	.03-.06 in.	1000 (RT)	300 (RT)	1.4 (1000°F)						
General Electric	Alumina (99.5%)	>4000	3-6	d	.03-.06 in.	500 (RT)	400 (RT)	1.0 (1000°F)						
	Silica (99.5%)	>4000	3-6	d	.03-.06 in.	1000 (RT)	300 (RT)	1.4 (1000°F)						
General Electric	Alumina (99.5%)	>4000	3-6	d	.03-.06 in.	500 (RT)	400 (RT)	1.0 (1000°F)						
	Silica (99.5%)	>4000	3-6	d	.03-.06 in.	1000 (RT)	300 (RT)	1.4 (1000°F)						
General Electric	Alumina (99.5%)	>4000	3-6	d	.03-.06 in.	500 (RT)	400 (RT)	1.0 (1000°F)						
	Silica (99.5%)	>4000	3-6	d	.03-.06 in.	1000 (RT)	300 (RT)	1.4 (1000°F)						
General Electric	Alumina (99.5%)	>4000	3-6	d	.03-.06 in.	500 (RT)	400 (RT)	1.0 (1000°F)						
	Silica (99.5%)	>4000	3-6	d	.03-.06 in.	1000 (RT)	300 (RT)	1.4 (1000°F)						
General Electric	Alumina (99.5%)	>4000	3-6	d	.03-.06 in.	500 (RT)	400 (RT)	1.0 (1000°F)						
	Silica (99.5%)	>4000	3-6	d	.03-.06 in.	1000 (RT)	300 (RT)	1.4 (1000°F)						
General Electric	Alumina (99.5%)	>4000	3-6	d	.03-.06 in.	500 (RT)	400 (RT)	1.0 (1000°F)						
	Silica (99.5%)	>4000	3-6	d	.03-.06 in.	1000 (RT)	300 (RT)	1.4 (1000°F)						
General Electric	Alumina (99.5%)	>4000	3-6	d	.03-.06 in.	500 (RT)	400 (RT)	1.0 (1000°F)						
	Silica (99.5%)	>4000	3-6	d	.03-.06 in.	1000 (RT)	300 (RT)	1.4 (1000°F)						
General Electric	Alumina (99.5%)	>4000	3-6	d	.03-.06 in.	500 (RT)	400 (RT)	1.0 (1000°F)						
	Silica (99.5%)	>4000	3-6	d	.03-.06 in.	1000 (RT)	300 (RT)	1.4 (1000°F)						
General Electric	Alumina (99.5%)	>4000	3-6	d	.03-.06 in.	500 (RT)	400 (RT)	1.0 (1000°F)						
	Silica (99.5%)	>4000	3-6	d	.03									

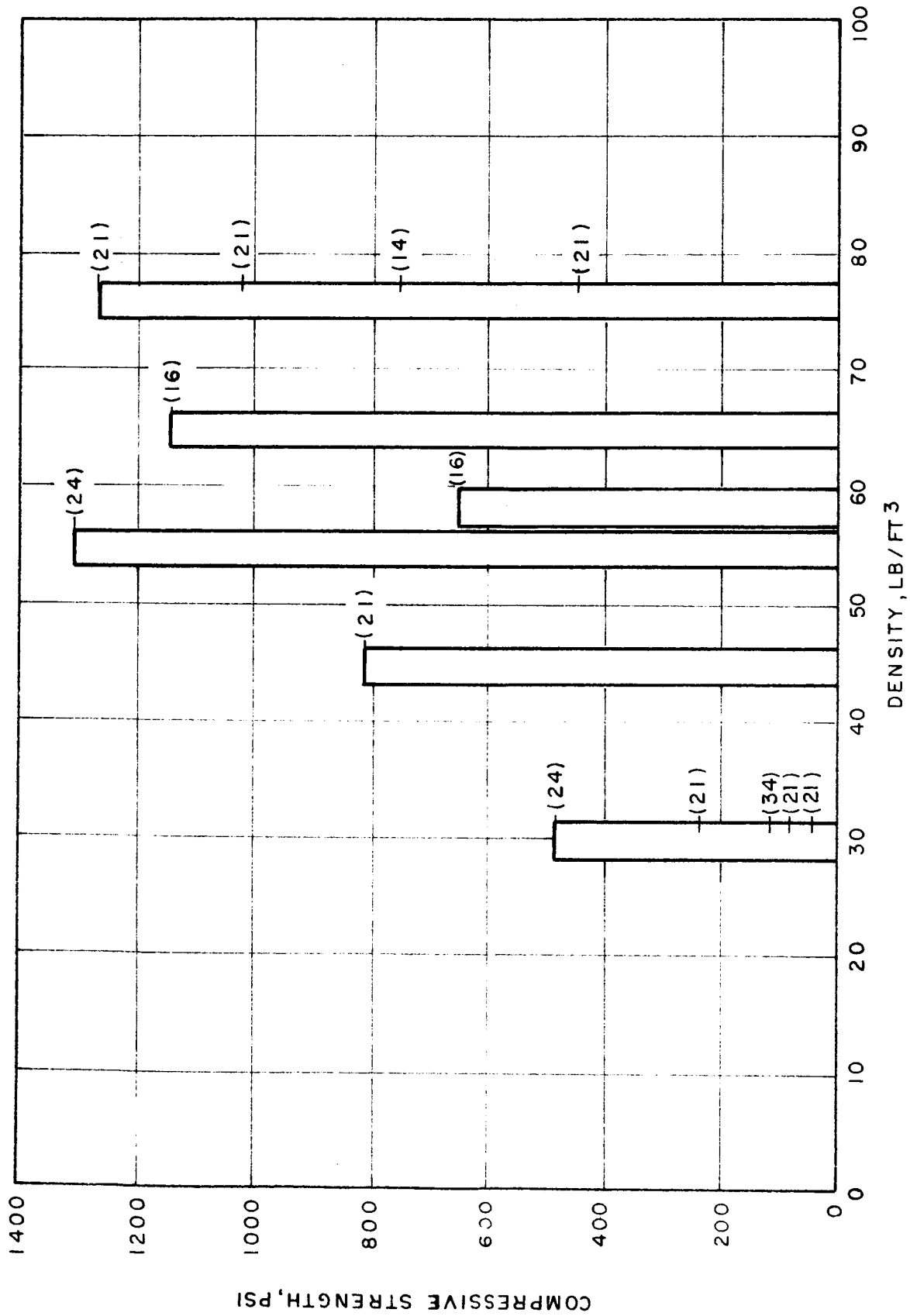


FIG. B-1 - COMPRESSIVE STRENGTH OF ALUMINA FOAMS AT ROOM TEMPERATURE (Numbers in parenthesis indicate References)

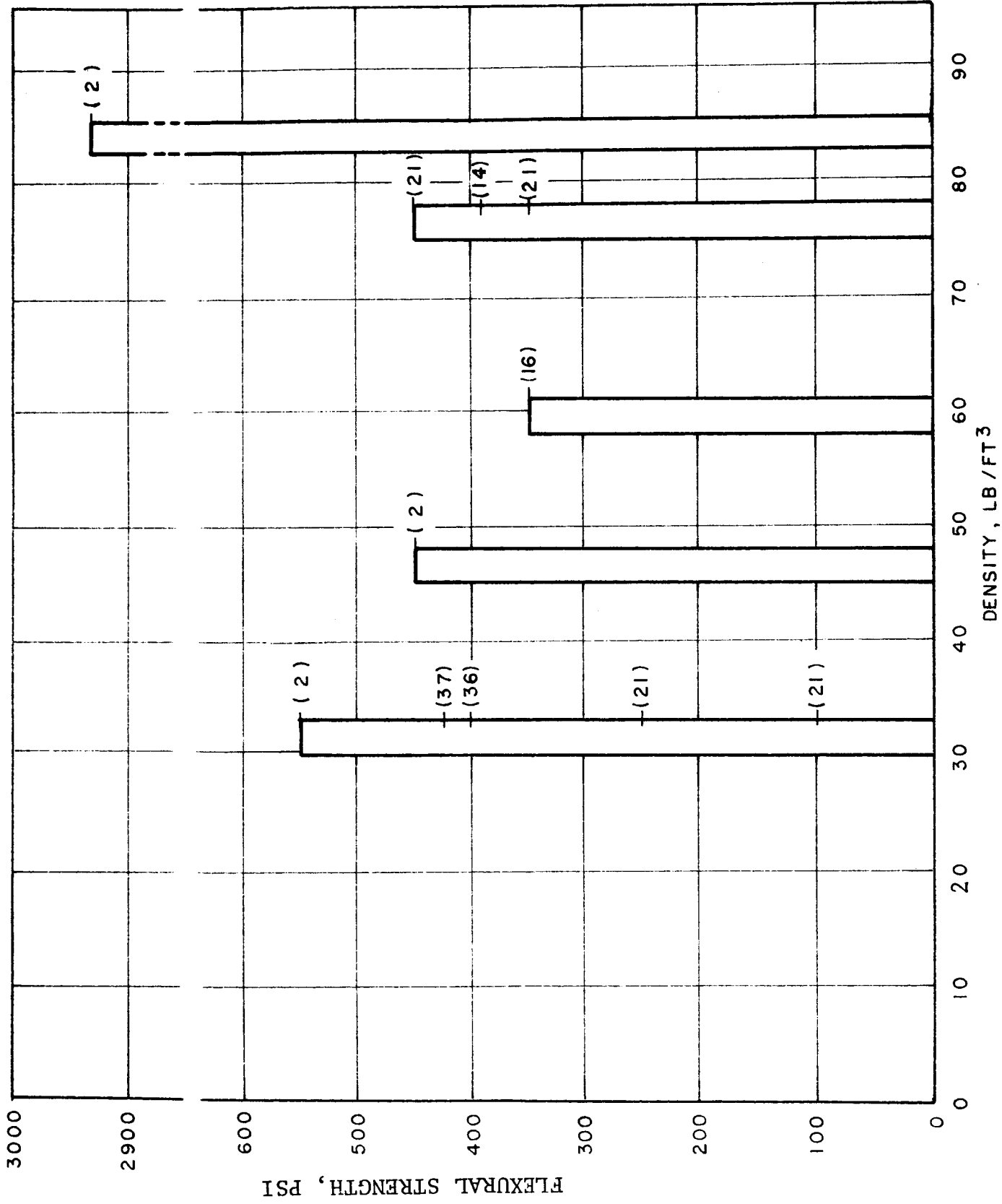


FIG. B-2 - FLEXURAL STRENGTH OF ALUMINA FOAMS AT ROOM TEMPERATURE (Numbers in parenthesis indicate References)

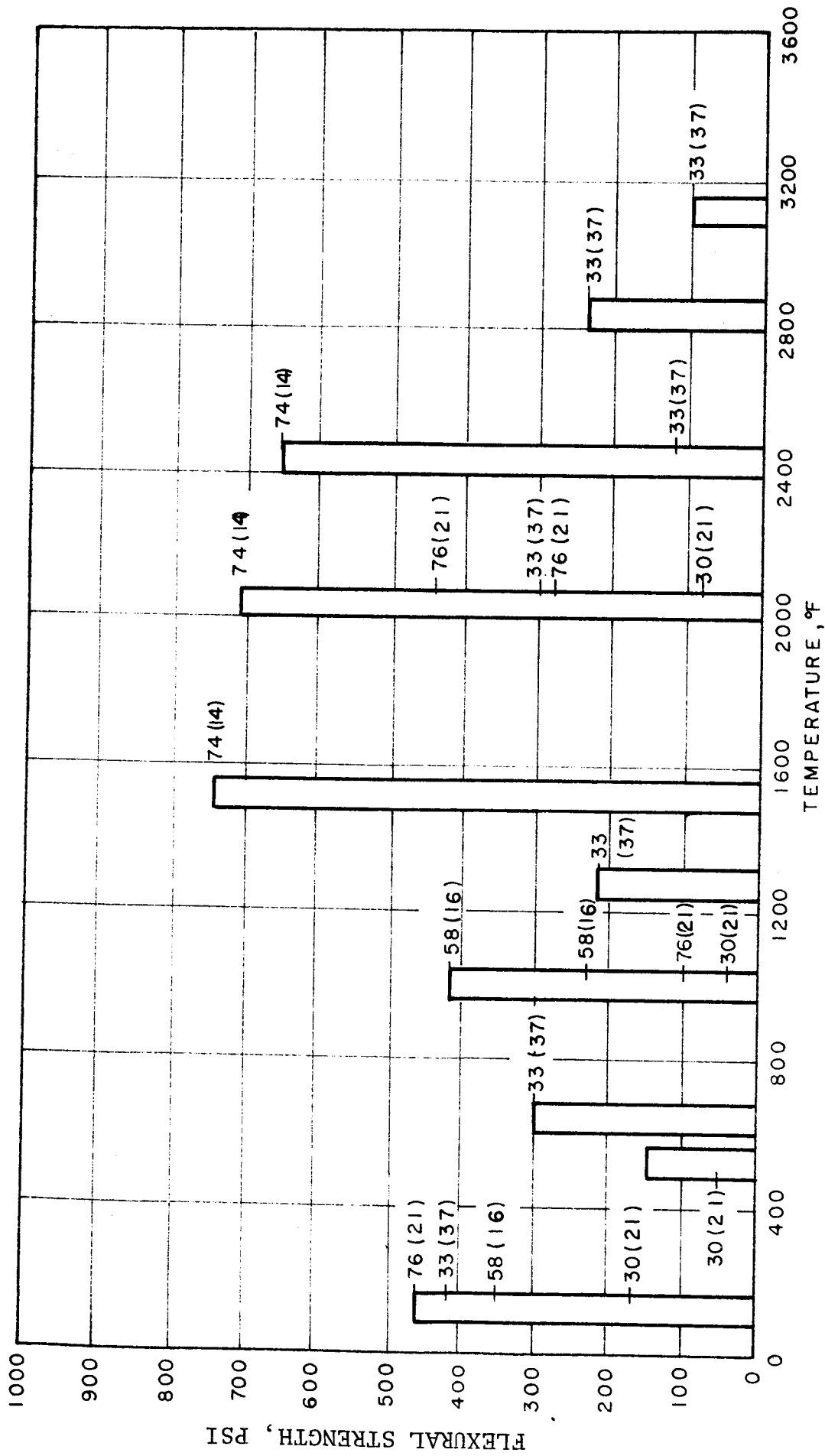


FIG. B-3 - EFFECT OF TEMPERATURE ON FLEXURAL STRENGTH OF ALUMINA FOAMS OF VARIOUS DENSITIES (Numbers in parenthesis indicate References and are preceded by foam density in lb/ft³)

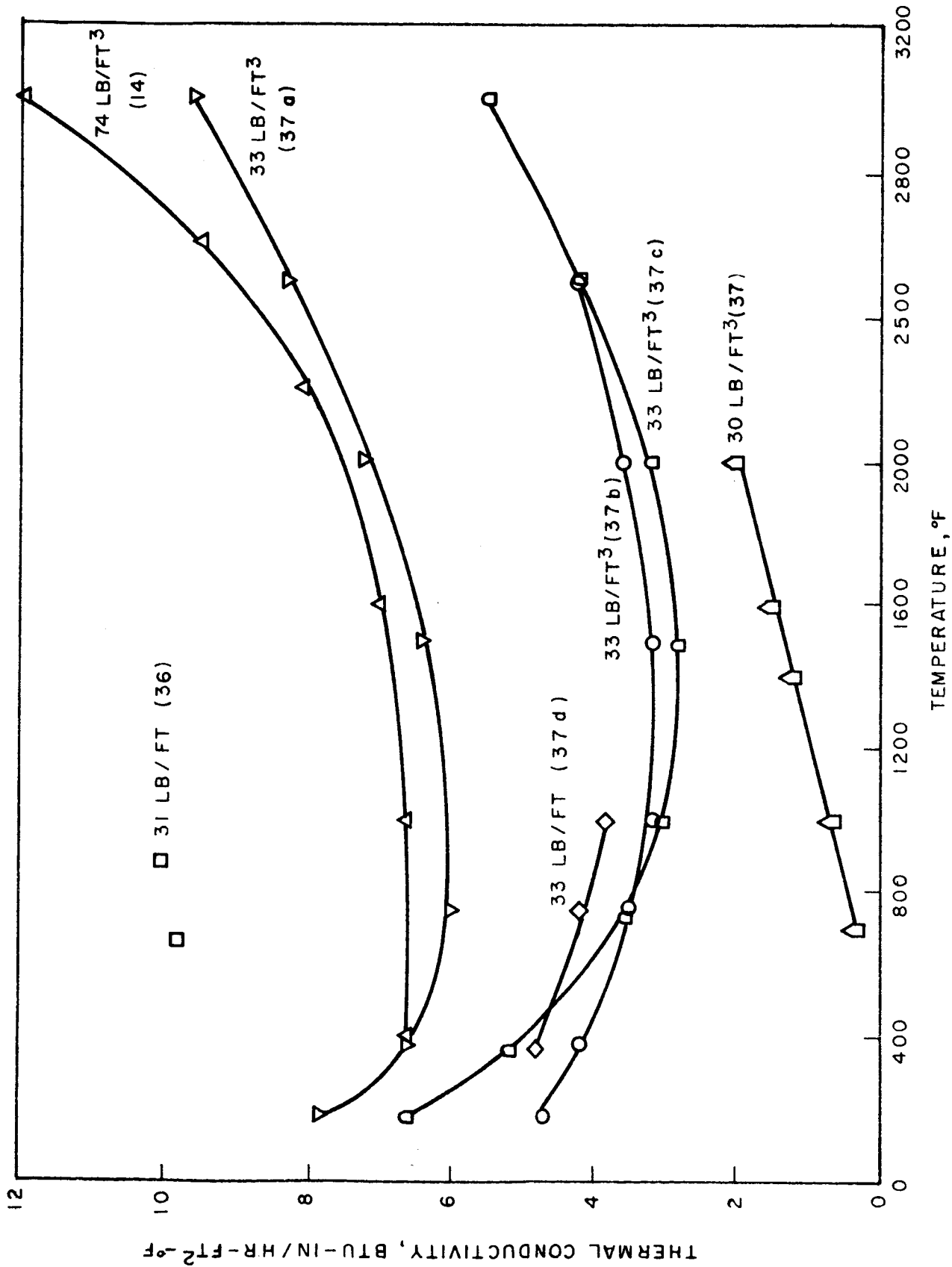


FIG. B-4 - EFFECT OF TEMPERATURE ON THE THERMAL CONDUCTIVITY OF ALUMINA FOAMS OF VARIOUS DENSITIES (Numbers in parenthesis indicate References and are preceded by density of foams; a,b,c,d refer to four different investigators)

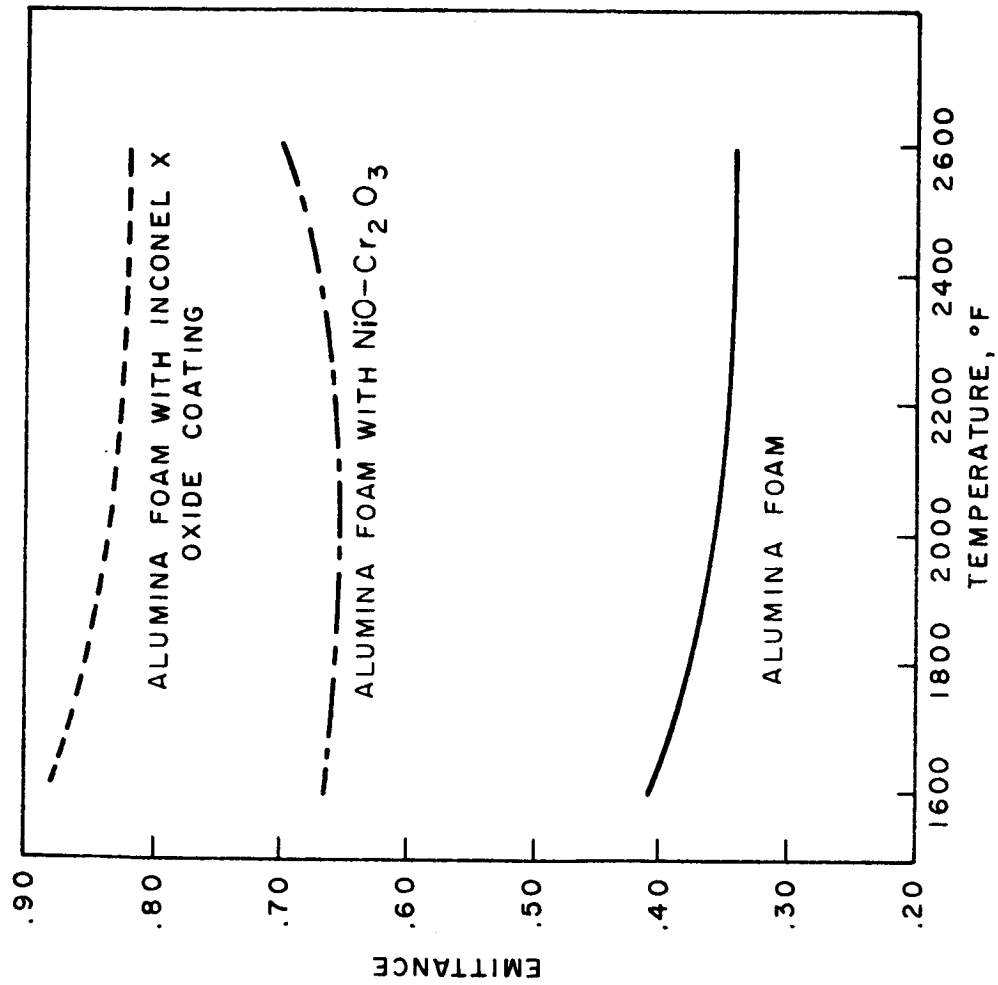


FIG. B-5 - EMMITTANCE OF VARIOUS ALUMINA-BASED FOAMS (16)

(Reproduced from J.N.Krusos et al.,
Aeronca Manufacturing Corporation)

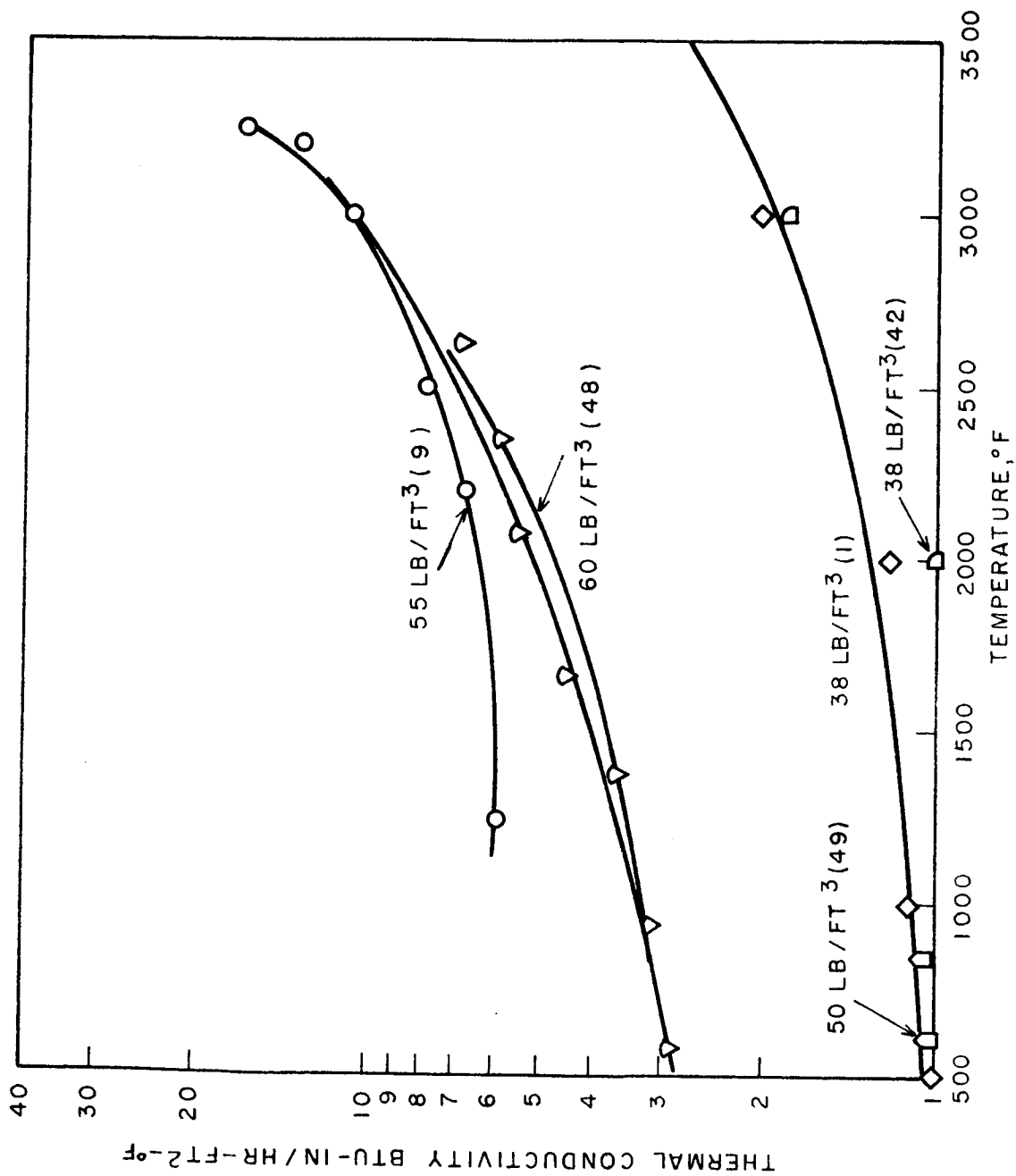


FIG. B-6 - EFFECT OF TEMPERATURE ON THERMAL CONDUCTIVITY OF ZIRCONIA FOAMS OF VARIOUS DENSITIES (Numbers in parenthesis indicate References and are preceded by density of foams)

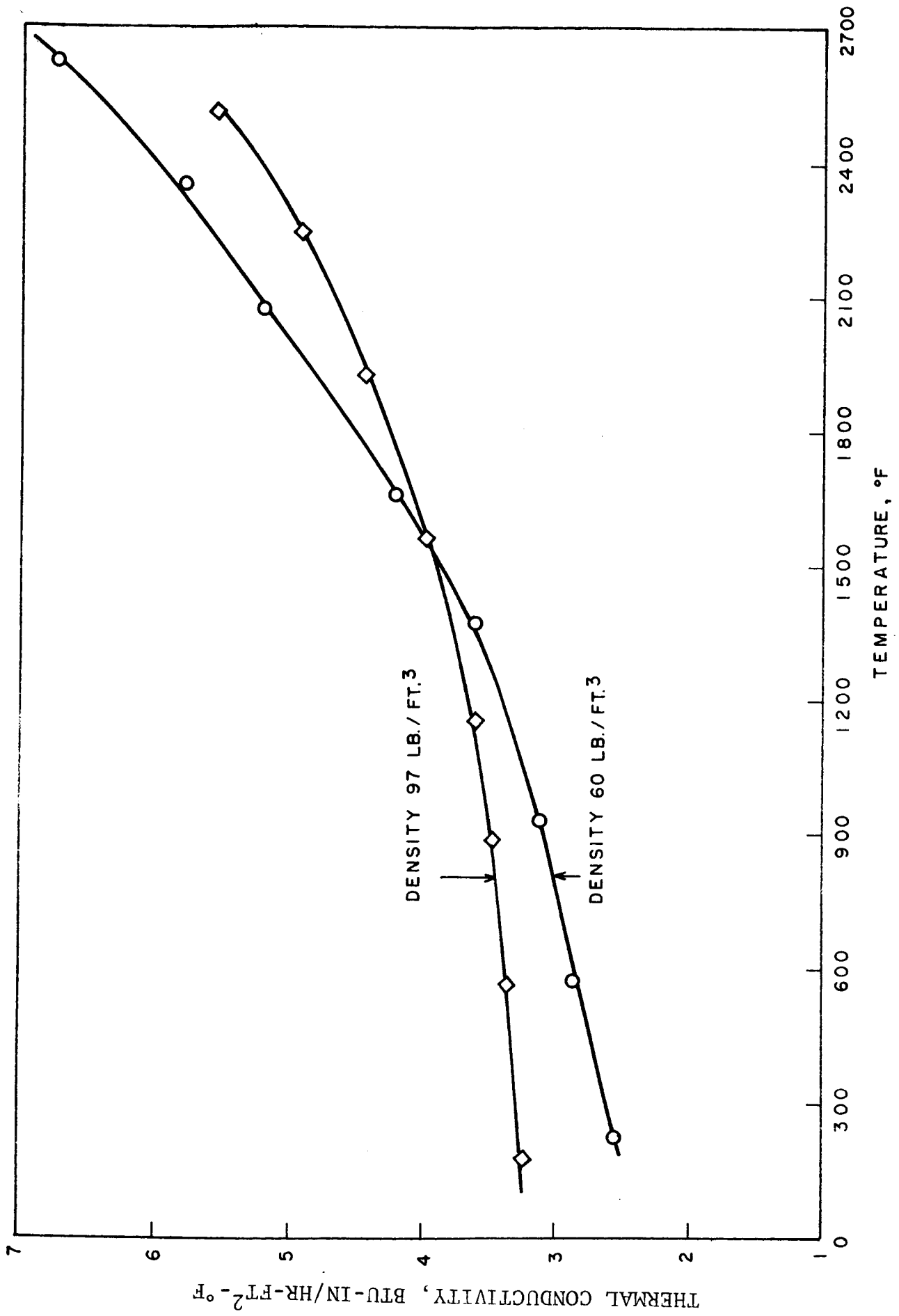


FIG. B-7 - THE EFFECT OF DENSITY ON THE THERMAL CONDUCTIVITY OF FOAMED ZIRCONIA (48)

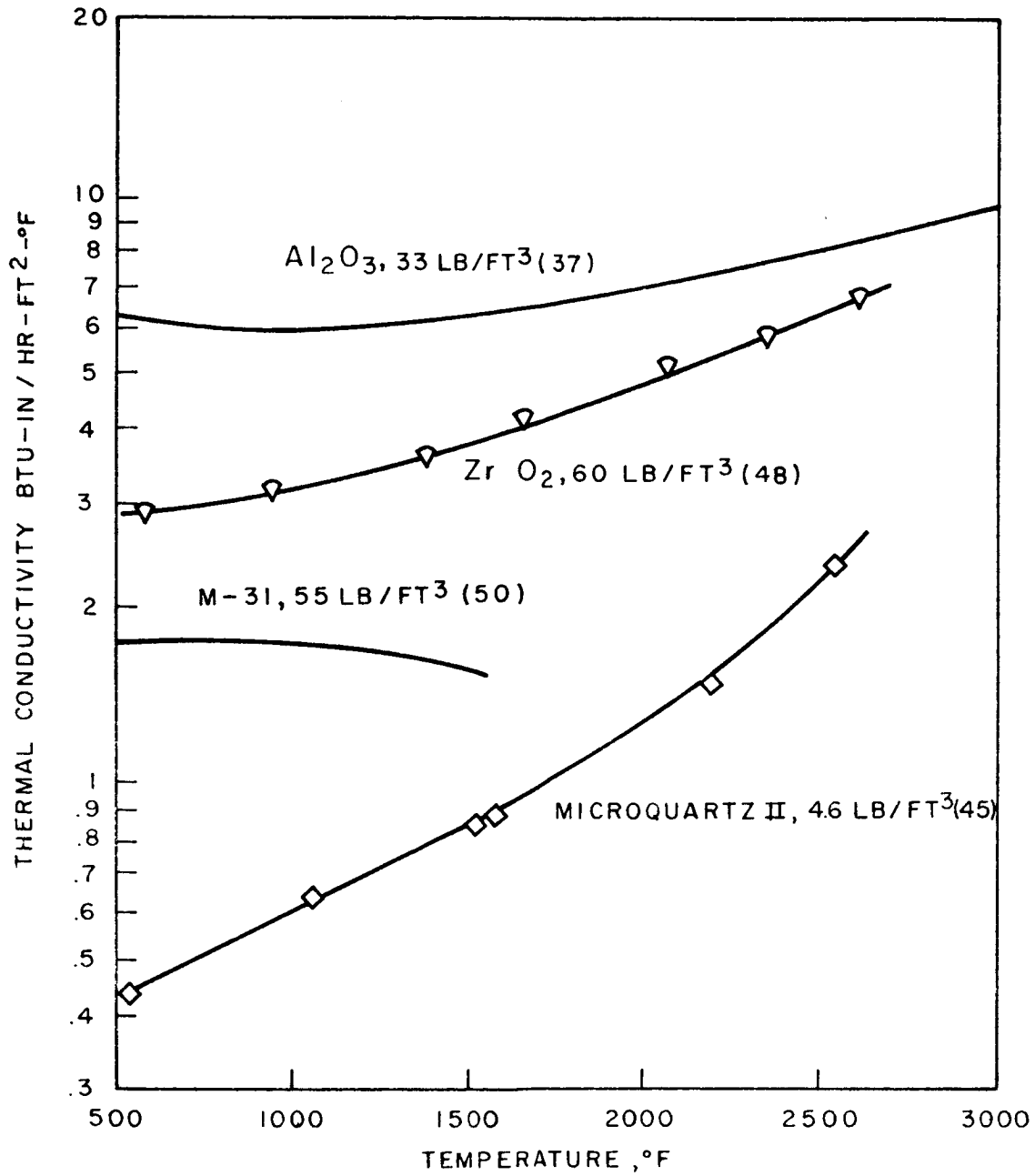


FIG. B-8 - THE THERMAL CONDUCTIVITY OF FOAMED AND FIBROUS MATERIALS (Numbers in parenthesis indicate references and are preceded by density of materials)

REFERENCES

1. D. L. Kummer et al., "Shielded Ceramic Composite," McDonnell Aircraft Corp., Report IR-7-997(1), Contract No. AF 33(657)-10996, 31 August 1963 (AD 417,116).
2. H. A. Pearl, J. M. Nowak, J. C. Conti, and R. J. Urode, (Bell Aircraft Corporation), "Refractory Inorganic Materials for Structural Applications," WADC-TR-59-432, Contract No. AF 33(616)-5930, February 1960.
3. C. M. Nicholson and G. A. Bole, "Cellulated Ceramics for the Structural Clay Products Industry, - J. Am. Ceram. Soc., 36 (4), 127-136 (1953).
4. J. W. Vogan and J. L. Trumbull (Boeing Company), "Metal-Ceramic Structural Composite Materials," ML-TDR-64-83, Contract No. AF 33 (616)-7815, June 1964.
5. J. K. Lindell and J. B. Cloud, et al., "Research on Method for Production of Thermantic Structural and/or Heat Shielding Materials, Phase 2--Process Development and Trial Production," Ipsen Industries, Inc., Interim Report IR-8-117 (2), Contract No. AF 33(657)-11286, 1 October 1963-30 April 1964.
6. J. D. Walton, "Fused Silica Ceramics," Ceramic Age, 77, 52-58, May 1961.
7. S. Pawlowski, "Highly Refractory Insulating Foam Products," Prace Inst. Min. Hutnictwa, 6, 65-73 (1954), (in Polish, English Summary--see Chem. Abstr. 49, 2044h, 1955.)
8. S. Pawlowski, "The Manufacture of Insulating Refractories by the Foam Method," Prace Inst. Min. Hutnictwa, 6, 305-313 (1954), (in Polish, English Summary--see Chem. Abstr., 48, 7271a, 1954).
9. K. H. Styhr, Jr., (National Beryllia Corporation), "Research on Low-Density Thermal Insulation Materials for Use Above 3000°F," Third Quarterly Status Report, Contract No. NASr-99, 31 December 1962.
10. J. S. Griffith, R. S. Olsen, and H. L. Rechter (IITRI Patent assigned to DuPont), "Compositions and Processes for Making Foamed Alumina Refractory Products and Articles So Produced," U. S. Patent 3,040,190, 26 June 1962.
11. "Baymal" Coloidal Alumina, brochure describing properties and uses, by E. I. duPont de Nemours and Company.

IIT RESEARCH INSTITUTE

REFERENCES (continued)

12. J. H. Fishwick, "Manufacture of Foamed Ceramics Based On Petalite and Beta Spodumene," J. Am. Ceram. Soc., 42, (3), 110-113, (1963).
13. News release: (a) Materials in Design Engineering, July 1964, p. 113, (b) Electronic News, 31 July 1964.
14. W. F. Zimmerman and R. S. Haeckl (General Electric Co.), "Cellular Lightweight Alumina Ceramic," U. S. Patent 2,966, 421; 7 December 1960.
15. W. F. Zimmerman, "Development of a Foamed Alumina Cement," Am. Ceram. Soc. Bull., 38 (3), 97-98 (1959).
16. J. N. Krusos, A. S. Kjelby, J. Borosic, and T. J. Byrne (Aeronca Manufacturing Corporation), "Beryllium Composite Structures, Volume II--Materials and Processes," ASD-TR-61-706 Volume II, Contract No. AF 33(616)-7050, May 1962 (AD 278-526).
17. M. F. Grandey and J. F. Kulp (General Electric Company), "Method of Preparing Silicon Nitride Foam Material," U.S. Patent 3,085,886, 16 April 1963.
18. M. F. Grandey (General Electric Company), "Method of Making Foam Material From Nickel Powder," U.S. Patent 2,917,384, 15 December 1959.
19. M. F. Grandey (General Electric Company), "Copper Foam Material and Method," U.S. Patent 3,078,552, 26 February 1963.
20. I. M. Logan, D. C. Wise, J. J. McGahan, and C. Von Doenhoff (Carborundum Co.), "Development of Non-Oxidic Refractory Foams" WADD-TR-60-124, Contract No. AF 33(616)-6294, April 1960.
21. M. S. Howeth, H. R. Thornton, and J. E. Burroughs (General Dynamics, Fort Worth, Texas), "Developments in Thermal-Structural Composites at General Dynamics/Fort Worth" FZM-4037, Presented at the Eighth Refractory Composites Working Group Meeting, January 1964.
22. S. Fernhof (Sweden), "Method of Manufacturing Porous Ceramic Products," U.S. Patent 2,996,389, 15 August 1961.

IIT RESEARCH INSTITUTE

REFERENCES (continued)

23. K. Schwartzwalder and A. V. Somers (General Motors Corp.), "Method of Making Porous Ceramic Articles," U.S. Patent 3,090,094, 21 May 1963.
24. I. J. Holland (Consolidated Beryllium, Ltd., England), "Method of Making Porous Shape of Sintered Refractory Material," U.S. Patent 3,097,930, 16 July 1963.
25. W. D. Ford (Pittsburgh-Corning Corporation), "Production of Cellulated Glass," U.S. Patent 2,758,937, 14 August 1956.
26. C. M. Riley, "Relation of Chemical Properties to Bloating of Clays," J. Am. Ceram. Soc., 34 (4), 121-128 (1951).
27. G. A. Bole (Laclede Christy Clay Products Co.), "Heat Insulating Material," U.S. Patent 2,073,138, 9 August 1930.
28. E. Ryshkewitch, "Compression Strength of Porous Sintered Alumina and Zirconia--9th Communication to Ceramography," J. Am. Ceram. Soc., 36 (2), 68 (1953).
29. W. Duckworth, "Discussion of Ryshkewitch's Paper," J. Am. Ceram. Soc., 36 (2), 68 (1953).
30. L. J. Trostel, Jr., "Strength and Structure of Refractories as a Function of Pore Content," J. Am. Ceram. Soc., 45, (11), 563-564 (1962).
31. S. D. Brown, R. B. Biddulph, and P. D. Wilcox, "A strength-Porosity Relation Involving Different Pore Geometry and Orientation," J. Am. Ceram. Soc., 47 (7), 320-322 (1964).
32. S. M. Lang, "Properties of High-Temperature Ceramics and Cermets," National Bureau of Standards Monograph 6, March 1, 1960.
33. J. Francl and W. D. Kingery, "Thermal Conductivity: IX, Experimental Investigation of Effect of Porosity on Thermal Conductivity," J. Am. Ceram. Soc., 37 (2), 99-107 (1954).
34. A. E. Wechsler, P. E. Glaser (Arthur D. Little, Inc.), "Investigation of the Thermal Properties of High-Temperature Insulation Materials," ASD-TDR-63-574, Contract No. AF 33 (657)-9172, July 1963 (N63-22592).
35. A. L. Loeb, "Thermal Conductivity: VIII, A Theory of Thermal Conductivity of Porous Materials," J. Am. Ceram. Soc., 37 (2), 96-99 (1954).

IIT RESEARCH INSTITUTE

REFERENCES (continued)

36. D. J. Powers (Bell Aerosystems Co.), "Modulus of Rupture, Thermal Conductivity, and Thermal Exposure Tests on Foamed Aluminum Oxide and Foamed Zirconium Oxide," Bell Lab. Report 63-13(m), Contract No. AF 33(657)-8555, March 1963 (AD-401-854).
37. R. M. David and C. Milewski (Martin Company, Baltimore), "High-Temperature Composite Structure," ASD-TDR-62-418, Contract No. AF 33(616)-7497, June 1962.
38. R. H. Stutzman, J. R. Salvaggi, and H. P. Kirschner, (Cornell Aeronautical Laboratory), "An Investigation of the Theoretical and Practical Aspects of the Thermal Expansion of Ceramic Materials, Volume I--Literature Survey," PI-1273-M-4, Contract No. NOrd-18419, 31 August 1956 (AD 220-685).
39. Boeing Company Aerospace Division, "Evaluation of Impregnated Porous Refractory Oxide Composites," Quarterly Progress Report No. 3, Contract No. AF 33(657)-11222, April 1964.
40. K. H. Styhr (National Beryllia Corp.), "Research on Low-Density Materials for Use Above 3000°F," Seventh Quarterly Status Report, Contract No. NASr-99, 31 December 1963.
41. J. F. Judge, "Glasrock Applications Described Limitless," Missiles and Rockets, 8, 26-28, 10 April 1961.
42. C. W. Hallett, et al., (Ipsen Industries), "Research on Method for Production of Thermantic Structural and/or Heat Shielding Materials, Phase I, Survey of the State-of-the-Art for the Processing of Foamed Metals and Ceramics and Composite Structures," IR-8-117(1), Contract No. AF 33(657) 11286, 30 September 1963.
43. Glasrock Products, Inc., Atlanta, Georgia Private Communication (1964).
44. A. L. Hansen, "Evaluation of Low Density, High Temperature (to 2000°F) Thermal Insulation," Northrop Aircraft Norair Division Report NOR-60-251, 7 December 1961.
45. R. H. Lange, H. Jones, et al., (General Dynamics/Astronautics), "Lightweight Thermal Protection System Development, Volume II," ASD-TDR-63-596, Vol. II, Contract No. AF 33(657)-9444, June 1963 (AD 422-941).

IIT RESEARCH INSTITUTE

REFERENCES (continued)

46. Thermal Insulations, Johns-Manville Insulation Product Information, Form IN-475A, 12 June 1963.
47. V. F. Seitzinger (NASA-MSFC), "Development of Ceramic Insulation for Radiant Heating Environments," Presented at the Annual Meeting of the American Ceramic Society in Chicago, April 1964, Paper 13-3S-64.
48. Unpublished data on an Air Force sponsored program at IITRI.
49. E. L. Strauss (Martin Company, Baltimore), "Recent Martin Investigation of Refractory Composites, ER 11853," Presented at the Fifth Meeting of the Refractory Composites Working Group, August 1961.
50. J. M. Carroll, and C. D. Pears (Southern Research Institute), "The Thermal Conductivity of 'M-31' Coating Material," Final Report on Task 4, Contract No. NAS8-5196, 9 September 1963.

IIT RESEARCH INSTITUTE